M M

TP 3988E

TANK CAR THERMAL MODELLING-Phase 1

PREPARED FOR:

TRANSPORT CANADA
TRANSPORTATION DEVELOPMENT CENTRE

BY:

H.G. ENGINEERING LIMITED
&
HOOPER & ANGUS LIMITED

CA1
DTC 801
8
R17
c.

SS CONTRACT NO: 11SA.T8200-1-1540

Library and Information Centre /
Centre de Documentation (GSLA)
RECEIVED – REÇU LE
APR AVR 6 1983
Transport Canada / Transports Canada

TP 3988E

RAIL TANK CAR THERMAL MODELLING

Prepared for: Transport Canada
Transportation Development Centre

DSS Contract No: 11SA.T8200-1-1540

By: H.G. Engineering Ltd. & Hooper and Angus Associates Ltd.

Principal Investigators: A. Firmin, F.C. Hooper, G.T. Williams

H.G.E. Job No: 10202

H.G. Engineering Ltd., 260 Lesmill Rd., Don Mills, Ontario
Phone: (416) 447-5535

The contents of this report reflect the views of the contractor and not necessarily the official views or policies of the Transportation Development Centre of Transport Canada.

REPORT DOCUMENTATION FORM

1. Transport Canada Report No.
TP 3988E

2. TDC Project No.
4468

3. Recipient's Catalogue No.

4. Title and Subtitle
RAIL TANK CAR THERMAL MODELLING - Phase I

5. Report Date
AUGUST 31, 1982

6. Performing Organization Report No.

7. Author(s)
A. Firmin, F.C. Hooper and G.T. Williams

8. Transport Canada File No.
D1465-302-C-3

9. Performing Organization Name and Address
H.G. Engineering Ltd.
260 Lesmill Road
Don Mills, Ontario M3B 2T5

10. DSS File No.
11SD.T8200-1-1540

11. DSS or Transport Canada Contract No.
OSD81-00164

12. Sponsoring Agency Name and Address
Transportation Development Centre (TDC)
1000 Sherbrooke Street West
Place de l'aviation
Montreal, Quebec H3A 2R3

13. Type of Report and Period Covered
Technical

14. Sponsoring Agency Code
TDC 4468

15. Supplementary Notes

16. TDC Project Officer
D.W. Dibble

17. Abstract

This report forms part of the Tank Car Explosion Protection Program - Phase II, with the primary goal of developing a mathematical model of heat transfer processes in a rail tank car under fire conditions. Models will be used to analyse the results of an experimental testing program, to understand the role of EXPLOSAFE (a tank car protective system) in a tank car fire, and to develop preferred design alternatives and configurations for tank car thermal protection.

Models have been developed in particular for the study of propane-filled rail tank cars, but are not limited to this. It has been necessary to propose three models, the engulfing pool fire, the impinging torch fire (liquid zone) and the impinging torch fire (vapour zone). These fire conditions and the manner of tank car failure are sufficiently different that they have been modelled separately. The proposed models not only handle the calculation of temperature and pressure with time, but also include the effects of mass flow through the pressure relief valve.

18. Key Words
Mathematical model, Rail tank car, Thermal model, Fire, Heat transfer, Pressure relief valves

19. Distribution Statement
Copies available from TDC.

20. Security Classification (of this report)
nil

21. Security Classification (of this page)
nil

22. No. of Pages

23. Price
--

TDC/CDT 79-005

FORMULE DE DOCUMENTATION POUR RAPPORT

1. Nº du rapport Transports Canada
TP 3988E

2. Nº de l'étude — CDT
4468

3. Nº de catalogue du destinataire

4. Titre et sous-titre
RAIL TANK CAR THERMAL MODELLING - Phase I

5. Date du rapport
31 août 1982

6. Nº du rapport de l'organisme exécutant

7. Auteur(s)
A. Firmin, F.C. Hooper et G.T. Williams

8. Nº de dossier Transports Canada
D1465-302-6-3

9. Nom et adresse de l'organisme exécutant
H.G. Engineering Ltée
260 Lesmill Road
Don Mills, Ontario
M3B 2T5

10. Nº de dossier — ASC
11SD.T8200-1-1540

11. Nº de contrat — ASC ou Transports Canada
0SD81-00164

12. Nom et adresse de l'organisme parrain
Centre de développement des transports (CDT)
1000 o., rue Sherbrooke
Place de l'aviation
Montréal, Québec H3A 2R3

13. Genre de rapport et période visée
Technique

14. Code de l'organisme parrain
CDT 4468

15. Remarques additionnelles

16. Agent de projet — CDT
D.W. Dibble

17. Résumé

Ce rapport porte sur le programme Protection des wagons-citernes Phase II, visant l'étude d'un modèle mathématique pour la modélisation des transferts thermiques ayant lieu dans un wagon-citerne pris dans un incendie. Divers modèles serviront à analyser les résultats des expérimentations prévues par ce programme , de manière à mettre en lumière l'apport du système EXPLOSAFE dans la protection d'un wagon-citerne soumis à l'action des flammes et à trouver les meilleures solutions et configurations à mettre en oeuvre.

Des modèles ont été élaborés, notamment pour l'étude de wagons-citernes remplis de propane, mais leur utilité ne s'arrête pas à cette application. Il a été jugé nécessaire d'élaborer trois modèles mathématiques pour étudier trois situations distinctes: l'incendie enveloppant, l'effet torche (phase liquide) et l'effet torche (phase gazeuse). Ces trois situations et les types de défaillance structurelle qu'elles entraînent se démarquent suffisamment les unes des autres pour justifier une modélisation distincte. Les modèles mathématiques élaborés tiennent compte non seulement de la montée des températures et des pressions dans le temps, mais aussi de l'effet de l'écoulement massique par les soupapes de sûreté.

18. Mots-clés
Modèle mathématique, wagon-citerne, modèle thermique, incendie, transferts thermiques, soupapes de sûreté

19. Diffusion
Le CDT dispose d'un certain nombre d'exemplaires

20. Classification de sécurité (de ce rapport)
aucune

21. Classification de sécurité (de cette page)
aucune

22. Nombre de pages

23. Prix
aucun

(i) ABSTRACT

This report describes in detail the procedure for developing a computer model to study the changing state of a fluid filled cylinder under an engulfing or locally impinging flame. The model has been developed in particular for the study of propane filled rail tank cars but is not limited to this. The proposed model not only handles the calculation of temperature and pressure with time but also includes the effects of mass flow through the pressure relief valve.

RAIL TANK CAR THERMAL MODELLING

TABLE OF CONTENTS

Page No.

(i) ABSTRACT

(ii) TABLE OF CONTENTS

(iii) NOMENCLATURE

(iv) LIST OF FIGURES

(v) LIST OF TABLES

1.0 INTRODUCTION 1

2.0 REVIEW AND INTERPRETATION OF CANADIAN AND AMERICAN FIELD TESTS

2.1 Review of approaches to field trials 3
2.2 Explanation of observed sequence of events 7
2.3 Interpretation of test results 9
2.3.1 The superheating and vapour venting processes 9
2.3.2 Homogeneous boiling and flashing 18
2.3.3 Liquid temperature zoning 18
2.3.4 Temperature gradients in the vapour 21
2.3.5 Liquid level effects 23
2.3.6 Pressure relief valve operation 23

3.0 THE ROLE OF EXPLOSAFE IN RAIL TANK CAR FIRES

3.1 Notes on a preliminary qualitative comparative boiling test with and without EXPLOSAFE 24
3.2 Relevant characteristics of EXPLOSAFE 25

4.0 VENT VALVE CHARACTERISTICS

4.1 Mass discharge rates 28
4.2 Valve open and close set points 31

5.0 THE MODEL CONCEPT

5.1 Model building 32
5.2 Model objectives 34
5.3 Model features 36
5.4 Heat transfer processes 39
5.5 Distinguishing the role of EXPLOSAFE 39
5.6 Engulfing pool fire model concept 44
5.7 Impinging torch fire concept 49
5.8 Future extensions of the model concepts 52

6.0 MODEL FORMULATION

6.1 Governing equations 53
6.2 Overall model logic 58
6.2.1 Engulfing pool fire 58
6.2.2 Impinging torch fire 67

TABLE OF CONTENTS (cont'd)

6.3 Model component description and logic 76
- 6.3.1 Location of phase boundaries 76
- 6.3.2 Location of zonal boundaries 76
- 6.3.3 Nodal configuring 76
- 6.3.4 Heat input functions - pool fire 84
- 6.3.5 Heat input functions - impinging torch fire 84
- 6.3.6 Heat input functions - plume radiation 84
- 6.3.7 Fluid properties subroutine 92
- 6.3.8 Steel properties subroutine 92
- 6.3.9 Insulation properties subroutine 92
- 6.3.10 EXPLOSAFE properties subroutine 92
- 6.3.11 Heat transfer coefficients subroutine 92
- 6.3.12 Coefficients subroutine 98
- 6.3.13 R_m subroutine 109
- 6.3.14 Thermal network 110
- 6.3.15 PRV subroutine 114
- 6.3.16 State equations - liquid phase 115
- 6.3.17 State equations - vapour phase 118
- 6.3.18 Process equations - Stage.1 119
- 6.3.19 Process equations - Stage 2 119
- 6.3.20 Vapour pressure equation 123
- 6.3.21 Mass transfer equation - vaporization 124
- 6.3.22 Mass transfer equation - condensation 125
- 6.3.23 Failure subroutine 125
- 6.3.24 PRV set points 125

7.0 STRUCTURAL CONSIDERATIONS AND THE FAILURE CRITERIA

- 7.1 Pressure induced stresses 129
- 7.2 Experimental data 131
- 7.3 Thermal stresses due to wall temperature variations 133
- 7.4 The model failure criteria 135

8.0 PHYSICAL DATA

- 8.1 Requirements for physical data 136
- 8.2 Boiling curves for propane 136
- 8.3 EXPLOSAFE effects on heat transfer 137
- 8.4 Thermodynamic properties of propane 138
- 8.5 Heat transfer coefficients and properties 140
- 8.6 Mechanical properties and tank materials 140

9.0 EXPERIMENTAL WORK REQUIRED

- 9.1 Overall considerations 141
- 9.2 Boiling curve determination 141
- 9.3 Mixing resistance scale effect 142
- 9.4 Further data on EXPLOSAFE 144
- 9.5 Vent valve characteristics 145

TABLE OF CONTENTS (cont'd)

10.0 COMPUTER PROGRAM DEVELOPMENT

10.1 Software considerations 146
10.2 Background of heat transfer software 147
10.3 Background in structural analysis software 147

11.0 SUMMARY 148

12.0 REFERENCES

13.0 BIBLIOGRAPHY

APPENDIX

(III) NOMENCLATURE

A - liquid saturation flag
- surface area
A^* - critical valve area
B - liquid boil-off flag
BLEVE - boiling liquid expanding vapour explosion
C - heat capacitance
C_p - specific heat
D - tank diameter
D_f - damping factor
DT - steel thickness
DN - nodal distance
e - emissivity
F - configuration factor
G - mass flux rate
g - gravitational constant
g_c - dimensional constant
h - heat transfer coefficient
- distance to plume from tank top
h_{fg} - latent heat of vaporization
j - time step iteration number
k - ratio of specific heats
- material thermal conductivity
L - tank car length
m - mass
M_o - molecular weight
n - polytropic exponent
NN - number of nodes
P - system pressure
PRV - pressure relief valve
Q - heat flux
R - universal gas constant
- tank radius
- link thermal resistance
R_m - mixing resistance between saturated and sub-cooled liquid zones
t - time
T - fluid temperature
TOL - tolerance
TE - EXPLOSAFE thickness
TI - insulation thickness
Δt - time step
v - specific volume
v_e - fluid velocity
V - volume
x - distance to liquid surface from tank top
Z - compressibility factor
Δz - static head

Greek symbols

α - absorptivity
α_T - coefficient of isothermal compressibility
β - angle defining location of PRV
γ - specific gravity
δ - condensation layer thickness
Δ - difference
κ_T - isothermal compressibility
ρ - density
σ - stress
θ - angle defining location of liquid surface
ϕ - angle defining location of a node
χ - fluid quality

Superscripts

e - external
  - efflux
i - inner
l - liquid phase
lv - liquid/vapour
s - steel
v - vapour phase
• - rate of change

Subscripts

a - ambient
c - close
cond - condensation
e - efflux
f - flame
i - nodal location reference index
l - liquid
n - iteration number
o - open
  - reference state
sat - saturated state
v - vapour phase
vap - vaporization
1 - saturated liquid zone
2 - sub-cooled liquid zone
T - total

Other symbols

$\{\ \}$ - matrix
$[\ ]$ - vector
$\|\ \|$ - matrix norm

LIST OF FIGURES

		Page No.
FIGURE 2.1	FLAMES AND SMOKE FROM A 19-CAR DERAILMENT	4
FIGURE 2.2	EXPLODED RAIL TANKER CAR CONTAINING PROPANE GAS	5
FIGURE 2.3	TIME HISTORY FOR ENGULFED TANK CAR	6
FIGURE 2.4	PROPANE MOLLIER DIAGRAM	10
FIGURE 2.5	PROPANE MOLLIER DIAGRAM	11
FIGURE 2.6	PROPANE MOLLIER DIAGRAM	12
FIGURE 2.7	PROPANE MOLLIER DIAGRAM	13
FIGURE 2.8	PROPANE MOLLIER DIAGRAM	14
FIGURE 2.9	PROPANE MOLLIER DIAGRAM	15
FIGURE 2.10	VARIATION OF POLYTROPIC EXPONENT	19
FIGURE 2.11	TEMPERATURES IN VAPOUR SPACE	20
FIGURE 2.12	VAPOUR SPACE TEMPERATURE GRADIENTS	22
FIGURE 4.1	MASS DISCHARGE THROUGH PRV	29
FIGURE 5.1	MODEL BUILDING	33
FIGURE 5.2	RAIL TANK CAR MODEL TYPES	43
FIGURE 5.3	EQUIVALENT THERMAL NETWORK	45
FIGURE 5.4	EQUIVALENT THERMAL NETWORK - TWO NODE	47
FIGURE 5.5	IMPINGING TORCH MODEL - LIQUID ZONE	48
FIGURE 5.6	IMPINGING TORCH MODEL - VAPOUR ZONE	50
FIGURE 6.1	GOVERNING EQUATIONS	54
FIGURE 6.2	ENERGY FLOWS IN A GENERAL THERMODYNAMIC SYSTEM	55
FIGURE 6.3	OVERALL MODEL ORGANIZATION - ENGULFING FLAME	57
FIGURE 6.4	ENGULFING FLAME MODEL - TWO LIQUID ZONES	59
FIGURE 6.5	CALCULATION OF MASS EXCHANGES BETWEEN PHASES	66
FIGURE 6.6	OVERALL MODEL ORGANIZATION - IMPINGING FLAME	68
FIGURE 6.7	IMPINGING FLAME MODEL	70
FIGURE 6.8	LOCATION OF PHASE BOUNDARIES	77
FIGURE 6.9	LOCATION OF ZONAL BOUNDARIES	79
FIGURE 6.10	NODAL CONFIGURING - ENGULFING FLAME MODEL	81
FIGURE 6.11	NODAL CONFIGURING - TORCH - LIQUID ZONE	85
FIGURE 6.12	NODAL CONFIGURING - TORCH - VAPOUR ZONE	86
FIGURE 6.13	POSSIBLE FLAME TEMPERATURE PROFILES	87
FIGURE 6.14	HEAT INPUT FUNCTION - POOL FIRE	88
FIGURE 6.15	HEAT INPUT FUNCTION - IMPINGING TORCH	89
FIGURE 6.16	HEAT INPUT FUNCTION - PLUME RADIATION	91
FIGURE 6.17	FLUID PROPERTIES SUBROUTINE	93
FIGURE 6.18	STEEL PROPERTIES SUBROUTINE	94
FIGURE 6.19	INSULATION PROPERTIES SUBROUTINE	95
FIGURE 6.20	EXPLOSAFE PROPERTIES SUBROUTINE	96
FIGURE 6.21	HEAT TRANSFER COEFFICIENTS SUBROUTINE	97
FIGURE 6.22	INFRARED SPECTRUM OF GASEOUS PROPANE	99
FIGURE 6.23	COEFFICIENTS SUBROUTINE - ENGULFING FLAME	100
FIGURE 6.24	COEFFICIENTS SUBROUTINE - IMPINGING TORCH	103
FIGURE 6.25	COEFFICIENTS SUBROUTINE - IMPINGING TORCH	105
FIGURE 6.26	R_m SUBROUTINE	109
FIGURE 6.27	THERMAL NETWORK	112

		Page No.
FIGURE 6.28	PRV SUBROUTINE	114
FIGURE 6.29	STATIC LIQUID LEVEL ON PRV (ΔZ)	116
FIGURE 6.30	STATE EQUATIONS - LIQUID PHASE	117
FIGURE 6.31	STATE EQUATIONS - VAPOUR PHASE	118
FIGURE 6.32	COMPRESSIBILITY CHART FOR PROPANE (2)	120
FIGURE 6.33	PROCESS EQUATIONS - STAGE 1	121
FIGURE 6.34	PROCESS EQUATIONS - STAGE 2	122
FIGURE 6.35	VAPOUR PRESSURE EQUATIONS	123
FIGURE 6.36	MASS TRANSFER EQUATIONS - VAPORIZATION	124
FIGURE 6.37	MASS TRANSFER EQUATIONS - CONDENSATION	126
FIGURE 6.38	FAILURE SUBROUTINE	127
FIGURE 6.39	PRV SET POINTS	128
FIGURE 7.1	TWO TYPICAL STRUCTURAL MODELS OF A TANK CAR	130
FIGURE 7.2	STRENGTH VS TEMPERATURE FOR A285 STEEL	132
FIGURE 8.1	HEAT ABSORPTION RATES AT DIFFERENT ELEVATIONS	139

LIST OF TABLES

		Page No.
TABLE 2.1	DISCHARGE CHARACTERISTICS FOR POLYTROPIC EXPONENT	17
TABLE 5.1	ENGULFING FLAME MODEL	35
TABLE 5.2	IMPINGING TORCH MODEL	37
TABLE 5.3	HEAT TRANSFER PROCESSES	40
TABLE 6.1	MODEL COMPONENTS	75
TABLE 7.1	TEST TEMPERATURES AND PRESSURES	131

1.0 INTRODUCTION

This report summarizes work performed by H.G. Engineering Ltd. and Hooper and Angus Associates Ltd. on the project, "Tank Car Thermal Modelling" for the Transportation Development Centre, Transport Canada, under D.S.S. Contract No.: 11SD.T8200-1-1540. This project is part of the Tank Car Explosion Protection Program-Phase II, with the primary goal of developing a mathematical model of heat transfer processes in a rail tank car under fire conditions. This model will be used to analyse the results of an experimental testing program, to understand the role of EXPLOSAFE (a tank car protective system) in a tank car fire, and to develop preferred design alternatives and configurations for tank car thermal protection.

The thrust of the overall program is to develop improved safety measures for rail tank cars carrying propane, a liquifed petroleum gas, classified as a dangerous commodity [1]. In a series of experiments, conducted both in Canada and the United States, it became evident that new designs have the potential of being effective. These include using EXPLOSAFE, a fine metal mesh which is installed inside the tank against the inner walls, and thermal insulation. These measures have been studied in detail in this work, as it has been necessary to describe their role throughout an accident in order to develop concepts of the physical processes for the model. The field test program results provide the essential physical evidence. Sections 2.0 and 3.0 present interpretations of these results in the context of model development.

The pressure relief valve (PRV) is a safety measure used on all propane tanks. Their behaviour under accident conditions is discussed in Section 4.0.

With these data, it has been possible to build the model concept, presented fully in Section 5.0. It has been necessary to propose three models, the engulfing pool fire, the impinging torch fire (liquid zone), and the impinging torch fire (vapour zone). These fire conditions and the manner of tank car failure are sufficiently different that we have distinguished between these models.

The detailed mathematical formulation of the proposed models is given in Section 6.0. Governing equations are listed. The overall model logic is described and in subsequent subsections, model component (subroutine) logic is detailed. In essence, the model(s) is developed to the point where the next stage is computer programming of the described algorithms.

The model can be used to simulate the heat transfer behaviour during the accident. It is not capable of providing a detailed analysis of the tank car structure. Other approaches are required, should stress-strain profiles for the tank car be needed. Section 7.0 describes the approach which has been adopted for this model and reviews the options which are possible should a structural analysis be desired.

In order to use the model as formulated, it is necessary that some physical data be obtained. These include fundamental property data for propane. Additionally, data with EXPLOSAFE present with the propane are needed. These data requirements are fully discussed in Section 8.0 and in Section 9.0, experimental work which would be undertaken to obtain these data is described.

The course of development of the model is presented in Section 10.0 accounting for the availability of physical data.

The work is reviewed in total in the Summary, Section 11.0, with recommendations highlighted.

2.0 REVIEW AND INTERPRETATION OF CANADIAN AND AMERICAN FIELD TESTS

In the development of predictive heat transfer models of rail tank car fire accidents, it has been very useful to draw up on the available experimental evidence. This evidence consists of accounts of tank car derailments (eg. Mississauga Inquiry [2] and controlled tests conducted by Canadian and American Authorities [3 to 7]. Observations of real accidents, see Figures 2.1, 2.2 and the cover photo, have provided important background to assessing the severity of such accidents, identifying the dominant mechanisms, and determining the adequacy of simulating such accidents by a field test approach. In this Section, a general review of the field test approach is presented and the results of such tests are discussed in the present context.

2.1 REVIEW OF APPROACHES TO FIELD TRIALS

It is not within our terms of reference to review field testing methods in detail and to make recommendations concerning their possible improvement. If this is to be done, then it should follow the completion of the system model when further testing can be used to validate the model and to assess the success of design alternatives which may result from the modelling process.

Field tests conducted both in Canada and the U.S. have provided invaluable information used in building the proposed models. The American field test program started with a 1/5-scale examination of tank car fires in the early seventies [7]. Work was extended to full-scale tests on uninsulated and insulated tank cars in the mid-seventies [4,5,6]. This program led to significant revisions in tank car design (eg. shelf couplers, head shields, and insulation). Additionally, modelling activity was undertaken by the Calspan Corporation (1975)[8] and more recently by the University of Maryland (1981) [9], to understand the causes and find solutions to tank car disasters. A vigorous program of research into tank car safety valves is also being pursued at the University of Maryland [10 to 23].

A series of field tests was undertaken in Canada throughout 1979 and 1980 at the Defence Research Establishment (Suffield) to investigate the impact that EXPLOSAFE has on tank car explosions [3]. This was performed on a number of 1/5-scale tanks. These tests have provided a qualitative basis to develop model concepts.

Figure 2.1 Flames and smoke billow from burning freight cars following a 19-car derailment on the British Columbia Railway line 18 miles north of Prince George. (CP Wirephoto) 1976

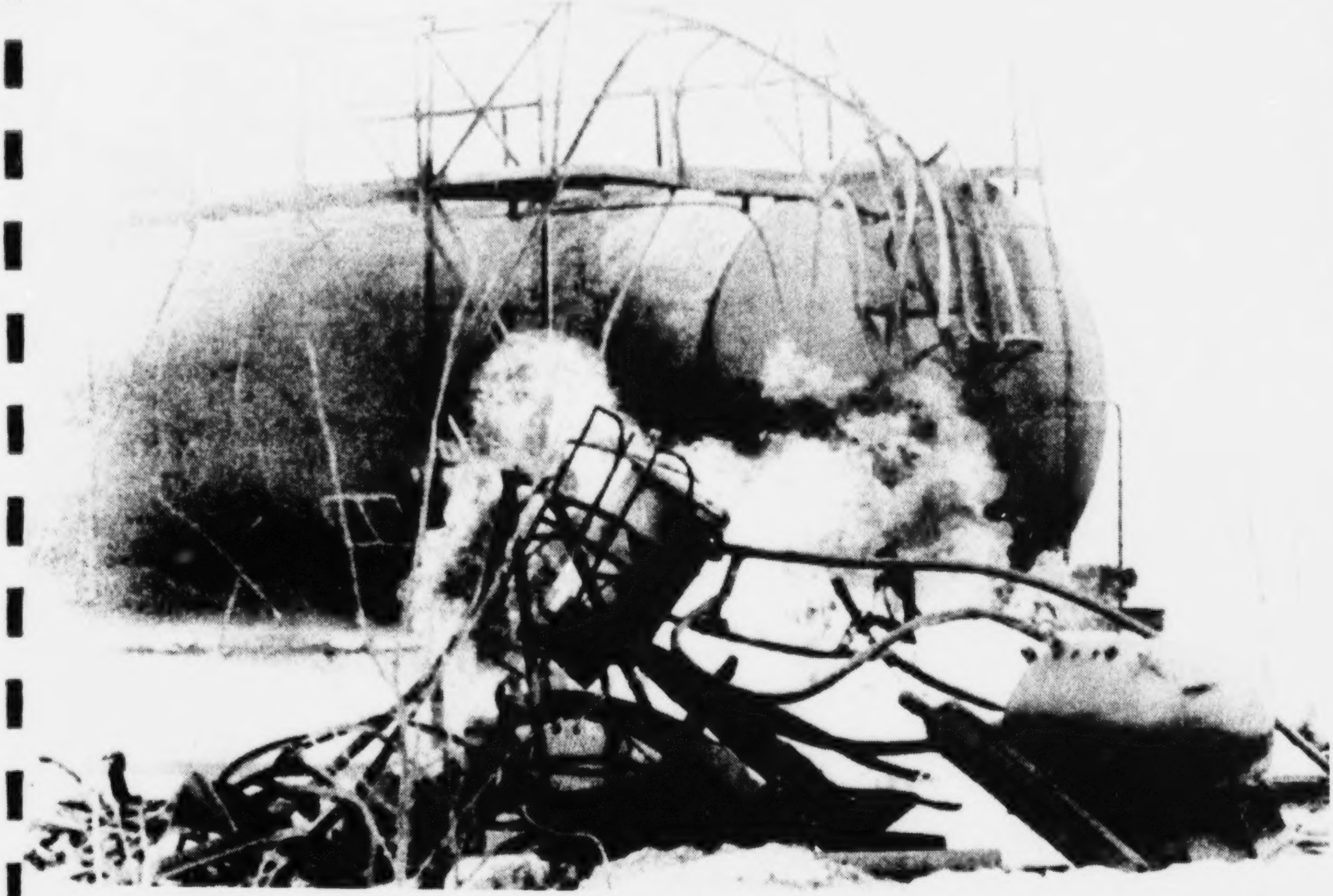

Figure 2.2 A rail tanker car containing propane gas exploded near Sylvan Lake, Alberta. (March 14, 1980)- One loading dock worker was injured and farm houses in the area were evacuated. (CP Laserphoto - Dale Lunan)

CHARACTERISTIC PRESSURE - TIME HISTORY FOR ENGULFED TANK CAR

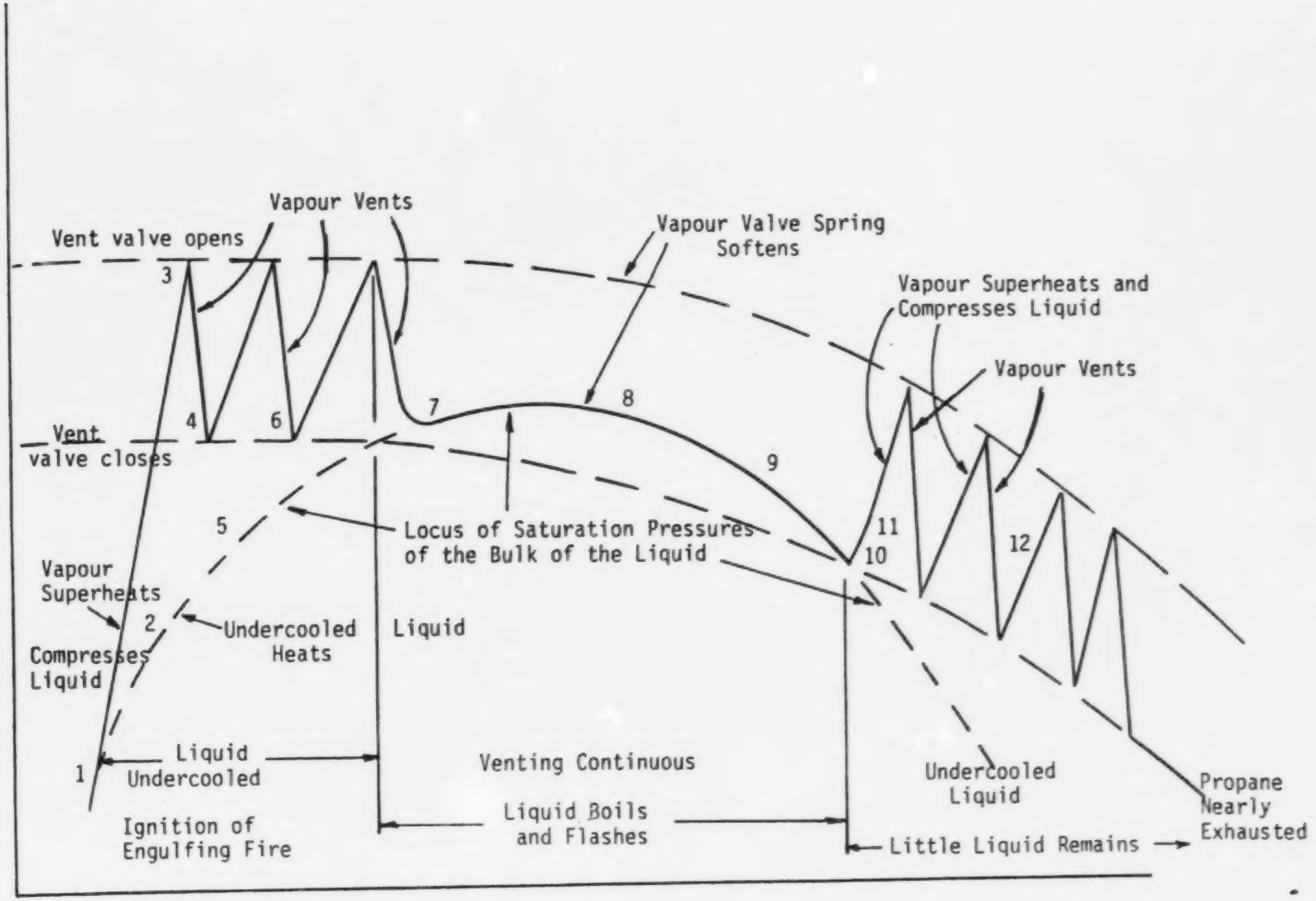
Vapour Vents
Vent valve opens
Vapour Valve Spring Softens
Vapour Superheats and Compresses Liquid
Vapour Vents
3
4
6
7
8
9
10
11
12
Vent valve closes
5
Locus of Saturation Pressures of the Bulk of the Liquid
Vapour Superheats
2
Undercooled Heats
Liquid
Compresses Liquid
1
Liquid Undercooled
Venting Continuous
Undercooled Liquid
Propane Nearly Exhausted
Ignition of Engulfing Fire
Liquid Boils and Flashes
Little Liquid Remains

FIGURE 2.3

In general, tank cars were equipped with monitoring equipment, filled with propane, (in some cases with EXPLOSAFE), and surrounded by a flaming pool of JP-4 fuel. Data were taken until either the tank failed or the propane fully boiled away. No data are available for the impinging torch case.

Results of the engulfing pool tests are discussed in the following Sections.

2.2 EXPLANATION OF OBSERVED SEQUENCE OF EVENTS

All of the tests of the propane filled tanks reported in TP 2740 [3] followed remarkably similar patterns. The sequence of events following ignition is seen in terms of pressure and time in Figures B-1 to B-5 inclusive in that Report. In the accompanying Figure 2.3 the general characteristics shown in all of the engulfment tests are apparent, including those both with and without EXPLOSAFE.

1. At the moment of ignition the tank was about 85% filled with liquid propane, the top 15% being filled with propane vapour. The liquid and vapour were in equilibrium at the saturated condition corresponding to the atmospheric temperature.

2. The engulfing fire begins to heat all of the outside surfaces of the tank.

3. Because the thermal capacity of the vapour is much smaller than that of the liquid, the vapour rises much more rapidly in temperature, as seen in the temperature data reported on pages 125 to 204 inclusive. The vapour space being closed, the pressure in the vapour space, and hence throughout the vessel, rises also. The vapour is in a superheated condition and the liquid is undercooled. This is a non-equilibrium condition and some of the vapour begins to condense onto the cooler liquid. The rate of heat transfer to the vapour remains higher than its rate of heat loss to the liquid, and the pressure and temperature of the superheated vapour continue to rise until the vent valve opening pressure of approximately 300 psi is reached.

4. The vent valve opens and superheated vapour is released. The pressure and temperature of the vapour fall as the remaining vapour in the vapour space expands, until the vent valve closing pressure of about 200 psi is reached.

5. The bulk of the liquid has at this point not yet risen to the saturation temperature of about 110°F corresponding to the 200 psi pressure, so the vapour remains slightly superheated with respect to the liquid, and no evaporation from the liquid surface takes place.

6. The heating continues and the vapour again rises in temperature and pressure until the vent valve opening pressure is again reached. The superheated vapour is vented, reducing the pressure and temperature in the vapour space. During this period, the temperature varies from point to point in the vapour space depending on the local heat transfer conditions. Some of the liquid near the heating surface will have risen in temperature to, or near to, the saturation temperature corresponding to the pressure and this warm liquid will have partially convected to the top. The bulk of the liquid will , however, still be well below the saturation temperature.

7. The vapour again superheats and vents, but by this time the upper surface of the liquid will have been heated to above the saturation temperature corresponding to the closing pressure of the vent valve. As the pressure falls nearly to this pressure, surface evaporation and some homogeneous nucleation and flashing of vapour from within the bulk of the warmest part of the liquid takes place. The rate of heat transfer to the liquid from the flame is now sufficient to maintain the pressure at a level above the valve closing pressure, and boiling becomes continuous on the heated surfaces of the liquid.

8. The spring in the vent valve is apparently temperature sensitive, and it "softens" as the tank metal temperatures rise. This causes it it open more widely at a given pressure and hence to allow the pressure to fall, even though the vapour generation rate may remain nearly constant. The opening and closing pressures are both correspondingly reduced. Some reduction in vapour generation rate may occur as the available boiling surface decreases as the liquid level falls.

9. The metal temperatures continue to rise, especially those near the top of the vessel as the vapour space grows; the cooling effect of the vapour being less than that of the liquid on the tank wall.

10. Failure may occur at this time as the metal weakens with increasing temperature and pressure, and hence the stress, remains high. As the vent valve spring weakens further,the pressure falls and the risk of failure decreases.

11. As the liquid boils away the available boiling surface is further reduced and the rate of vapour generation is no longer sufficient to keep even the weakened valve continuously open, and it closes.

12. The vapour rapidly superheats when the valve closes because there is much wall-to-vapour contact surface and high wall temperatures, and a further series of valve cycles follows until the liquid is exhausted.

2.3 INTERPRETATION OF TEST RESULTS

Although in the investigation of a complex phenomenon, such as a propane tank fire, there is never enough reliable physical evidence to meet all of the data requirements, our review of the Suffield tests reported in TP 2740 has provided us with a useful data base for the analysis of the events during an engulfment type of fire. Some comments on the specific component phenomena are included in this Section. Many of these phenomena can be understood only in relation to the thermodynamic state of the propane in the liquid and vapour spaces of the tank. To display the sequence of states observed we have plotted the observed data on Mollier (pressure-enthalpy) charts, displayed as Figures 2.4 to 2.9 in this report.

2.3.1 The Superheating and Vapour Venting Processes

The characteristic vapour superheating and venting process, described in overall terms in Section 2.2 and which occurs in the first two or three minutes, can be observed for each of the five complete engulfment trials; DRES Special, Howler, Nova, Diablo and Enigma. The data used to make these property variation plots for the superheated vapour states shown were taken from the pressure-time history curves reported in Figures B1 to B5 of TP 2740, and from the readings of the uppermost

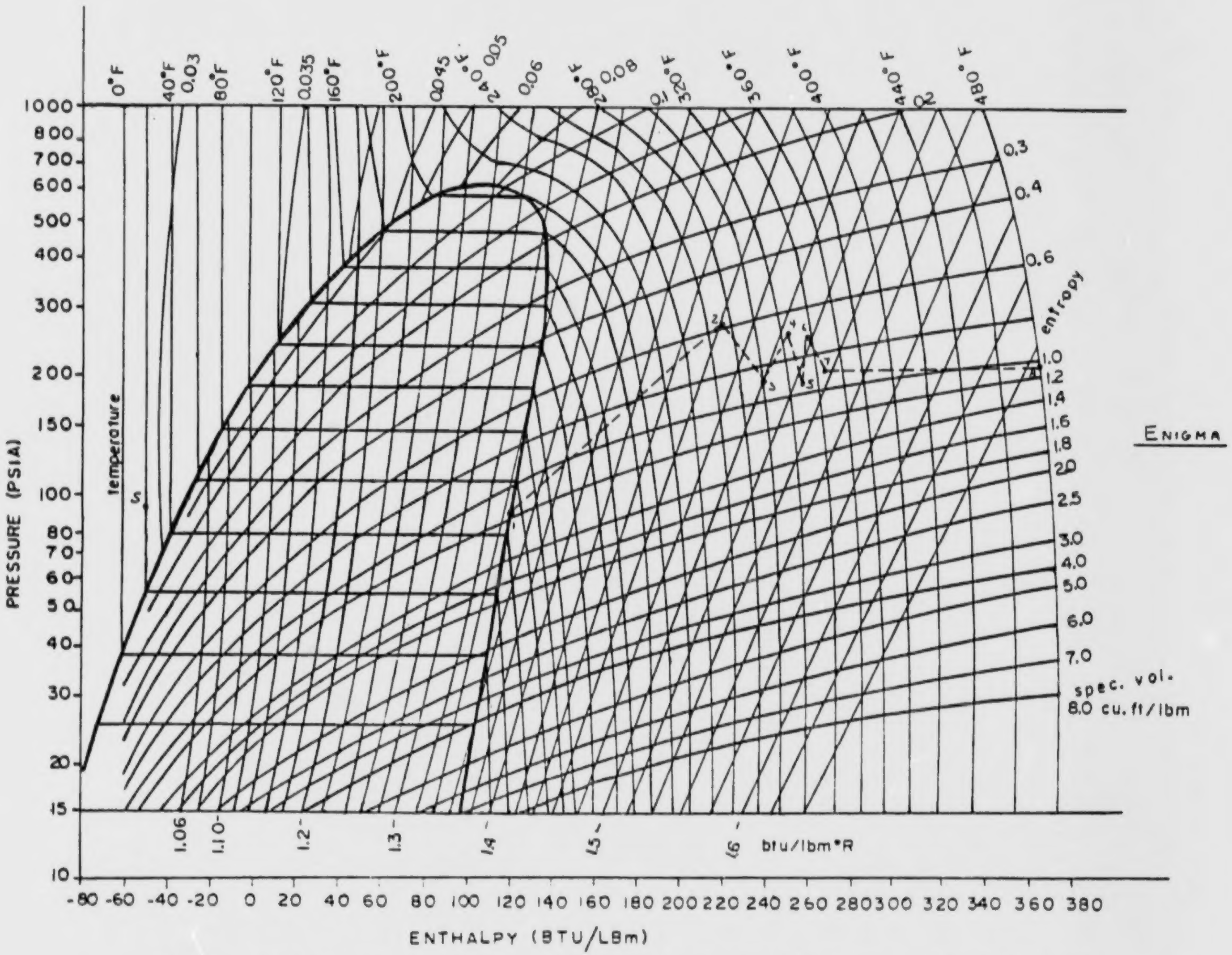

PROPANE MOLLIER DIAGRAM H=0 AND S=0 AT 0°R AND IDEAL GAS STATE

FIGURE 2.4

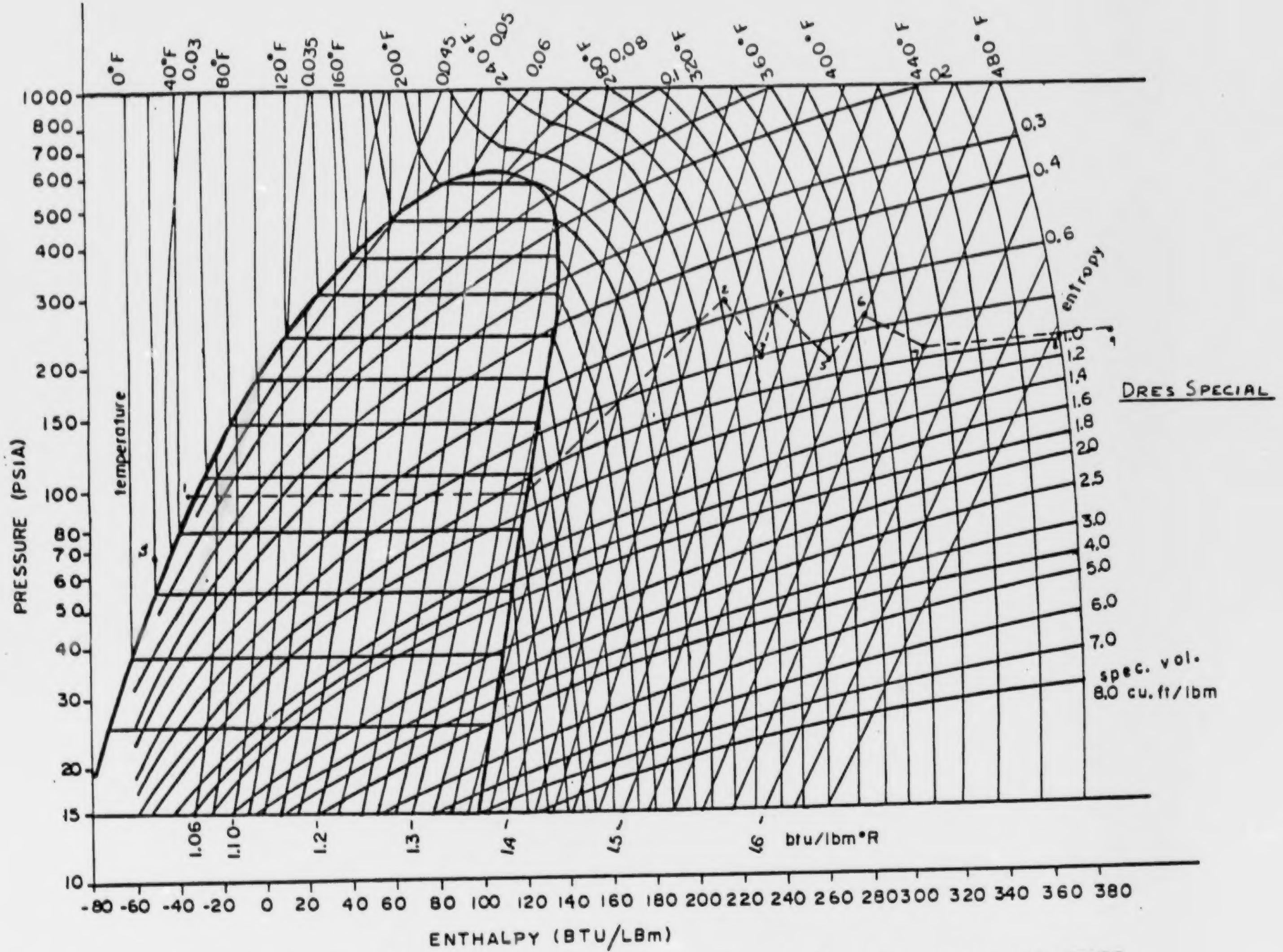

PROPANE MOLLIER DIAGRAM H=0 AND S=0 AT 0°R AND IDEAL GAS STATE

FIGURE 2.5

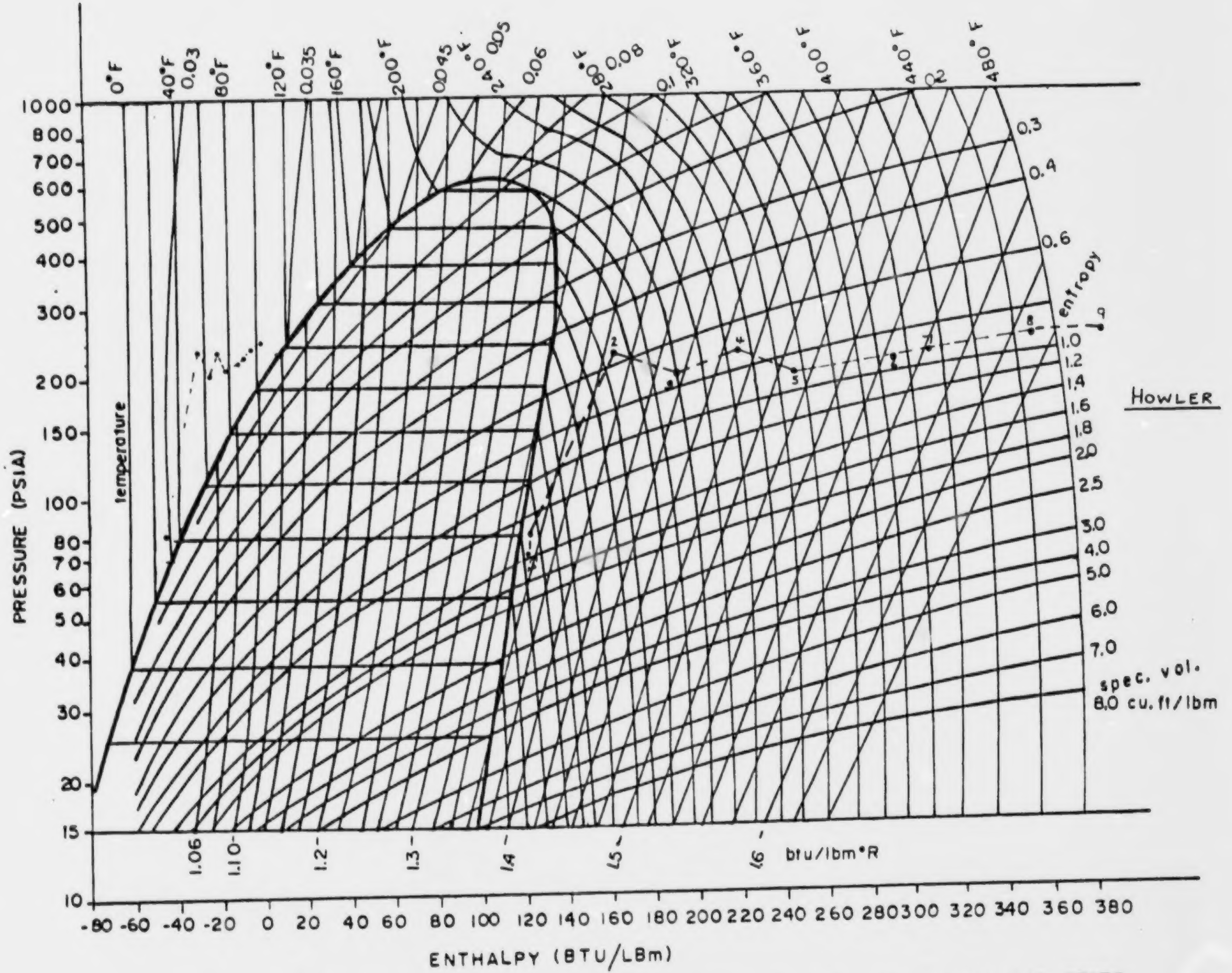

PROPANE MOLLIER DIAGRAM H=0 AND S=0 AT 0°R AND IDEAL GAS STATE

FIGURE 2.6

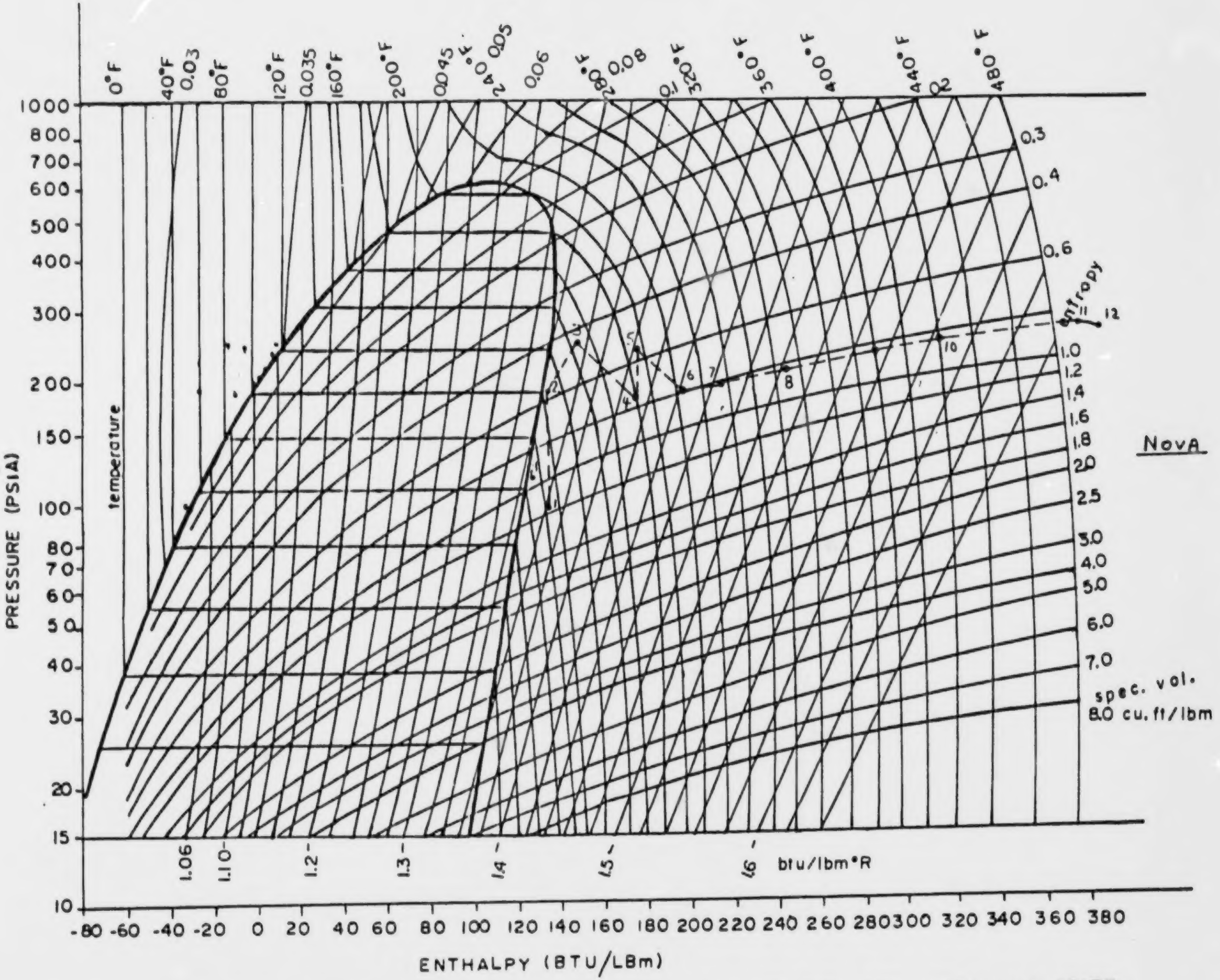

PROPANE MOLLIER DIAGRAM H=0 AND S=0 AT 0°R AND IDEAL GAS STATE

FIGURE 2.7

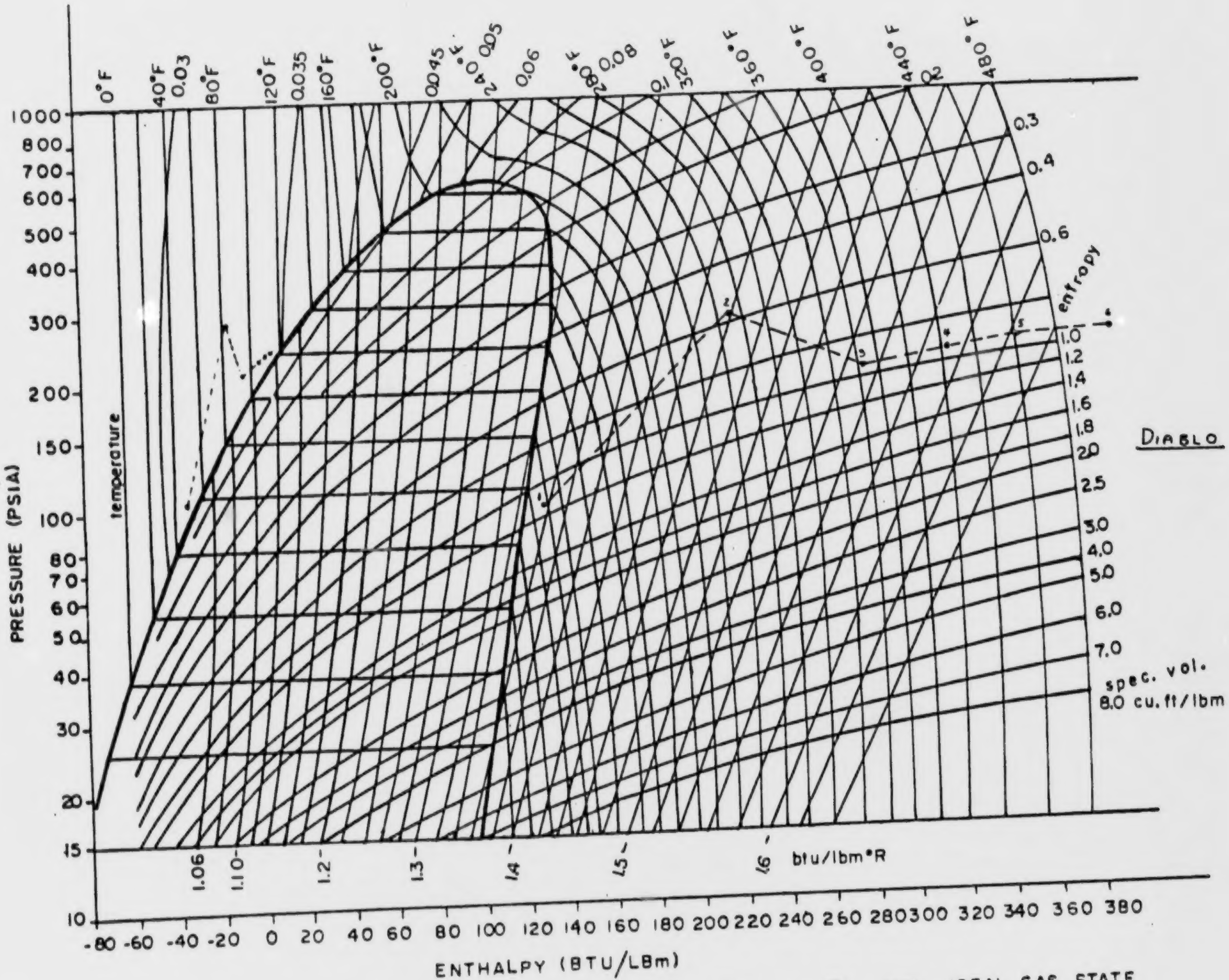

PROPANE MOLLIER DIAGRAM H=0 AND S=0 AT 0°R AND IDEAL GAS STATE

FIGURE 2.8

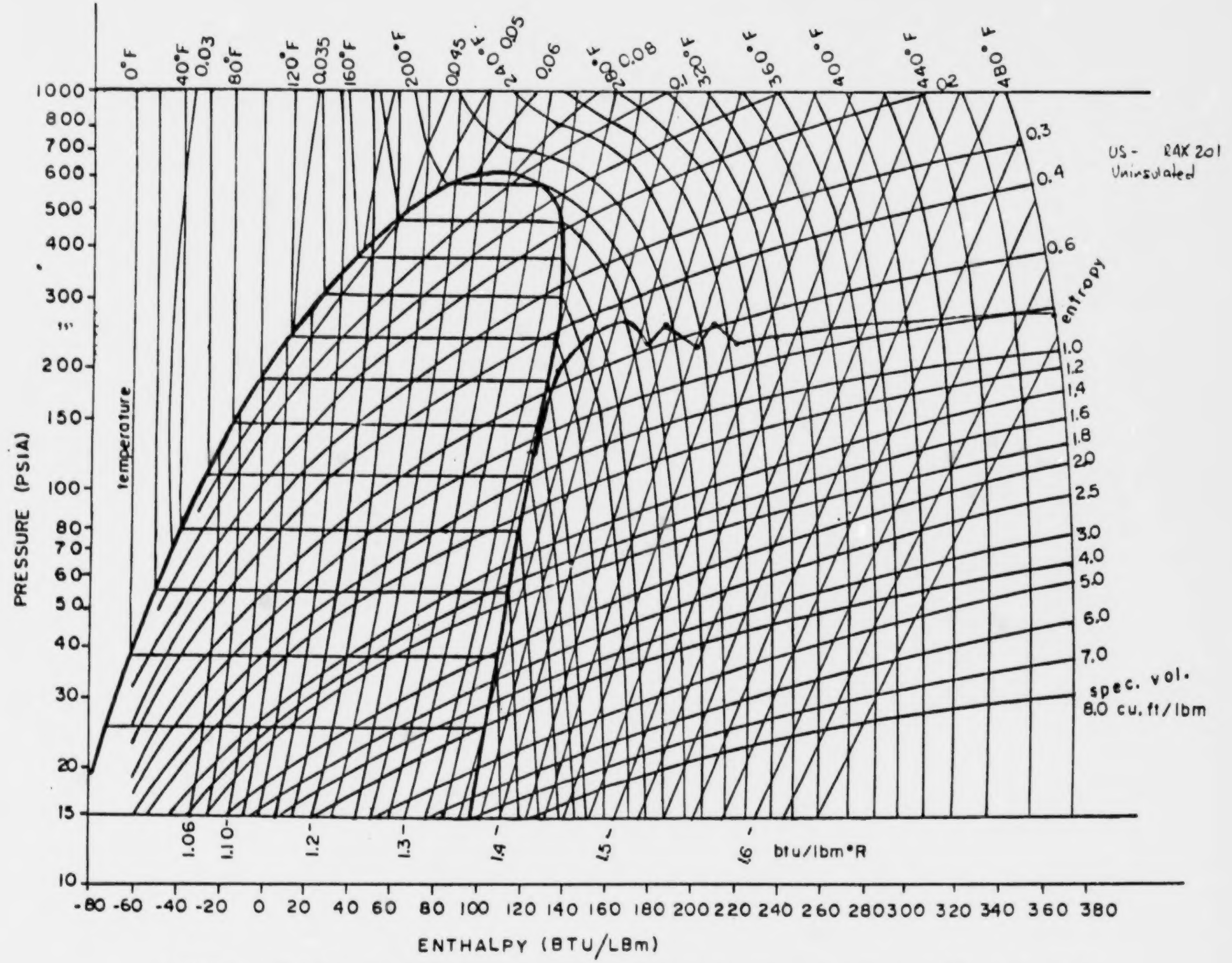

PROPANE MOLLIER DIAGRAM H=0 AND S=0 AT 0°R AND IDEAL GAS STATE

FIGURE 2.9

]

thermocouple in the vapour at corresponding times taken from the temperature cross-sections on pages 125 to 204. This provided the state of the vapour nearest to the vent valve inlet and represents, for the valve open condition, the state of the vented vapour.

In order to model these superheating and venting operations, their characteristic behaviour must be estimated. For the superheated operations, represented by the "rising temperature with rising pressure" segments, physically this is close to a constant entropy process for the vapour, although some evaporation or condensation may occur at the liquid surface. No boiling, and therefore no foaming or droplet release at the surface, would be expected.

However, in the initial stages of the engulfing fire, starting with a vapour space only about 15% of the total volume, the rapid warming of the liquid causes an expansion of the liquid volume and thereby a compression of the vapour volume. The result is that the first temperature and pressure rise operation approaches an adiabatic compression operation (in the limit, a constant entropy process) as seen in all five trials, but most clearly in the Howler and Nova cases.

As the liquid body approaches more nearly to a constant temperature limit, corresponding to saturation at the vent valve pressure relief setting, and as the venting process reduces the total volume of liquid in the tank and hence increases the volume of the vapour cushion, the compression effect is reduced. In the subsequent pressure rises, the heating processes in most cases approaches a constant volume heating operation (seen as constant specific volume).

Because the actual process involves both heat transfer and compression, and is certainly under non-equilibrium conditions, no simple assumption will be correct. However, by following the liquid expansion process for the first series of pressure rises, and assuming constant volume for subsequent pressure rises, we believe the model will approximate the real case, see also Section 6.3.18 for more detail.

DISCHARGE CHARACTERISTICS TO DETERMINE POLYTROPIC EXPONENT

TEST CASE	P_o (psig)	T_o (°F)	v_o (ft³/ lb_m)	P_c (psig)	T_c (°F)	V_c (ft ³/lb_m)	$\overline{T}^v$ (°F)	n
Enigma	265	272	0.59	185	300	0.90	286	0.85
	260	325	0.68	185	330	0.95	328	1.02
	255	338	0.72	195	345	0.90	342	0.97
Nova	257	138	0.45	188	180	0.75	159	0.61
	250	192	0.55	183	225	0.80	209	0.83
Dres	280	262	0.55	200	284	0.80	273	0.90
	273	305	0.61	200	335	0.90	320	0.80
	260	370	0.75	211	408	0.95	389	0.90
Diablo	280	270	0.58	196	365	0.95	318	0.72
Howler	220	172	0.57	182	220	0.84	196	0.84
	217	268	0.72	182	316	0.90	292	0.90
US-RAX201	275	180	0.47	242	198	0.59	189	0.56
(uninsulated)	273	215	0.53	239	235	0.65	225	0.65
	275	250	0.59	241	265	0.70	258	0.77

NOTES: P_o = valve open pressure; P_c = valve closing pressure
T_o = vapour temperature of opening; T_c = vapour temperature at closing; $\overline{T}^v$= average temperature
v_o = vapour specific volume at opening ; v_c = vapour specific volume at closing
n = polytropic exponent based on $P \cdot v^n = C$.

TABLE 2.1

For the falling pressure processes corresponding to the "vent valve open" periods, the residual superheated vapour in the vapour space expands as it pushes out the vented vapour. If this were rapid it might be expected to approach a reversible adiabatic expansion. In fact it is a relatively slow process and heat transfer to and from the surroundings can take place. For such cases, often encountered in reciprocating compressors and engines, a polytropic expansion curve of the form $pv^n = C$ is often found to fit the data. We have evaluated the polytropic exponent "n" for each of the initial series of venting operations for all the Suffield trials, and for one full scale test conducted in the U.S.A. The results are shown in Table 2.1 and the fourteen values plotted in Figure 2.10 as a function of the average temperature of the vapour in the vapour space T^V. For experimental data, the correlation is good. A least squares linear fit shows a correlation coefficient of 0.760, and gives support for the use of this relation in the model.

2.3.2 Homogeneous Boiling and Flashing

Under normal (equilibrium) conditions both the liquid and the vapour in a propane tank will be at saturated conditions. If the system is heated and the vent valve is opened, the pressure will drop below the saturation value corresponding to the previous equilibrium temperature, putting the liquid into a superheated condition. Flashing of a part of the liquid into vapour will sponteneously occur, from nucleation sites on the boundary or (homogeneously) in the bulk of the liquid.

In the present case, the rapid heating of the vapour and expansion of the liquid overpressures the liquid over almost all of the periods of blowdown. Only as the liquid heats up to temperatures above the saturation temperature corresponding to the minium vent valve setting would homogeneous nucleation and flashing occur. This point is noted in Figure 2.3, and the overpressure condition of the liquid is clearly seen on the Mollier diagrams for Diablo, Nova and Howler. Flashing does not play an important part in the engulfing flame events observed at Suffield.

2.3.3 Liquid Temperature Zoning

Following the time-temperature history in the liquid zones for any of the Suffield trials [3] shows considerable temperature differentials from point to point. These

VARIATION OF POLYTROPIC EXPONENT WITH
MEAN VAPOUR TEMPERATURE DURING TANK BLOWDOWN

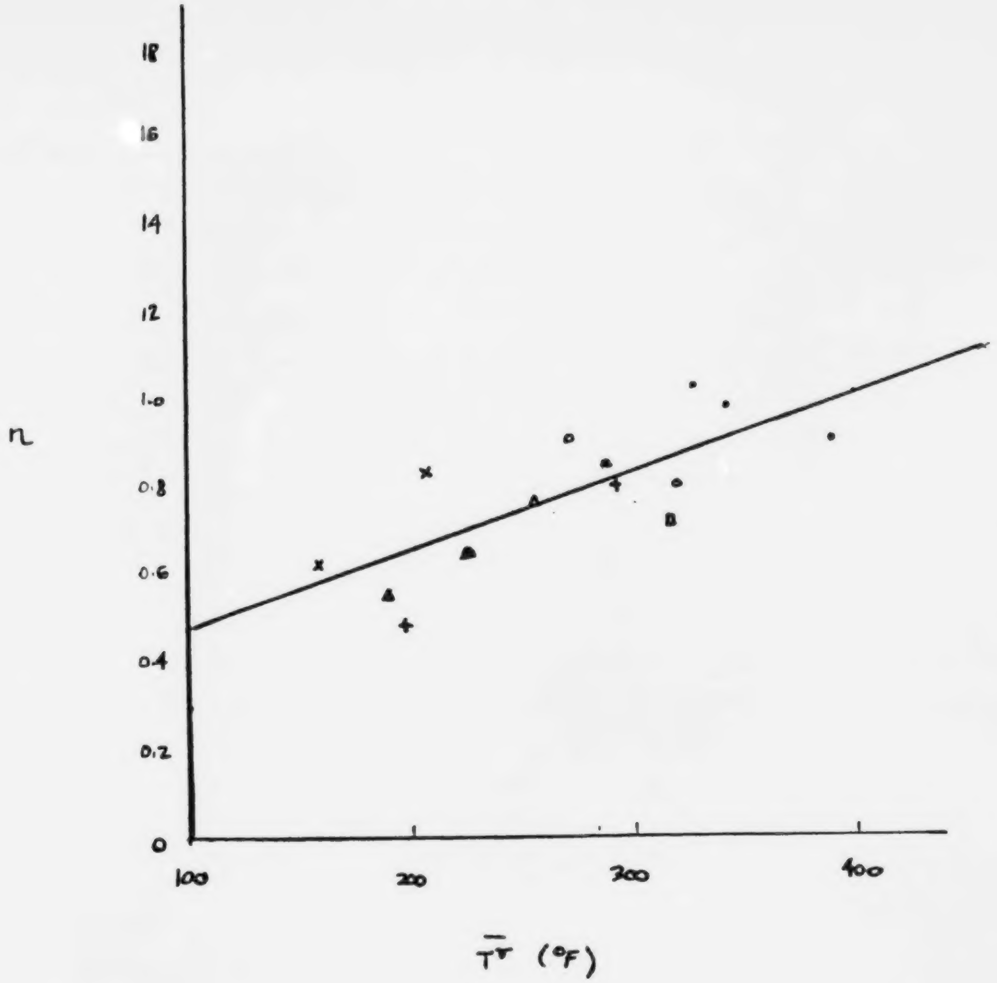

$$n = 1.773 \times 10^{-3} \cdot \bar{T}^{v} + 0.296$$

Correlation coefficient = 0.760

FIGURE 2.10

TEMPERATURES IN VAPOUR SPACE

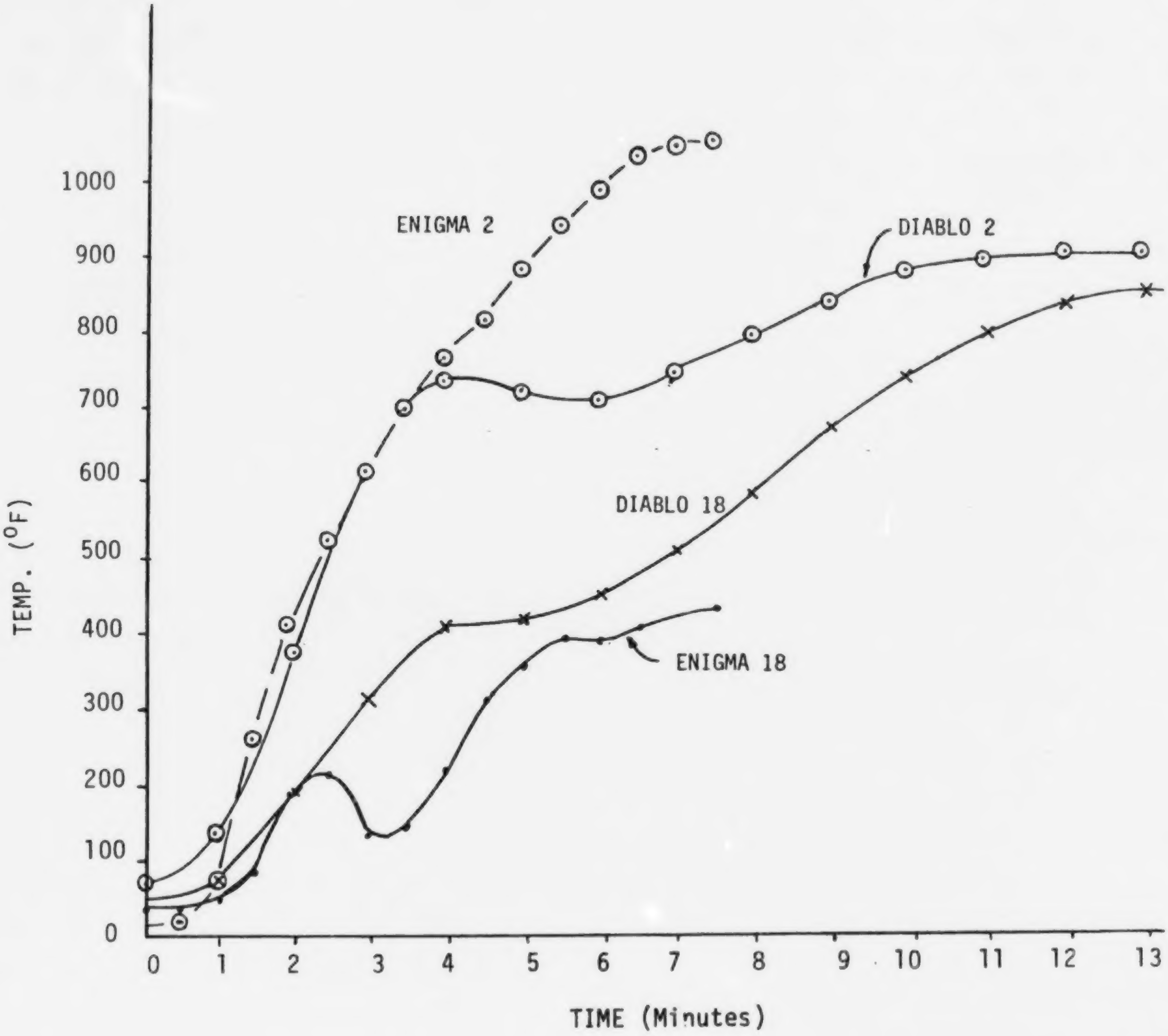

FIGURE 2.11

temperature differentials are much more persistent in the tanks in which EXPLOSAFE was fitted, apparently due to the inhibition of natural circulation in the liquid by the matrix of aluminum.

Examination in detail shows that a cool zone, at well below the saturation temperature persists in the zone most remote from the walls for at least 13 minutes after ignition. This is very near the end of the process and it indicates the need to consider this factor in the model.

It is apparent that mixing of the saturated liquid near the walls and at the surface is the process by which the cool zone is heated. To model the process, it is apparent that at least two zones of the liquid must be identified, and a mixing coefficient established to represent the temperature (heat) diffusion mechanism. These coefficients will clearly be different in cases with and without EXPLOSAFE fitted.

2.3.4 Temperature Gradients in the Vapour

Strong temperature gradients are observed in the superheated vapour, both with and without EXPLOSAFE present. The observed gradients are functions of the heat transfer rates in the space and depend as well upon the radiation within the space. Very little radiant interchange can be expected for cases in which EXPLOSAFE fills the volume. In the absence of EXPLOSAFE, radiation plays an important role. Some of the differences between the Enigma condition (no EXPLOSAFE) and the Diablo condition (with EXPLOSAFE) can be seen in Figure 2.11, which shows the temperatures on the tank surface adjacent to the vapour space (2) and those at a point a small distance from the wall (18). Further evidence of the difference is seen in Figure 2.12.

The interpretation of this information is complex, since both radiation and convection effects are present, but it is clear that differences are too big to be ignored. The model should include both radiation and convective components within this space.

VAPOUR SPACE TEMPERATURE GRADIENTS

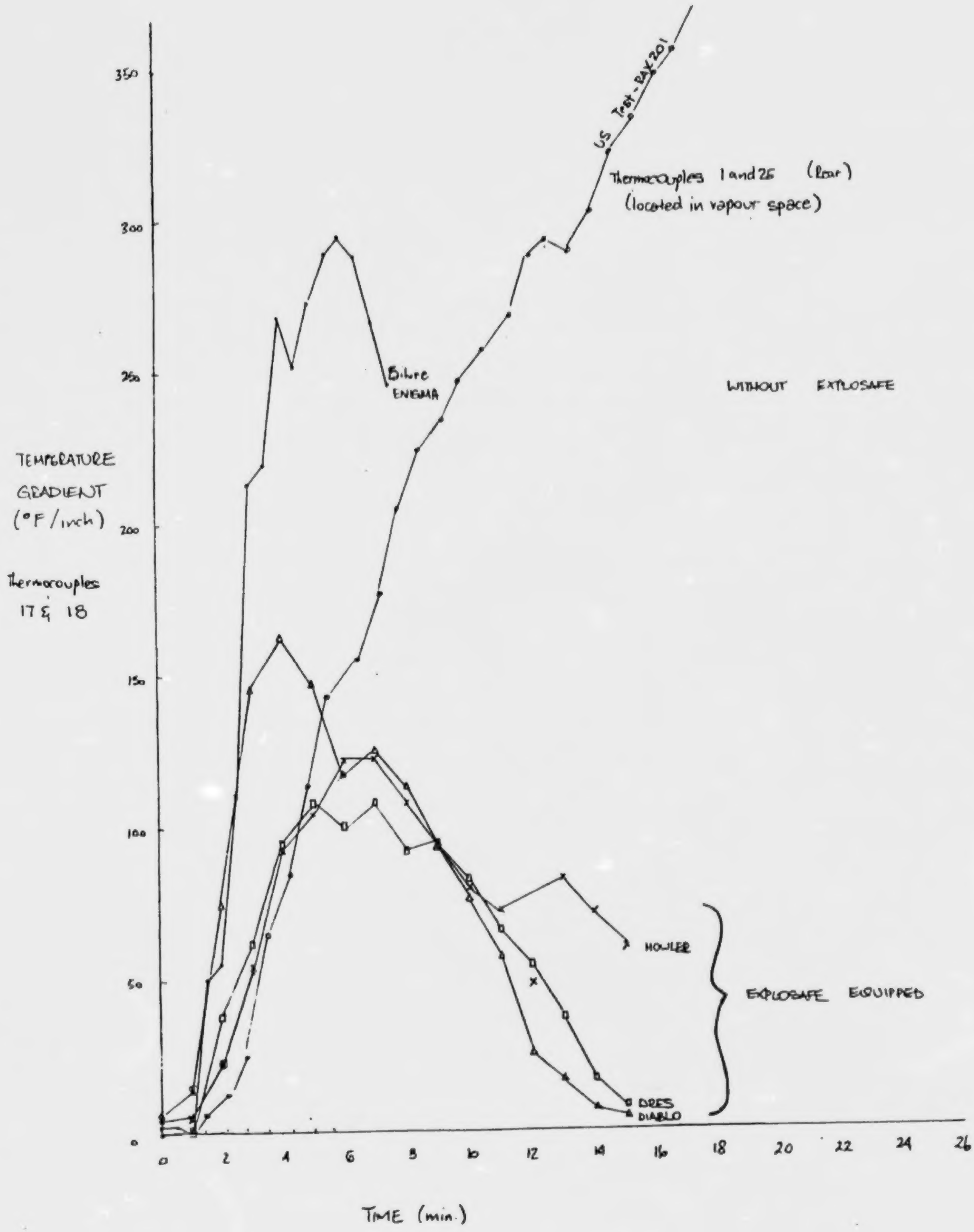

FIGURE 2.12

2.3.5 Liquid Level Effects

Because the heat transfer rate is greater from the wall to the liquid than from the wall to the vapour, the wall temperatures are observed to be much higher adjacent to the vapour zone. This makes it almost certain that tank failure would be initiated in the vapour region of the vessel. It also indicates that a bending or "hogging" of the tank due to thermal expansion occurs and that if it is restrained, additional stresses would develop in the walls. Provisions should be made to account for point-to-point variations in heat transfer at the wall and for lateral wall conduction in order to differentiate between the hazards of failure associated with different thermal insulation or between other alternative designs of the tank car.

The liquid level can be inferred from the point of step change in the wall temperatures or from the point in the liquid at which the temperature increases above the saturated value. For most of the Suffield tests, these two criteria do not give agreement. This would appear to be due either to vapour droplets holding the vapour space near the liquid surface to the saturation temperature or to a departure from the nucleate boiling curve at that point on the tank wall due to the angle of surface or some other effect in the propane. If the latter is true, it has important implications for the case of intense impinging flames. The need for boiling curve data for propane on surfaces with EXPLOSAFE fitted is further emphasized.

2.3.6 Pressure Relief Valve Operation

The opening and closing set points, and the flow capacity of the tank vent valve are of great importance. The valves in the Suffield trials appear to have functioned well, except in all cases, they displayed dropping values of the opening and closing pressures as the test proceeded. This effect has a substantial influence on the course of the test and could have controlled whether or not failure occurred in some of the tests.

In Section 4 the vent valve function is discussed in more detail.

3.0 THE ROLE OF EXPLOSAFE IN RAIL TANK CAR FIRES

In order to assist in the development of the model concept and the formulation of the model into a mathematically convenient form, and to appropriately incorporate into the model the effects that EXPLOSAFE has on the thermodynamic processes, a qualitative boiling test was performed, allowing both field and lab bench tests to be more fully interpreted.

3.1 NOTES ON A PRELIMINARY QUALITATIVE COMPARATIVE BOILING TEST WITH AND WITHOUT EXPLOSAFE

A limited laboratory experiment was carried out in the following manner. An EXPLOSAFE sample was prepared (approx. 6.1 kg/m^3 density) to fit into a one litre Pyrex beaker which was subsequently filled, to about three-quarters of the total volume, with city water. The water was brought to a boil and the behaviour noted. The EXPLOSAFE was removed and the test was repeated. The comparative observations noted are discussed below.

Without EXPLOSAFE	With EXPLOSAFE
- vapour bubble sizes were relatively large during boiling	- vapour bubble sizes were noticeably much smaller during boiling
- at "rolling" boil the surface of the water was greatly agitated	- at corresponding conditions the surface of the water was much less agitated
- bubble motion showed the liquid motion to be quite turbulent	- bubble motion showed much slower and less turbulent liquid motion
- there was much foaming and priming at the suface, and clouds of droplets were sprayed upward	- the intensity of the foaming and droplet spray was much lower
- during the heating up period, prior to boiling, dissolved gases formed bubbles which rose to the surface of the liquid and left	- during the heating up period, prior to boiling, the gas bubbles mostly adhered to the aluminum surfaces and did not leave the liquid
- during boiling the vapour bubbles were more or less uniformaly distributed across the beaker	- during boiling the vapour bubbles tended to move up the beaker walls to the surface.

3.2 RELEVANT CHARACTERISTICS OF EXPLOSAFE

The Suffield field trials, our own preliminary boiling tests, and rational considerations of the heat transfer and fluid mechanics effect, indicate that EXPLOSAFE influences the fire exposure event in a complex manner. Some of these effects are noted below.

1. We have shown that the temperature gradients in the vapour during the Suffield trials were lower with EXPLOSAFE than without, see Figures 2.11 and 2.12. This appears to be a complex effect, probably involving radiation within the vapour space, the reduction of vapour circulation, and the droplet release from the surface of the liquid during venting periods.

2. The EXPLOSAFE probably thickens the boundary layer at the liquid-metal surface, reducing the heat transfer rate by liquid conduction and by liquid convection, but increases the rate of heat transfer from the surface into the liquid by metallic conduction. The relative magnitude of these effects should be investigated in the proposed boiling curve experiments. Contact pressure of the EXPLOSAFE will be a factor to consider.

3. EXPLOSAFE will lead to the onset of the departure from nucleate boiling (also called the boiling crisis or the burnout point) at a lower heat flux but not necessarily at an earlier time, by inhibiting the vapour bubble departure from the surface. This was not an apparent factor in the tests at the field trials at Suffield. However, in other conditions, such as would occur with local impinging flames or in very intense fires, this would be expected to be a factor. The need to determine the effect of EXPLOSAFE on the departure from nucleate boiling by boiling experiments is clear.

4. The EXPLOSAFE reduces the intensity of turbulence at the liquid-vapour interface, reducing the number of droplets of liquid thrown into the vapour space. These droplets in the vapour space would tend to reduce the superheat in the vapour and raise the apparent value of the specific heat of the vapour. This, in turn, will effect the temperature-pressure relation in the vapour during relief valve operation.

5. EXPLOSAFE can be expected to reduce the circulation and mixing rate in the bulk of the liquid, and so give rise to greater temperature differences and temperature gradients in the liquid.

6. Other factors concerning EXPLOSAFE include its ability to reduce the flame speed in a combustion explosion of air and vapour in a tank, reducing the severity of the explosion. It could also absorb some of the energy of the expanding vapour or gas during a BLEVE or a combustion explosion.

7. Some concern for the melting point of aluminum must be shown. Howler showed wall temperatures of 695 to 716 °C at 15 minutes, whereas the melting point of aluminum is 660 °C. With impinging flames, as burnout is approached, any aluminum in contact with the wall at the hot spot would certainly melt.

8. The EXPLOSAFE undoubtedly supplies an abundance of nucleation sites for bubble formation during homogeneous nucleation as flashing occurs from the bulk of the saturated liquid during pressure falls as the vent valve discharges vapour. Without EXPLOSAFE, nucleation might be expected to occur mainly at the tank wall.

9. From the visual evidence of the preliminary boiling tests we conducted and from a general appreciation of the characteristic behaviour of fluids in the spaces above boiling and flashing liquids, it can be assumed that almost no droplets would penetrate the EXPLOSAFE to the vent valve entry. The leaving vapour when EXPLOSAFE is present will always have a quality of unity and will generally be superheated. This is in contrast to the case without EXPLOSAFE, since during the boiling and flashing periods clouds of droplets will enter the vapour space. This will increase the density of the discharged vapour and reduce its quality and enthalpy, leading to a more rapid evacuation of the propane from tanks without EXPLOSAFE even at the

same rates of heat transfer to the tank. The response rate of the temperature sensors fitted to the test vessels was releatively slow and this effect would be expected to be obscured in the temperature readouts.

4.0 VENT VALVE CHARACTERISTICS

The dynamic behaviour of a pressure relief valve under tank car fire conditions is very complex. Mass discharge rates and the valve open and close set point characteristics which are required for the model, depend upon the fluid properties, temperature, pressure, time, and the specific design of the valve. The vapour fraction (quality) of the fluid discharged is difficult to measure on a laboratory-scale test, let alone on a full-scale field trial. No field data are available from the field trials which can be used to determine this quantity. It has been argued in Section 3.0, that EXPLOSAFE will affect the fluid quality and reduce the rate at which mass is discharged through the valve. Variations in the quality of the exiting fluid will have a significant impact on the time to safe blowdown or failure of the tank car. This Section addresses these concerns and presents a proposed method for modelling PRV operations.

4.1 MASS DISCHARGE RATES

Considerable work has been performed in determining flows through orifices and valves. Investigations which are relevant to the study of propane-laden rail tank cars have been undertaken at the University of Maryland. D.W. Sallet and others have been studying PRV operation through laboratory and analytical work for a number of years under the sponsorship of the U.S. Department of Transportation [10 to 23]. Guidelines for the sizing of PRV's are being developed for this and other applications [10, 11].

It is possible to define five cases which are useful in describing the mass efflux rates through a PRV. Figure 4.1 shows that the PRV can either be submerged or in the vapour space. In the latter case, the efflux can be expected to be primarily vapour when the liquid/vapour boundary is far from the PRV. On the other hand, if the boundary is close to the PRV and the liquid is boiling, with propane droplets being flung into the vapour space, then the quality is low. If submerged, the fluid on the high pressure side of the PRV is of zero-quality (100% liquid). Depending upon the design of the valve, boiling can occur at various locations in the PRV as the pressure drops as the fluid flows to atmosphere. That is, the flow can either be single-phase liquid, single-phase vapour, or two-phase.

MASS DISCHARGE THROUGH PRV

- Various Cases -

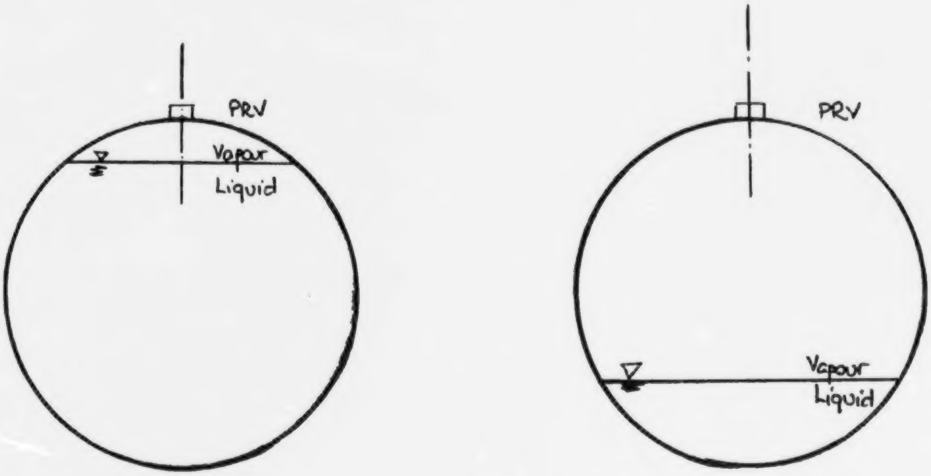
PRV
Vapour
Liquid
PRV
Vapour
Liquid

Case 1: Low quality efflux G_{v_2}

Case 2: High quality efflux G_v

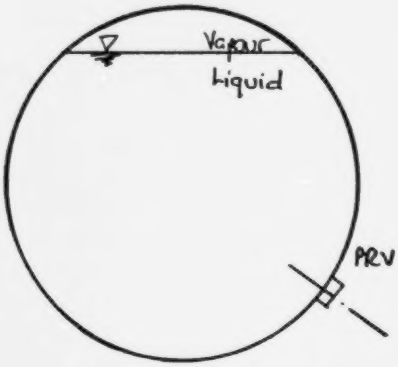
Vapour
Liquid
PRV

Case 3: no phase change, G_ℓ

Case 4: two-phase flow in valve passages, G_{ℓ_2}

Case 5: single phase vapour through valve, G_f

FIGURE 4.1

It would be difficult to separate cases 1 and 2 as no data exists from which it would be possible to calculate the variation in fluid quality with the distance from the PRV to the liquid surface. This quality will depend upon the rate of boiling and of course whether EXPLOSAFE is installed. The efflux rate, assuming 100% vapour, can be determined using the analysis of Sallet et al. [10],

$$\dot{m}_v = \rho^v A^* \cdot P \cdot (k \cdot (2/(k+1))^{(k+1)/(k-1)})/(ZRT/M_o g_c)^{\frac{1}{2}} \qquad (1)$$

where

A^* = critical valve section area

P = system pressure

k = C_p/C_v

M_o = molecular weight of propane

g_c = dimensional constant

Z = compressibility factor

R = universal gas constant

If the fluid is solely liquid flowing through the valve, then the efflux rate is,

$$\dot{m}_\ell = \rho^\ell \cdot A^* \cdot \left[\frac{2g(P-P_{atm})}{\gamma} + \Delta z\right]^{\frac{1}{2}} \qquad (2)$$

These flowrates set the lower and upper limits for the valve. A rough estimate of the flow through the valve if the quality, χ, is $0<\chi<1$, would be,

$$\dot{m}_T = \chi \cdot \dot{m}_v + (1-\chi) \cdot \dot{m}_\ell \qquad (3)$$

It is difficult to provide a useful definition of the quality. It should be noted that the tank-car/propane system is not in equilibrium throughout the fire. This is evident from the fact that the vapour is generally superheated, with the liquid phase being sub-cooled at times. A fluid quality is most properly defined when the system is at equilibrium.

As the engulfing pool fire model is a two-phase model, it is proposed that the efflux equations (1 and 2) be used to determine the flow through the PRV when it is located either above or below the liquid surface, respectively. As the "jury" is still out in the development of more comprehensive PRV models, accounting for variable fluid conditions, see Sallet [9], it is recommended that this approach be taken, that these developments be monitored, and that the overall model be designed to accomodate modifications to the PRV model.

4.2 VALVE OPEN AND CLOSE SET POINTS

It is clear from the experimental evidence that the open and close set points on the valve change throughout the fire. That is, the valve opens and closes at progressively smaller values of the pressure. As the vapour temperature increases throughout the event, this set point variation is both temperature and time dependent. For the proposed models which are more fully discussed in the following Sections, a function expressing this variation is to be supplied, that is,

$$P_o = P_o(T^v, t) \text{ and } P_c = P_c(T^v, t).$$

A careful examination of the valve spring material and the particular valve design (valve is in or out of the vapour space), as well as a detailed review of the Suffield and U.S. trials on this specific aspect of the problem would be necessary to determine the functional form for these variables.

5.0 THE MODEL CONCEPT

Models can prove to be useful tools for the quantitative analysis of complex systems. The sensitivity of a system to variations in the driving functions and the descriptive variables can be studied with a flexible model. The optimization of a design can be facilitated by modelling the system over the sensitive range of variables identified previously. A suitable model can often provide a designer with technically superior performance and a more cost-effective approach to complex system design than obtainable from a direct prototype development program. Properly used, modelling and prototype development activities can be merged to achieve reliable and cost-effective products within given time and cost constraints.

5.1 MODEL BUILDING

The model building process can generally be described by the block diagram presented as Figure 5.1. The most critical element in model building involves developing concepts of the physical system. This requires experience and imagination. This task is greatly aided by the availability of experimental evidence, which can be used to test hypotheses which are proposed as the concepts are being built. It is clear from this diagram that the validity of the end product, the numerical formulation of the model, is dependent upon the initial model concepts. It is for this reason that considerable effort during this project has been expended reviewing the experimental evidence and the available literature to develop supportable concepts of the system. These are then expressed mathematically (Section 6.0), and can then be developed into a numerical version of the model.

The program for model development, as described in the RFP and the terms of reference, places the emphasis of this Phase of the work on concept development and formulation of the mathematical relations describing the system. This process has been greatly assisted by the availability of test data which have clarified the system concepts.

It is evident from the available data that the rail tank car under fire conditions is a complex, dynamic system. As numerical models are not subject to many of the restrictive assumptions required for analytical solutions, a numerical approach has been selected. This means that the time-varying boundary conditions and initial

FIGURE 5.1 MODEL BUILDING

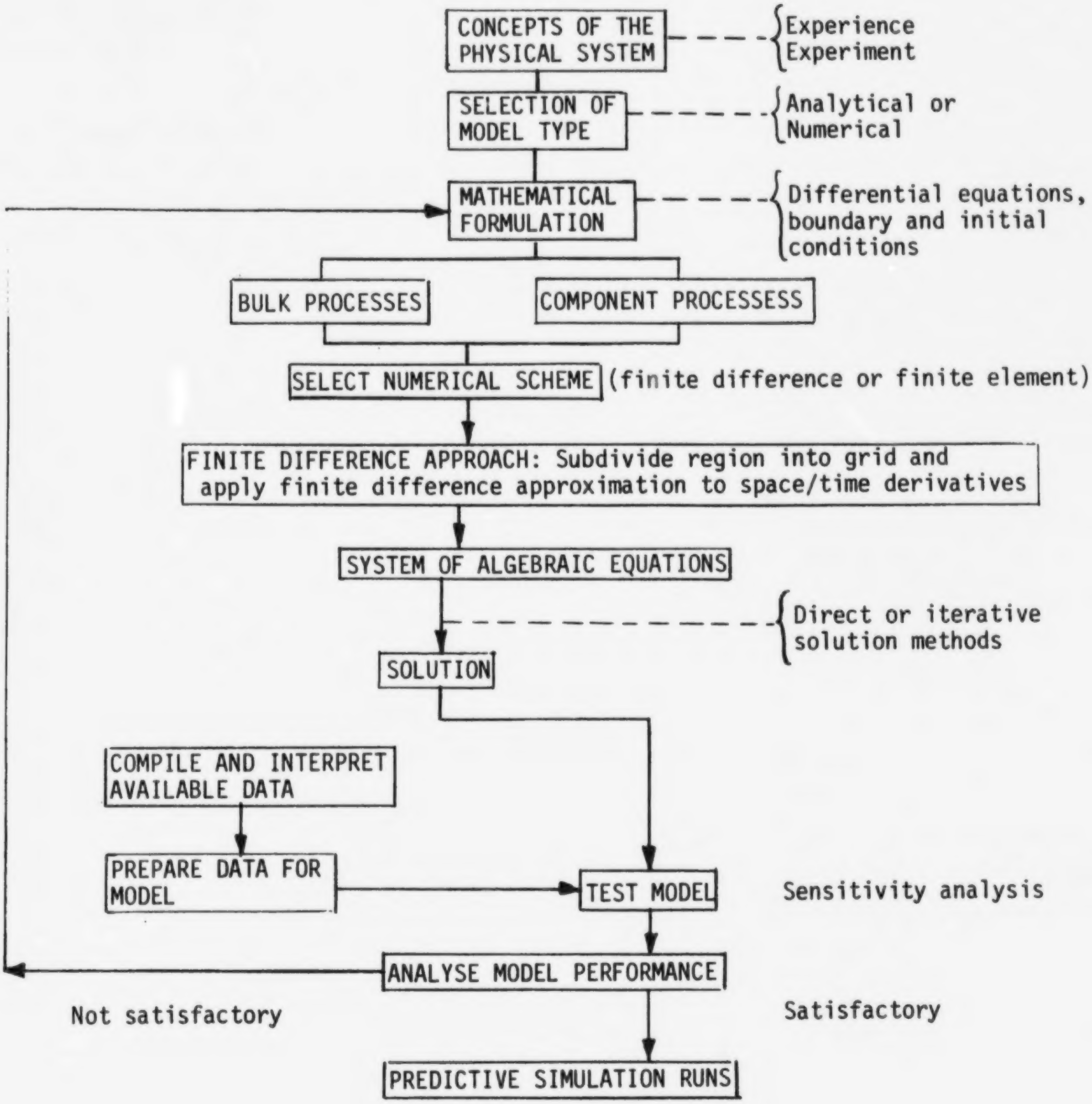
CONCEPTS OF THE PHYSICAL SYSTEM
Experience
Experiment
SELECTION OF MODEL TYPE
Analytical or Numerical
MATHEMATICAL FORMULATION
Differential equations, boundary and initial conditions
BULK PROCESSES
COMPONENT PROCESSESS
SELECT NUMERICAL SCHEME
(finite difference or finite element)
FINITE DIFFERENCE APPROACH: Subdivide region into grid and apply finite difference approximation to space/time derivatives
SYSTEM OF ALGEBRAIC EQUATIONS
Direct or iterative solution methods
SOLUTION
COMPILE AND INTERPRET AVAILABLE DATA
PREPARE DATA FOR MODEL
TEST MODEL
Sensitivity analysis
ANALYSE MODEL PERFORMANCE
Not satisfactory
Satisfactory
PREDICTIVE SIMULATION RUNS

processes are described at discrete points in time. This feature permits the modelling of rapidly varying conditions, and discontinuous processes such as intermittent tank blowdown, which would be otherwise impossible to predict using an analytical approach.

Two levels of complexity have been considered in formulating the models, these relate to bulk and component processes. Bulk behaviour is determined by relating the behaviour of the components through the bulk model. For example, system pressure and the representative temperatures of the vapour and liquid phases (bulk parameters) are functions of the rates at which heat is gained and lost by these respective bodies and the state of the pressure relief valve. These, in turn, depend upon a host of other factors with time varying properties.

The next step in building the rail tank car model involves detailing the relationships between the respective process models in a manner congruent with the model logic presented in Section 6.0. Additionally, the component models are detailed. This forms a set of equations which is then coded and packaged as a computer program. Thus, a solution exists, but must be tested and refined before it can be used as a design tool.

5.2 MODEL OBJECTIVES

The overall objective of the model development activity is to prepare an analysis tool to be used in quantitatively evaluating protective systems for propane laden rail tank cars under fire conditions. These systems specifically include thermal insulation and EXPLOSAFE. The model must describe the effect that EXPLOSAFE has on the system throughout the events from initiation to termination of the fire or tank failure.

The internal tank pressure and shell temperatures must be predicted by the model in order to determine the shell stresses. These stresses are to be compared against the failure criteria and the time to failure predicted. Predicting the time to failure is an important objective of the model as this is the principal measure of the success of a particular protective system.

TABLE 5.1 MODEL FEATURES

Engulfing Flame Model

- fully transient
- variable fluid properties
- variable fire temperatures
- mass and heat exchange across vapour/liquid boundary
- protective system configuration; bare tank, EXPLOSAFE, insulation, EXPLOSAFE and insulation
- thermal degradation of protective systems (insulation and EXPLOSAFE)
- variable pressure relief valve open and close set points
- two-phase flow through pressure relief valve
- effect of sub-cooling of liquid phase
- fluid mixing
- variable internal heat transfer coefficients
- radiation heat transfer in vapour space with and without EXPLOSAFE
- radiation heat ransfer to tank top from propane plume
- two-dimensional analysis with a fully three-dimensional model as a longer term objective:
    - 3-D model - longitudinal variation in heating input
      - enhanced heat transfer due to surface fins
      - longitudinal fluid mixing
      - tank pitch effects on tank shell temperatures
- tank roll
- flexible configuration of nodal network with shell temperature distribution resolution variable
- location of time and point of failure
- adaptable to shell materials with arbitary temperature-strength relationships
- adaptable to various shell thickness distributions

5.3 MODEL FEATURES

In order to predict the behaviour of the lading tank car system under wide-ranging, dynamic circumstances, the model concept has been developed to include a number of important features. Table 5.1 lists these features.

Two fire conditions have been considered, defining specific types of rail car fires involving propane. These are the engulfing pool fire and the impinging torch fire. In the former instance, a volatile liquid spills around an immobile tank car and, with liquid ignition, the car becomes almost totally engulfed by flames. At some point during the accident, the pressure relief valve will be triggered, releasing a cloud of propane which will be ignited. As the engulfing flame and torch fire represent two types of accidents which differ in mechanism, separate models have been proposed, Section 5.6 and 5.7. For the case in which both an engulfing flame and a torch fire occurs, or when a torch fire impinges upon a large area of the tank car, a more generalized model is proposed, Section 5.8.

5.3.1 Engulfing Flame Model

With temperatures and pressures varying considerably during the accident, fluid properties change accordingly. This is a necessary feature of the model. For example, the thermal expansion of both liquid and vapour are accounted for in this manner.

Both mass and heat exchange can occur across the boundary between the liquid and vapour phases. Evaporation and condensation are addressed.

The model features two types of "passive" protective systems, EXPLOSAFE and insulation (the insulation can be either internally or externally mounted). Four configurations are listed, with the thickness of the protection as a variable. High temperatures can have a deleterious effect upon the performance of the protective systems. Such effects can be accomodated in the model.

The pressure relief valve (PRV) is an "active" protection system. In a previous Section it was shown that the valve open and close set points vary throughout the accident. Variable PRV set points are featured. In addition, the model includes the effect of two-phase flow through the PRV.

TABLE 5.2 MODEL FEATURES

Impinging Torch Model

- fully transient
- variable fluid properties
- protective system configuration; bare tank, EXPLOSAFE, insulation, EXPLOSAFE and insulation
- thermal degradation of protective system (insulation and EXPLOSAFE)
- effect of sub-cooling of liquid phase
- variable internal heat transfer coefficients
- two-dimensional analysis
- pitch and roll
- assessment of type of failure

The experimental evidence from the field trials shows that a substantial zone within the liquid remains subcooled after the liquid near the heated boundary reaches saturation. There are significant differences in heat and mass transfer rates between the subcooled and saturated conditions, and significant differences in the temperature and extent of the subcooled zone at a given time between EXPLOSAFE and non-EXPLOSAFE filled cases. In order to differentiate between these relevant effects, the liquid zone was divided into two zones. The sub-cooled core zone is progressively reduced in size by thermal mixing as events proceed, eventually merging into the saturated zone.

Tank cars equipped with EXPLOSAFE are expected to have internal heat transfer coefficients considerably different from those of the tank car without EXPLOSAFE. A description of the relevant heat transfer processes featured in the model is given in Section 5.4.

The proposed model is two-dimensional, representing a typical cross-section of the tank, and offers a flexible nodal configuration network so that shell temperatures can be determined at variable spacing and so that external heating conditions and liquid level effects can be more accurately described. This two-dimensional aspect permits a progressive correlation between experiment and model, as the position of the liquid level can be determined by comparing model liquid node temperatures with field thermocouple measurements. Additionally, any roll of the tank following derailment can be accounted for as the valve position can be assigned to any point about the circumference of the shell with this model.

Insights gained during the development of the two-dimensional model will aid in the development of a three-dimensional model, a longer term objective. Such a model could incorporate a number of features which cannot be offered with a two-dimensional version, these being listed in Table 5.1.

Whenever the failure criteria, stated as a function of both pressure and temperature, is exceeded, failure occurs. The time to failure and the point of failure can be determined with the model.

5.3.2 Impinging Torch Models

The torch models share some features of the engulfing flame model, but in other respects are quite different. See Table 5.2. A full description of these models is presented in Sections 5.6 and 5.7.

5.4 HEAT TRANSFER PROCESSES

The rate at which heat is transferred into the lading-tank car system is governed by the heat transfer mechanisms listed in Table 5.3. These processes are complex and are interrelated. For example, the heat externally supplied by the fire is transferred by convection and radiation, and depends upon the combustion characteristics of the flame and the surface temperature of the tank car.

These processes are incorporated in the model and are described in detail in Section 6.0, Model Formulation.

5.5 DISTINGUISHING THE ROLE OF EXPLOSAFE

EXPLOSAFE's role throughout the tank car accident is one of modifying the heat transfer processes described above. EXPLOSAFE does not provide improved structural support to the tank. As discussed in Section 3.0, EXPLOSAFE is seen to significantly alter the transfer mechanisms. In order to model these effects, a number of features have been included in both the engulfing pool and impinging flame models.

The engulfing pool model proposed distinguishes six specific effects between cases with and without EXPLOSAFE present. These effects are:

1. A substantial reduction in mixing and circulation in the liquid body occurs when EXPLOSAFE is present, so some regions reach saturation earlier than others. Thus a significant fraction of the liquid volume is in a sub-cooled state during the initial heating of the system. This effect is described in the model by dividing the liquid region into two liquid zones, one representing the saturated state and the other, the sub-cooled state. EXPLOSAFE is viewed as increasing the resistance to mixing between these zones.

2. A substantial reduction in both thermal radiation and convection heat transfer in the vapour space is evident when EXPLOSAFE is present. This effect is modelled by decreasing the heat transfer coefficients in the vapour space for the EXPLOSAFE case.

TABLE 5.3 HEAT TRANSFER PROCESSES

Combustion	• fire characteristics • plume ignition
Conduction	• heat transfer through steel shell
Boiling heat transfer	• heat transferred from shell to boiling liquid propane
Two phase flow	• energy and mass transfer through pressure relief valve
Convection	• external convection of hot combustion gases • internal fluid mixing • internal liquid or vapour to shell convection
Radiation	• heat transfer from flame to tank shell • plume heat transfer to tank top • internal heat transfer from tank walls through vapour to liquid surface
Evaporation/condensation	• heat and mass transfer across liquid/vapour boundary

3. An increase in thermal capacity per unit volume of vapour space is expected due to the presence of EXPLOSAFE. This observed condition is modelled in two fashions, by modifying the fluid properties of the vapour when EXPLOSAFE is present and by using values of the polytropic exponent (used in describing the blowdown process) obtained in the field experiments.

4. The presence of EXPLOSAFE effects the surface coefficients between the fluid and the steel wall. Several factors are significant, including the conduction of heat by the aluminum, the inhibition of liquid motion near the liquid/vapour surface by EXPLOSAFE, and reducing breaking-up of vapour bubbles during boiling at the surface. These factors are modelled by adjusting the internal heat transfer and mixing coefficients to match the experimentally obtained valves (field tests and proposed laboratory experiments).

5. The large surface of aluminum metal in the vapour space provides sites to which droplets of liquid may adhere after the first foaming up during the first blowdown. This is seen to be equivalent to increasing the specific heat of the vapour.

6. The fraction of liquid exhausted through the PRV will be lower with EXPLOSAFE, since EXPLOSAFE reduces foaming and priming, and collects liquid droplets on its surface, while the high turbulence of the surface of the non-EXPLOSAFE equipped vessel releases clouds of droplets. Hence, the mass flow rate through the valve at a given tank pressure without EXPLOSAFE will be higher. Boil down is more rapid for non-EXPLOSAFE equipped tanks. The discharge coefficients of the PRV and the polytropic exponent of the blowdown process equation are the key variables which will be affected by the presence of EXPLOSAFE in the manner described.

The impinging torch model addresses the following specific effects which are anticipated to occur with EXPLOSAFE protection:

1. The heat transfer coefficient between the tank shell and the liquid propane
   will be primarily affected. As discussed above, the net effect will be
   influenced by the conduction of heat through the aluminum mesh, the in-
   hibition of liquid circulation, and the retention and break-up of vapour
   bubbles. The heat transfer coefficients used for this model will be ob-
   tained by experimentation.

2. As the impinging torch fire is viewed as being considerably more intense
   than the engulfing flame case, with higher heat fluxes, higher wall
   temperatures will result. It is quite probable that these temperatures
   may exceed the melting point of the EXPLOSAFE mesh as well as cause the
   insulation protection to degrade. The principal influence that this thermal
   degradation has on the system is the modification of the heat transfer
   coefficient. Hence, the heat transfer coefficients used for this model
   will incorporate a temperature dependence.

3. If the flame impinges upon a sector of the tank which is adjacent to the
   vapour region, then EXPLOSAFE will reduce radiative and convective heat
   transport. Heat transfer between phases in this case will be dominated
   primarily by condensation of vapour onto the cooler liquid surface. It is
   unlikely that boiling of the liquid propane would occur in this case and
   hence many of the effects discussed above for the engulfing pool flame will
   not be encountered, although if the impinging flame is large the boiling
   condition may be reached.

4. For intense, high temperature impinging flames in the liquid region, the
   departure from nucleate boiling may be reached. This can result in a local
   melting failure of the tank wall, even at relatively low bulk pressures and
   temperatures. Accurate boiling curves are necessary in assessing this
   critical case.

5. For impinging flames of moderate size, an equilibium temperature and pressure
   in the bulk of the fluid in the tank which is below the relief valve pressure
   setting can be expected, leading to a steady state, non-failure condition.

RAIL TANK CAR MODEL TYPES

ENGULFING FLAME MODEL $\phi = \frac{A_F}{A_T} \rightarrow 1$

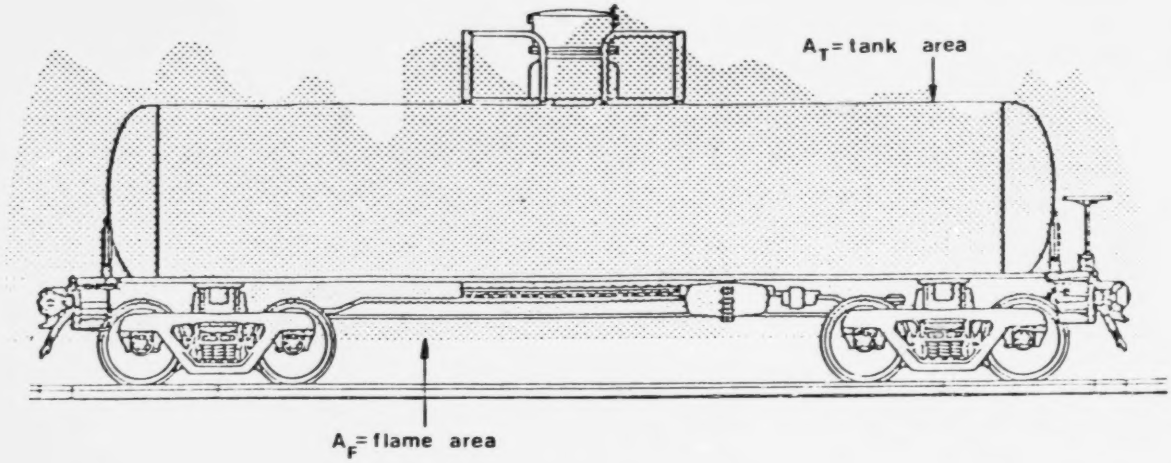
A_T = tank area
A_F = flame area

IMPINGING TORCH MODEL $\phi = \frac{A_F}{A_T} \rightarrow 0$

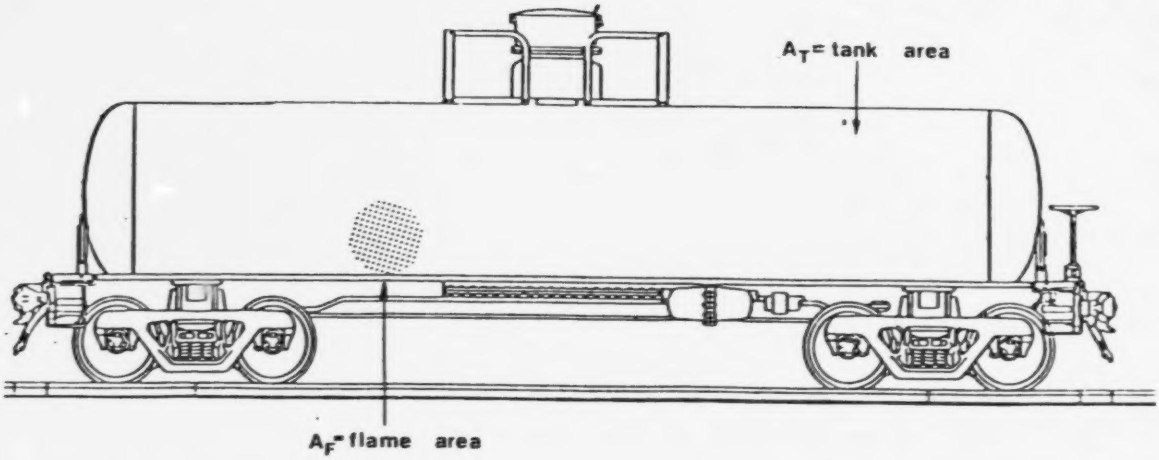
A_T = tank area
A_F = flame area

FIGURE 5.2

5.6 ENGULFING POOL FIRE MODEL CONCEPT

The engulfing pool fire model has been developed for the general conditon for which the area of the flame impinging upon the rail tank car, A_F, is almost equal to the tank surface area, A_T. Figure 5.2 shows the orientation of the flame with respect to the rail tank car.

If taken in cross-section, the lading is seen to consist of two bodies, a vapour and liquid phase, Figure 5.3. The section of the tank which is selected should be representative. In other words, though it is recognized that longitudinal temperature variations in the tank shell do occur because of wind effects and non-uniform spreading of the pool flame, it is proposed that a single cross-section can be defined and that the system temperatures are uniform longitudinally. As available data are presented in section (Suffield and US test reults), this approach is convenient for future model validation. It is recommended that this section be located through the PRV, i.e. mid-point of the tank,as the PRV is affected by the temperature of the vapour below the valve and the overall pressure.

It can be readily demonstrated that developing a three-dimensional version of this model (incorporating longitudinal temperature variations) is a very complex undertaking, see Section 5.8. More detailed information about the flame would be needed to make the model useful. Communication between tank sections would need to be determined; that is, fluid mixing and heat transfer. A two-dimensional version of the engulfing pool model is viewed as offering a level of sophistication and detail appropriate at this stage in the development of our understanding of this problem.

For the single node liquid model, a single temperature, T^{ℓ}, is taken to represent the liquid body and a single representative temperature, T^{v}, for the vapour. It would be assumed in this case that the liquid is well mixed. This assumption is seen to be reasonable for the case with no EXPLOSAFE in the tank. However, as was noted in previous sections, EXPLOSAFE reduces the mixing of the liquid, and a single node liquid model would not fully account for the degree of subcooling that was observed in some regions of the liquid. Though this model does offer an advantage of simplicity, a more complete version has been developed and is termed the "two-liquid node model".

EQUIVALENT THERMAL NETWORK -
SINGLE LIQUID NODE MODEL

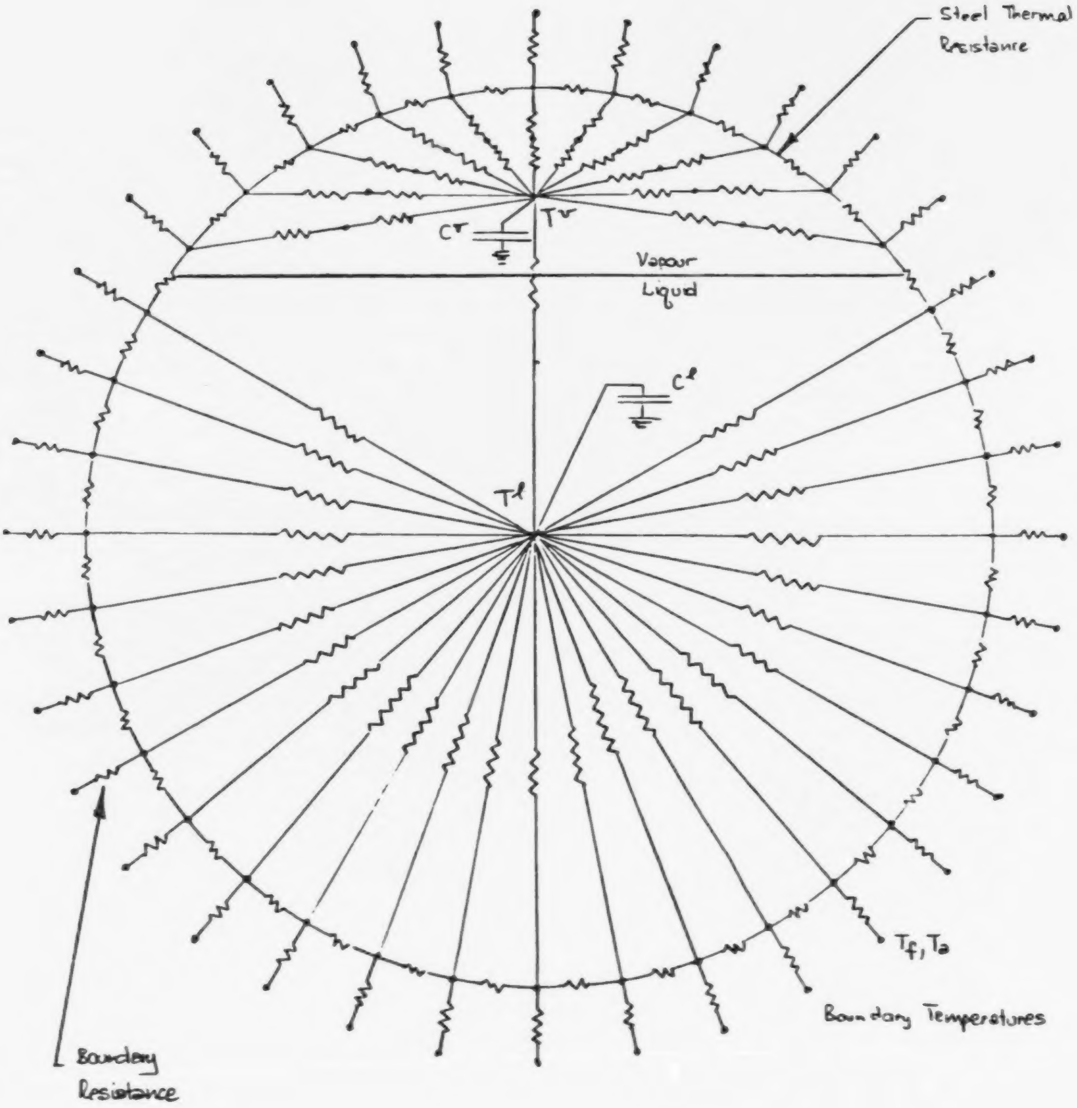
Steel Thermal Resistance
T^v
C^v
Vapour
Liquid
C^l
T^l
T_f, T_a
Boundary Temperatures
Boundary Resistance

Note: All steel nodes have an associated thermal capacitance.

FIGURE 5.3

Figure 5.4 is a schematic of this equivalent thermal network which can be used to determine the steel shell, sub-cooled liquid, saturated liquid, and vapour temperatures given the boundary temperatures, the internal and external heat transfer coefficients, and the state of the PRV. The liquid phase is considered to behave as two zones: a saturated and a sub-cooled zone. For the former case, the temperature, T_l , is determined by the system pressure at a given instant according to the saturated vapour pressure curve for propane. Heat can only be transferred from the tank wall and vapour to the saturated zone. Mass is transferred to the vapour phase only from the saturated zone. The subcooled zone communicates only with the saturated liquid zone, exchanging both heat and mass. The rate at which this heat (and mass) is transferred is a function of the mixing resistance, R_m. This parameter is larger for tanks equipped with EXPLOSAFE than for those without.

During the initial heating of the tank, most of the liquid zone is sub-cooled. The saturated zone at this time consists primarily of the body of liquid in the boundary layer between the tank wall and the subcooled zone and the liquid near the surface. It should be noted that the internal heat transfer coefficients in the liquid zone which will be used for this model will be those describing the saturated state. As the liquid heats up, circulation increases and the sub-cooled zone loses mass to the saturated zone until the liquid phase is fully saturated. When this condition is reached, the two-node model behaves identically to the single-node version.

An advantage of the two-node approach is the distinction that is made between the EXPLOSAFE-equipped versus the non-EXPLOSAFE-equipped tanks, through the mixing resistance. It is evident that R_m is a parameter that must be derived from the evidence of the field trials and by experiment. In Section 9.0, suggested approaches to determining R_m are given.

EQUIVALENT THERMAL NETWORK - TWO LIQUID NODE MODEL

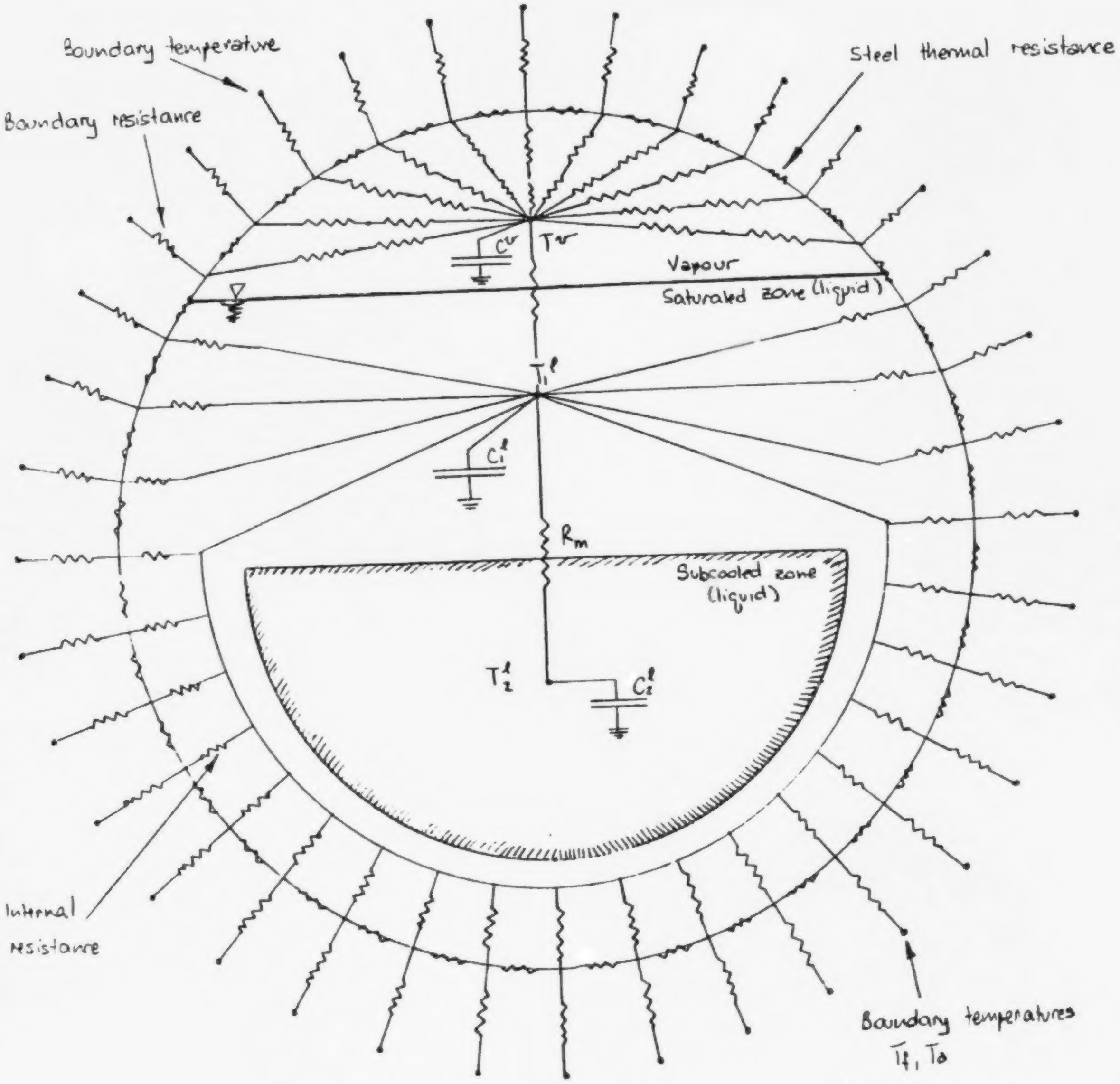
Boundary temperature
Boundary resistance
Steel thermal resistance
C^v
T^v
Vapour
Saturated zone (liquid)
T_1^l
C_1^l
R_m
Subcooled zone (liquid)
T_2^l
C_2^l
Internal resistance
Boundary temperatures T_f, T_a

Note: All steel nodes have an associated thermal capacitance.

FIGURE 5.4

IMPINGING TORCH MODEL - LIQUID ZONE

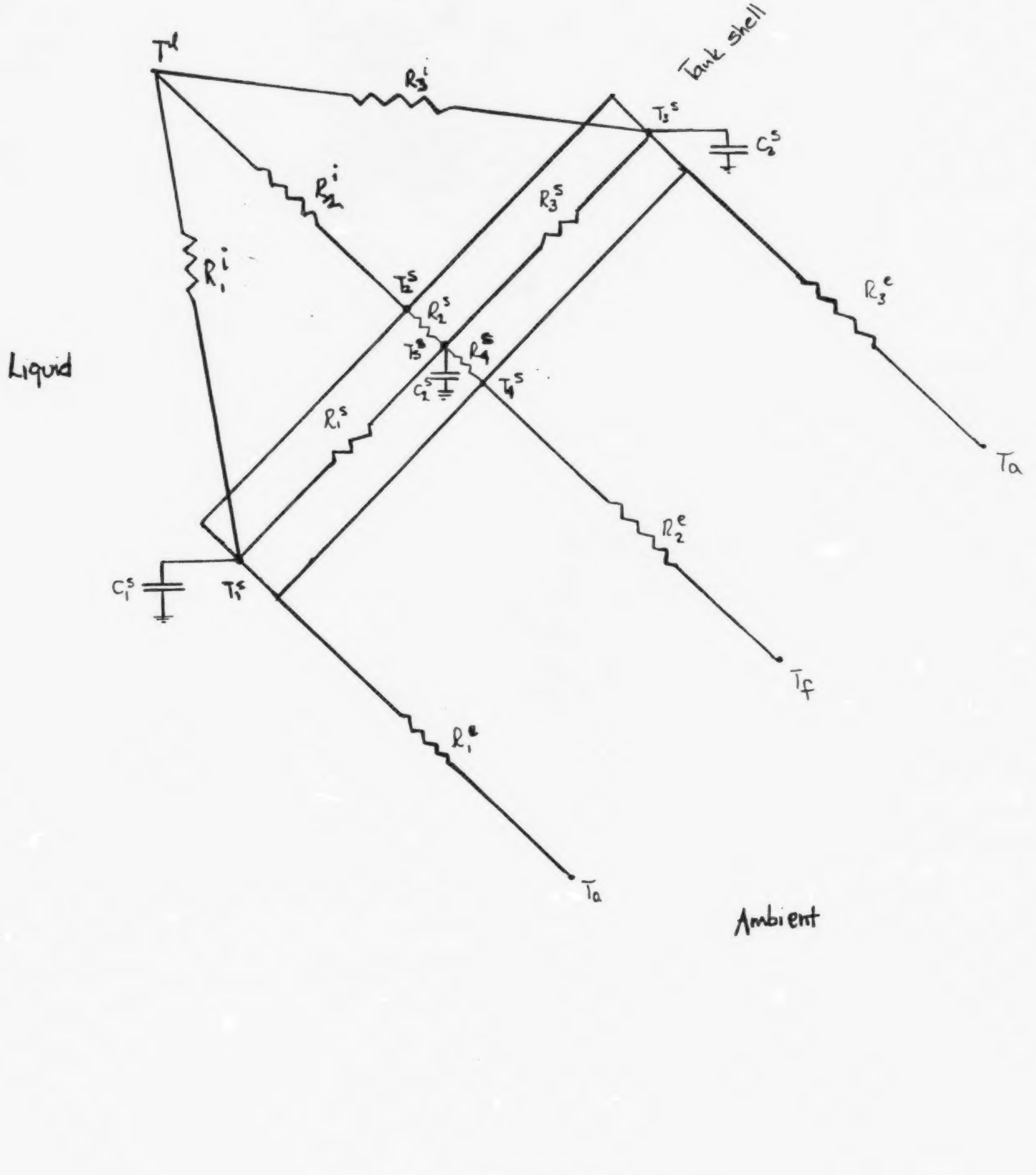

T^l
R_3^i
Tank shell
T_3^s
C_2^s
R_2^i
R_3^s
R_1^i
T_2^s
R_2^s
T_5^s
R_4^s
C_2^s
T_4^s
R_3^e
Liquid
R_1^s
Ta
R_2^e
C_1^s
T_1^s
Tf
R_1^e
Ta
Ambient

FIGURE 5.5

5.7 IMPINGING TORCH MODEL

As shown previously in Figure 5.2 the area of impingement upon the rail tank car is very small with respect to the overall tank area for the impinging flame. It is clear that this area could be considered to be adjacent to either the liquid or the vapour. Two versions of this model are proposed to describe these cases. The instance in which the flame is incident upon an area which includes the liquid to vapour boundary is considered rare and has not been modelled due to perceived model complexity.

5.7.1 Impingement upon area wetted by liquid

With a high intensity flame incident upon a bare steel wall with the obverse side in the liquid region, the heat flux to the liquid will depend upon the flame area and temperature, the external heat transfer coefficient, the steel thickness and properties, the internal coefficient, and the liquid temperature. These factors are indicated by the thermal network model presented in Figure 5.5.. The liquid is considered to be at saturation conditions with T^{ℓ} determined by a simple heat balance over the network.

The steel wall end temperatures are chosen outside of the flame area at a location where the temperature remains relatively constant throughout the accident. T^{f} represents a variable flame temperature, specified as program input.

With increasing steel temperatures during fire conditions, the degree of wall superheat increases. The internal thermal resistance, R_i (or the internal heat transfer coefficient), is a strong function of this temperature difference as described by the boiling curve, see Section 9.2. With superheat temperatures in excess of the critical heat flux condition burnout may occur. That is, the maximum heat flux is exceeded and the coefficient drops rapidly, causing the wall temperature to increase to a failure condition. The onset of failure will depend upon the thermal stresses established in the steel at the reference pressure and the physical characteristics of the steel (e.g. melting point). The presence of EXPLOSAFE is expected to modify the boiling curve of propane and affect the time to failure. Insulation will affect the steel temperatures which result. The effectiveness of these protective

IMPINGING TORCH MODEL - VAPOUR ZONE

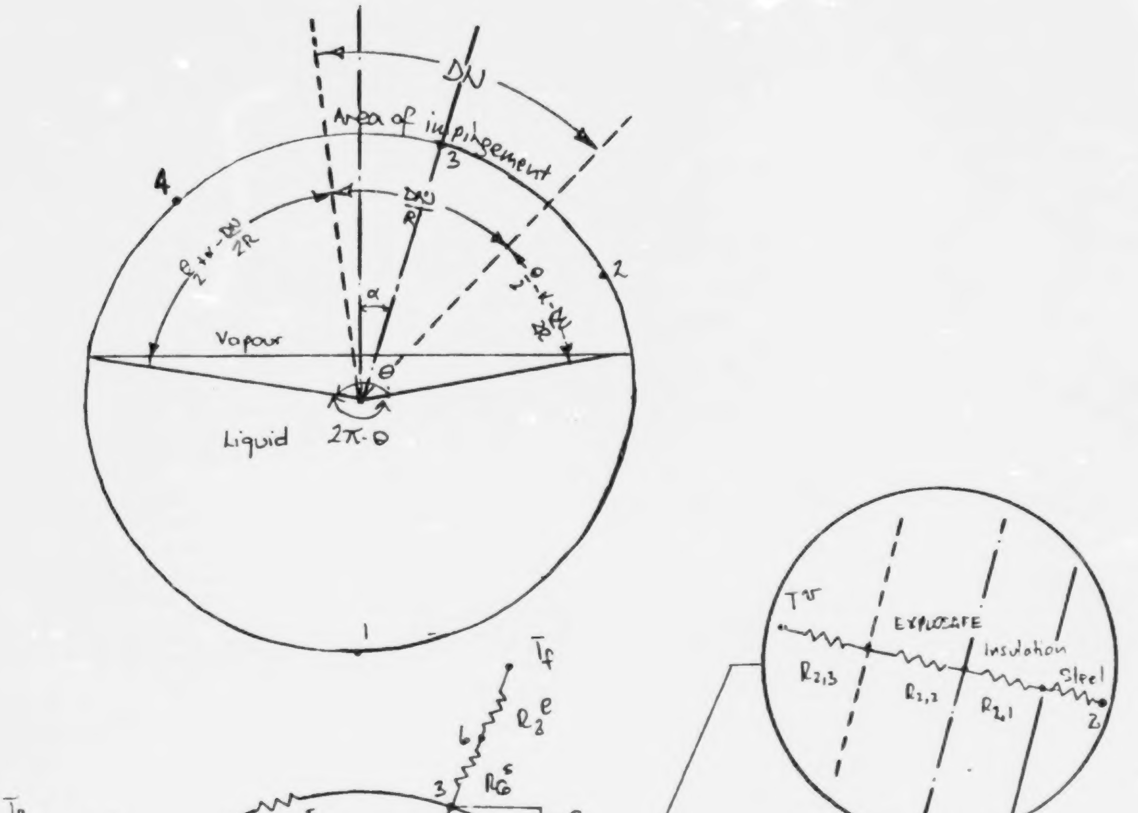
DW
Area of impingement
3
4
2
1
DW/R
α
θ
Vapour
Liquid
2π-θ
T_f
R_8^e
6
3
R_6^s
C_3
T_a
R_4^e
R_3^s
5
R_2^s
R_1^s
4
C_4
R_4^i
T^v
R_3^i
C^v
R_2^i
C_2
2
T_a
R_2^e
Vapour
Liquid
R^vl
T^l
C^l
R_4^s
R_5^s
R_1^i
1
C_1
R_1^e
T_a
T^v
EXPLOSAFE
Insulation
Steel
R_2,3
R_2,2
R_2,1
2

FIGURE 5.6

systems is temperature dependent, particularly when temperatures exceed material melting points.

It is entirely possible that failure will not occur for low flame intensities as heat may be effectively dissipated into the liquid or through the steel to the ambient air. The threshold flame intensity which leads to the failure of a bare tank wall can be determined. The protective system will modify this threshold value.

5.7.2 Impingement upon area wetted by vapour

A torch fire incident upon the vapour region of the tank will lead to some events different from those described above. As the vapour space has a much lower thermal capacity than the liquid phase, it will heat much more rapidly. Hence, the vapour temperature cannot be taken to be constant. As the temperature increases, so too will the pressure, until the set point on the PRV may be reached. At this time, vapour will be discharged until the pressure is relieved. Like the engulfing pool fire case, liquid will be vapourized to maintain the liquid at saturatured conditions should the pressure dip below the saturation pressure of the liquid. The equivalent thermal network for this case is shown in Figure 5.6. The vapour capacitance varies with the reduction in mass of vapour. Wall temperatures are expected to be much higher with this type of flame as the heat transfer coefficient in the vapour phase is much lower than that in the liquid phase, and the vapour pressure will be higher. Hence, burnout can be expected to occur more rapidly.

It should be noted that because of the relatively small vapour space in a fully laden car, and its high position, local flame impingement on the vapour zone must have a much lower probability than that for impingement on the liquid zone.

5.8 FUTURE EXTENSIONS OF THE MODEL CONCEPT

It is clear from the discussion above that some specific accident cases cannot be modelled with a two-dimensional model. Significantly, pitch cannot be a model variable. Longitudinal heating and mixing of the lading require a third dimension. Combined engulfment and torch impingement cannot be modelled. Though such features are desireable, they introduce complexity into an already complex set of models. Through development of a two-dimensional model, insights will be gained which should prove useful to developing future extensions to the concept. Following the successful implementation of the proposed models, it would then be appropriate to determine the need for more sophisticated algorithms and to develop a program to upgrade the models.

Future extensions to the model concept are envisaged to have a number of applications in other sectors of the transportation industry. With a numerical model organized as a series of upgradeable subroutines (see Section 6.0), it would be possible to study the behaviour of other lading materials in a tank under fire conditions by interchanging the appropriate physical properties and boiling curve subroutines. Materials which could be studied include all liquids transported under pressure. This could prove to be of considerable benefit to improving designs of and standards for rail tank cars and tanker trucks transporting dangerous goods. What would limit the general utility of the extended version of the proposed model is the availability of physical data (properties and boiling curves for the lading materials).

6.0 MODEL FORMULATION

To describe the events which occur during a rail tank car fire accident it is necessary to distinguish between micro-level processes and macro-level behaviour. Macro-level behaviour is governed by a set of fundamental equations. These governing equations can be related through a logical structure. This structure, which is the essence of the model, calls upon micro-level (component-level) descriptions of the state of the system (eg. fluid properties), the system forcing function (rate of heat gain, eg. flame intensity), and factors which affect the rate of system change (eg. PRV characteristics and heat transfer coefficients). Detailed aspects of the model are described in this Section following a discussion of the governing system equations and a presentation of the logical structure for both the engulfing pool fire and impinging flame models.

6.1 GOVERNING EQUATIONS

Certain fundamental laws or conditions must be satisfied throughout the event. These are described in equation form in the figure opposite.

The statement of mass conservation means that mass either remains in the rail tank car or is exhausted to the environment through the PRV. Mass can be exchanged between the phases and when the PRV is closed, the amount of liquid mass which becomes vapour is equal to the increase in vapour mass and vice versa if the vapour condenses. Equivalently, if the PRV is closed then an increase in vapour volume results in a decrease in liquid volume, with the total volume and mass remaining constant.

Conservation of energy requires that all forms of energy be accounted for. As no nuclear reactions occur (that is, mass is conserved), changes in system energy are equal to the net flow of energy into the system. This can be expressed by equation (5) opposite. As no work is performed by the system, $\Delta W=0$. Reference is made to Figure 6.2 which shows the generalized thermodynamic system.

FIGURE 6.1

GOVERNING EQUATIONS

1. Conservation of mass (continuity):

$$\Delta M_T = \Delta M^v + \Delta M^\ell = \Delta M_e \qquad (4)$$

ΔM_T = change in total lading mass
ΔM^v = change in mass of propane vapour
ΔM^ℓ = change in mass of propane liquid
ΔM_e = mass efflux from tank car

2. Conservation of energy (first law of thermodynamics):

Energy in - energy out = increase in system energy

$$\Delta m_1 \cdot (h_1 + \frac{v_{e1}^2}{2} + z_1 g) - \Delta m_2 \cdot (h_2 + \frac{v_{e2}^2}{2} + z_2 g) + \Delta Q - \Delta W = dE \qquad (5)$$

Δm_1 = mass flow into system ($\Delta m_1 = 0$ for the specific problem)
Δm_2 = mass flow out of system
h = enthalpy
v_e = stream velocity across boundary
z = elevation above datum
g = gravitational constant
ΔQ = heat added to system
ΔW = work done by system
dE = change in system energy

3. Equations of state:

Vapour: $$PV^v = ZM^vRT^v \qquad (6)$$

P = system pressure
V = vapour volume
Z = compressibility factor
M^v = mass of vapour
R = universal gas constant
T^v = vapour temperature

Liquid: $$v^\ell = v_0^\ell \{1 + \alpha_T (T^\ell - T_0^\ell) - \kappa_T (P - P_0)\} \qquad (7)$$

v^ℓ = specific volume of liquid at (T^e, P)
v_0^ℓ = reference specific volume
α_T = coefficient of thermal expansion
κ_T = isothermal compressibility
T^ℓ = liquid temperature
T_0^ℓ = reference liquid temperature
P = system pressure
P_0 = reference pressure

4. Process equations:

$$P \cdot (v^v)^n = c \qquad (8)$$

v^v = specific volume of vapour
c = constant
n = Polytropic exponent (not necessarily constant)

ENERGY FLOWS IN A GENERAL THERMODYNAMIC SYSTEM

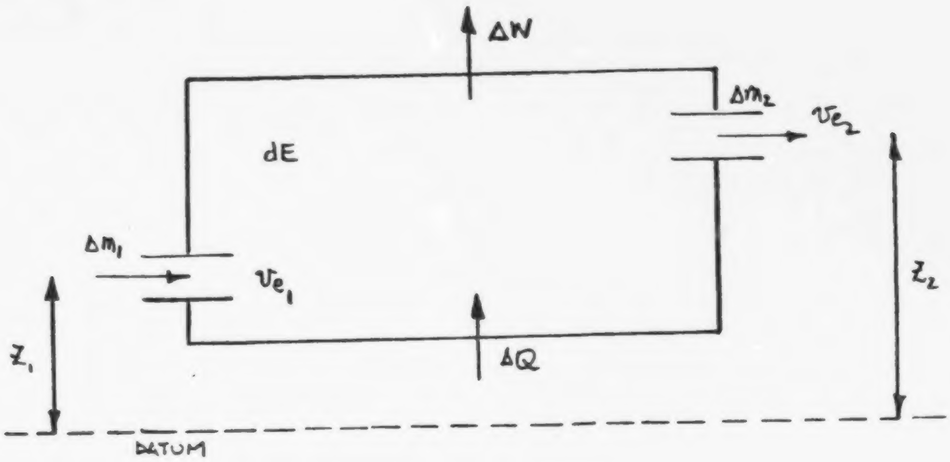
ΔW
Δm₂
v_{e_2}
dE
Δm₁
v_{e_1}
z_2
z_1
ΔQ
DATUM

FIGURE 6.2

Equations of state describe the relationship between the key thermodynamic variables. As the system is viewed as consisting of two bodies, liquid and vapour, two state equations are required. It is convenient to use a modified form of the ideal gas law, which incorporates the compressibility factor Z, to describe the propane vapour. This factor is empirically derived and represents deviation from ideality. It is a function of both temperature and pressure. Values of Z are presented in Section 6.3.17.

The state equation for a liquid is given by the general expression (7). The specific volume depends upon the state variables, temperature and pressure, as well as upon α_T and κ_T which are either presented as tabular values or can be deduced from the thermodynamic chart for propane.

As the state equations describe the conditions of a body at a given point in the thermodynamic space, the process equation describes the pathway that is taken between points. A general polytropic expression is given for the vapour in equation (8) This expression can be used to describe the compression and expansion of the vapour. The type of process which occurs is determined by the polytopic exponent, n. The selection of appropriate values of this parameter is discussed more fully in subsequent sections.

The thermodynamic process which occurs throughout the liquid phase is governed by the above expressions. Constraints which are imposed on the pathways taken are: (1) the liquid "pressure" is always equal to the vapour "pressure" and (2) the temperature of the bulk liquid cannot be greater than the saturation temperature corresponding to the system pressure; if it is greater, then propane vaporization occurs.

The above conditions represent the fundamental relationships which must be satisfied. State equations describe the thermodynamic conditions throughout a process specified by (8). Throughout the event, energy and mass must be conserved. The rate at which events occur is determined by the component-level effects related by the overall model structure presented below.

OVERALL MODEL ORGANIZATION
Engulfing Flame Model
MAIN PROGRAM

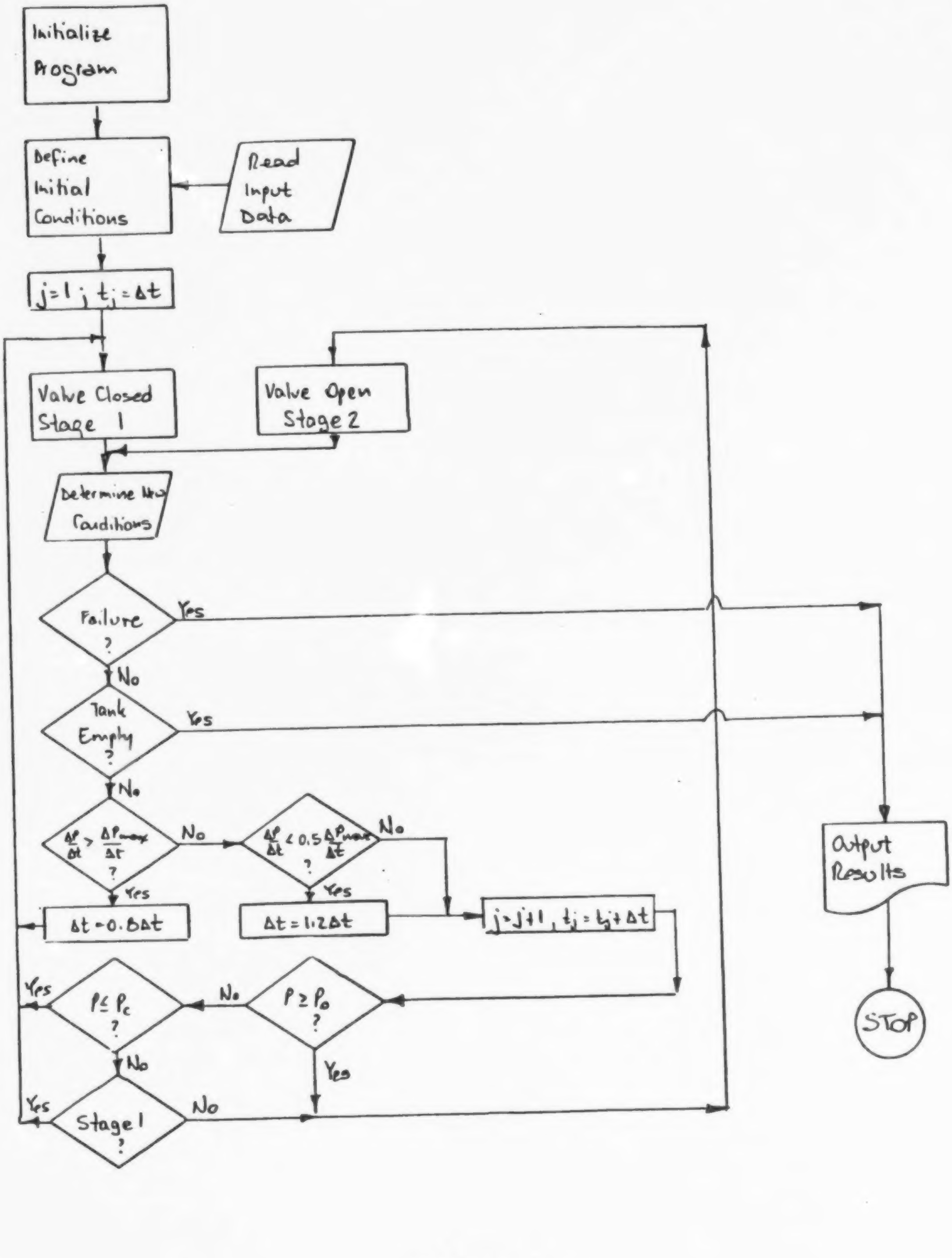
Initialize Program
Define Initial Conditions
Read Input Data
$j=1$; $t_j=\Delta t$
Valve Closed Stage 1
Valve Open Stage 2
Determine New Conditions
Failure ?
Yes
No
Tank Empty ?
Yes
No
$\frac{\Delta P}{\Delta t} > \frac{\Delta P_{max}}{\Delta t}$?
No
Yes
$\frac{\Delta P}{\Delta t} < 0.5\frac{\Delta P_{max}}{\Delta t}$?
No
Yes
$\Delta t = 0.8\Delta t$
$\Delta t = 1.2\Delta t$
$j=j+1$, $t_j = t_j + \Delta t$
Output Results
STOP
$P \geq P_o$?
No
Yes
$P \leq P_c$?
Yes
No
Stage 1 ?
Yes
No

FIGURE 6.3

6.2 OVERALL MODEL LOGIC (Bulk Process Description)

The logic structure represents the skeleton around which a complete model can be built. As these structures are different for each of the model cases, they are presented separately below.

6.2.1 Engulfing Pool Fire Model Logic

Figure 6.3 presents the overall organization for the engulfing pool fire model. The steps indicated constitute the main segment of the simulation program. Two states of the system are described; the PRV is either open or closed. The PRV is taken to be closed initially and the program steps through the event (under Stage 1) until Stage 2 is initiated when the PRV open set point is achieved. Stage 1 will be attained whenever the PRV close set point is reached. New system conditions are obtained following completion of the Stage steps. These results are then compared against the failure criterion to determine whether the simulation should be stopped. If not and the tank is not empty, the time step is adjusted so that computational accuracy and efficiency can be high. The system pressure is compared against the PRV set points and the subsequent Stage determined. The simulation continues until the tank fails or the tank becomes empty.

A description of the simulation procedure proposed for Stages 1 and 2 is given in Figure 6.4. The PRV condition is determined in the MAIN program. The state of the valve affects the subroutines which are called and the overall logic to be followed through an event. Initial conditions for the time step are taken to be those determined as a result of the previous step. The forcing function (heat input to the tank) is assumed constant over the time step and is calculated at the beginning of the step. Once these conditions are established, the locations of the phase and zonal boundaries are determined, with the configuration of the tank nodes following suit. Two flags, A and B, are defined and used to skip unnecessary steps. If the A flag is raised, all of the liquid is taken to be saturated and the liquid can be treated as one node. If the B flag is revised, all of the liquid has vaporized and the lading can be treated as a single phase system.

MODEL FORMULATION - Logic Diagram
Engulfing Flame Model -
Two Liquid Zones

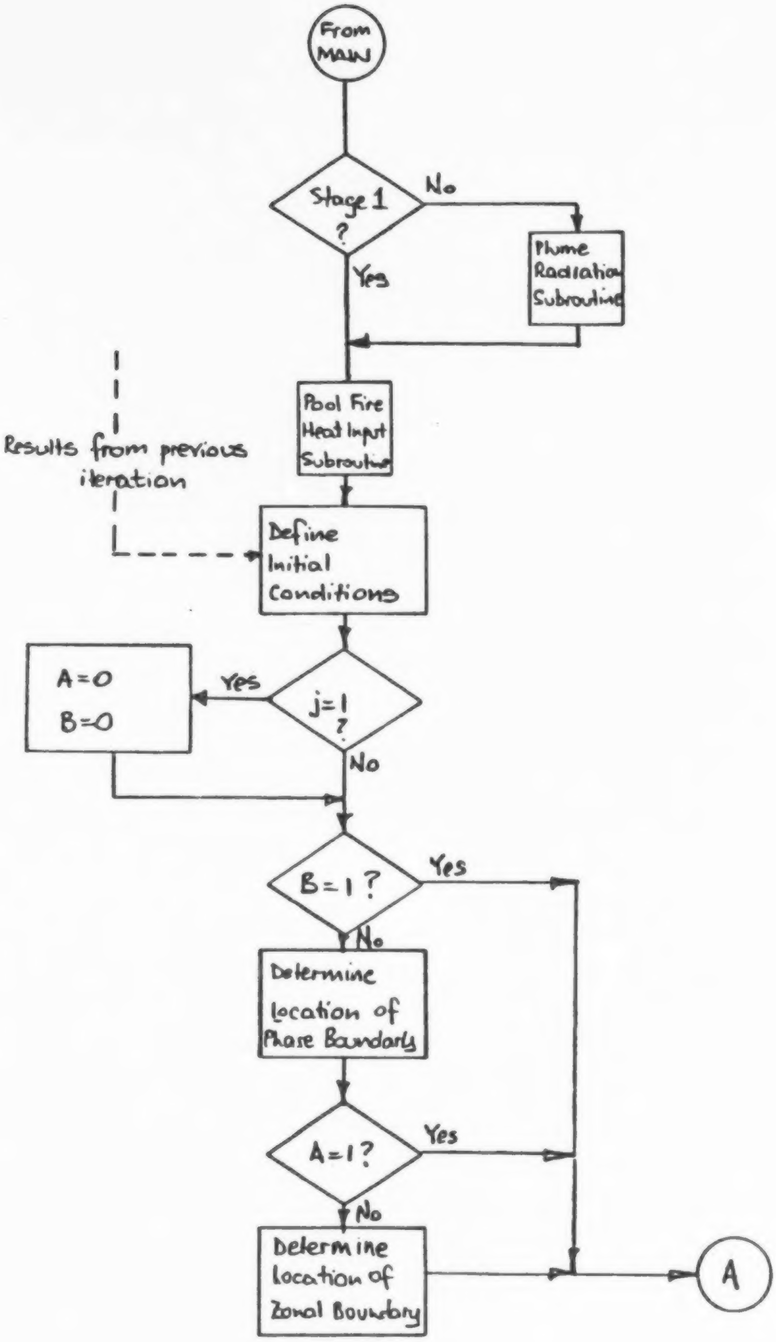
From MAIN
Stage 1 ?
No
Yes
Plume Radiation Subroutine
Pool Fire Heat Input Subroutine
Results from previous iteration
Define Initial Conditions
j=1 ?
Yes
No
A=0
B=0
B=1 ?
Yes
No
Determine location of Phase Boundary
A=1 ?
Yes
No
Determine location of Zonal Boundary
A

FIGURE 6.4

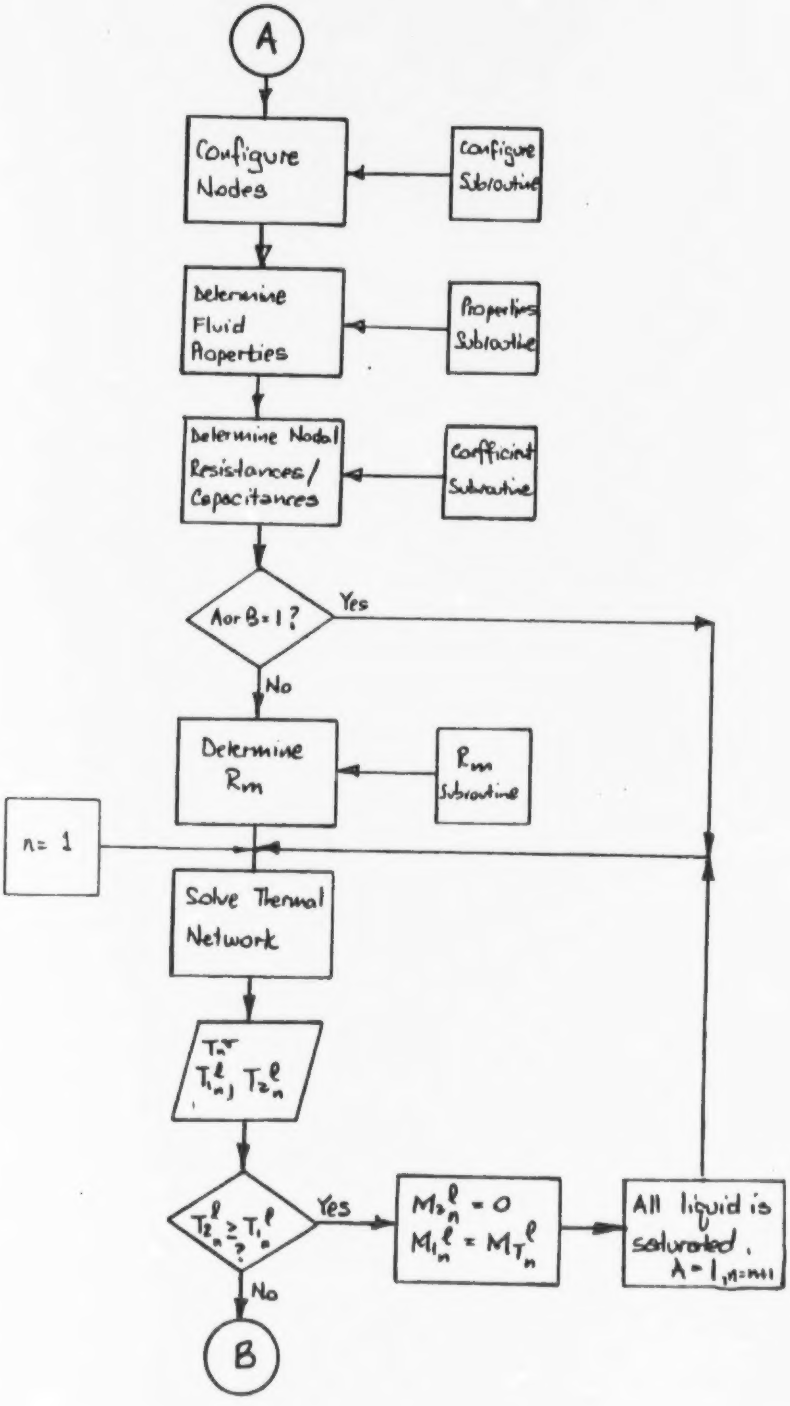
A
Configure Nodes
Configure Subroutine
Determine Fluid Properties
Properties Subroutine
Determine Nodal Resistances/ Capacitances
Coefficient Subroutine
A or B = 1 ?
Yes
No
Determine R_m
R_m Subroutine
n= 1
Solve Thermal Network
T_n^T
$T_{1_n}^\ell$, $T_{2_n}^\ell$
$T_{2_n}^\ell \geq T_{1_n}^\ell$?
Yes
$M_{2_n}^\ell = 0$
$M_{1_n}^\ell = M_{T_n}^\ell$
All liquid is saturated.
$\lambda = 1$, $n = n+1$
No
B

FIGURE 6.4 (cont'd)

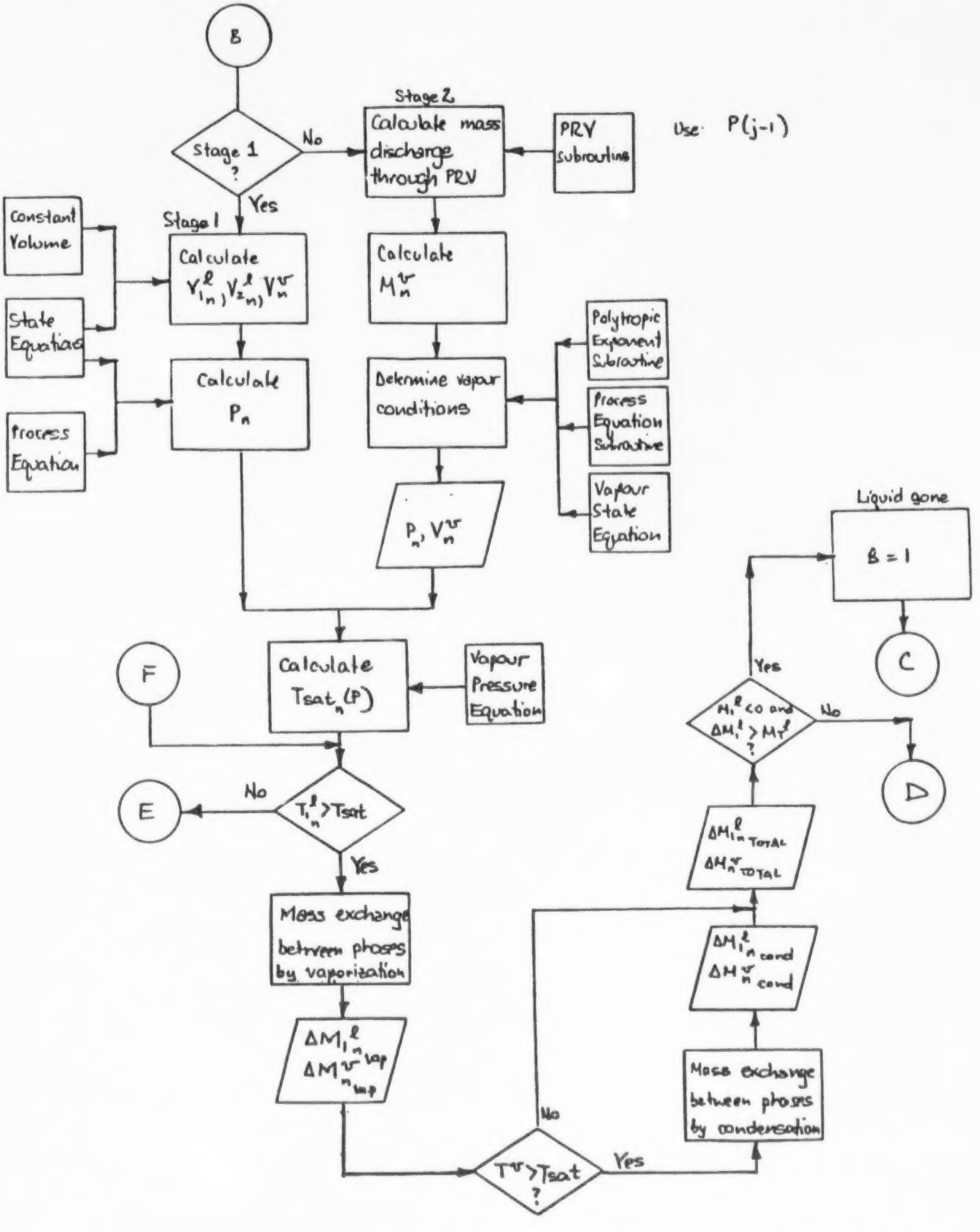
B
Stage 1 ?
No
Yes
Stage 2
Calculate mass discharge through PRV
PRV subroutine
Use $P(j-1)$
Stage 1
Constant Volume
State Equation
Process Equation
Calculate $V^{\ell}_{1n}, V^{\ell}_{2n}, V^{v}_{n}$
Calculate P_n
Calculate M^{v}_{n}
Determine vapour conditions
Polytropic Exponent Subroutine
Process Equation Subroutine
Vapour State Equation
P_n, V^{v}_{n}
Liquid gone
B = 1
C
Calculate $Tsat_n(P)$
Vapour Pressure Equation
F
E
No
$T^{\ell}_{1n} > Tsat$
Yes
Mass exchange between phases by vaporization
$\Delta M^{\ell}_{1n\,vap}$
$\Delta M^{v}_{n\,vap}$
$T^{v} > Tsat$?
No
Yes
Mass exchange between phases by condensation
$\Delta M^{\ell}_{1n\,cond}$
$\Delta M^{v}_{n\,cond}$
$\Delta M^{\ell}_{1n\,TOTAL}$
$\Delta M^{v}_{n\,TOTAL}$
$M^{\ell}_{1} < 0$ and $\Delta M^{\ell}_{1} > M^{\ell}_{T}$?
Yes
No
D

FIGURE 6.4 (cont'd)

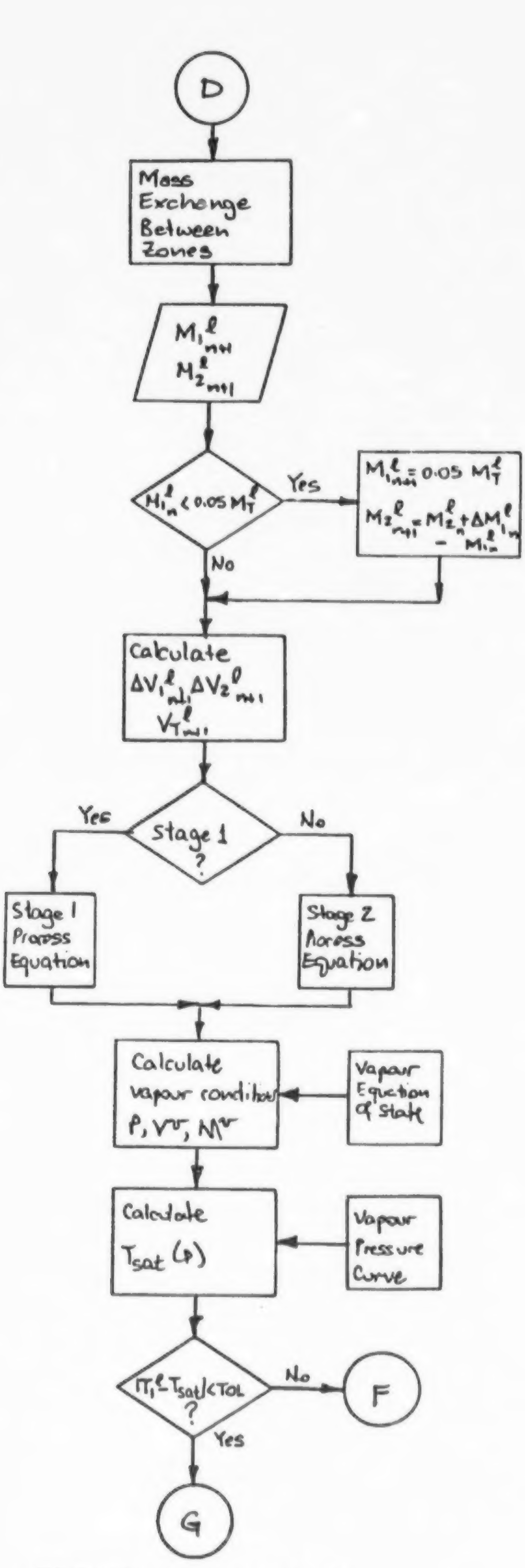
D
Mass Exchange Between Zones
$M_{1_{n+1}}^{\ell}$
$M_{2_{n+1}}^{\ell}$
$M_{1_n}^{\ell} < 0.05\, M_T^{\ell}$
Yes
$M_{1_{n+1}}^{\ell} = 0.05\, M_T^{\ell}$
$M_{2_{n+1}}^{\ell} = M_{2_n}^{\ell} + \Delta M_{1_n}^{\ell} - M_{1_n}^{\ell}$
No
Calculate
$\Delta V_{1_{n+1}}^{\ell}, \Delta V_{2_{n+1}}^{\ell}$
$V_{T_{n+1}}^{\ell}$
Stage 1 ?
Yes
No
Stage 1 Process Equation
Stage 2 Process Equation
Calculate vapour condition
P, V^v, M^v
Vapour Equation of State
Calculate $T_{sat}(P)$
Vapour Pressure Curve
$|T_1^{\ell} - T_{sat}| < TOL$?
No
F
Yes
G

FIGURE 6.4 (cont'd)

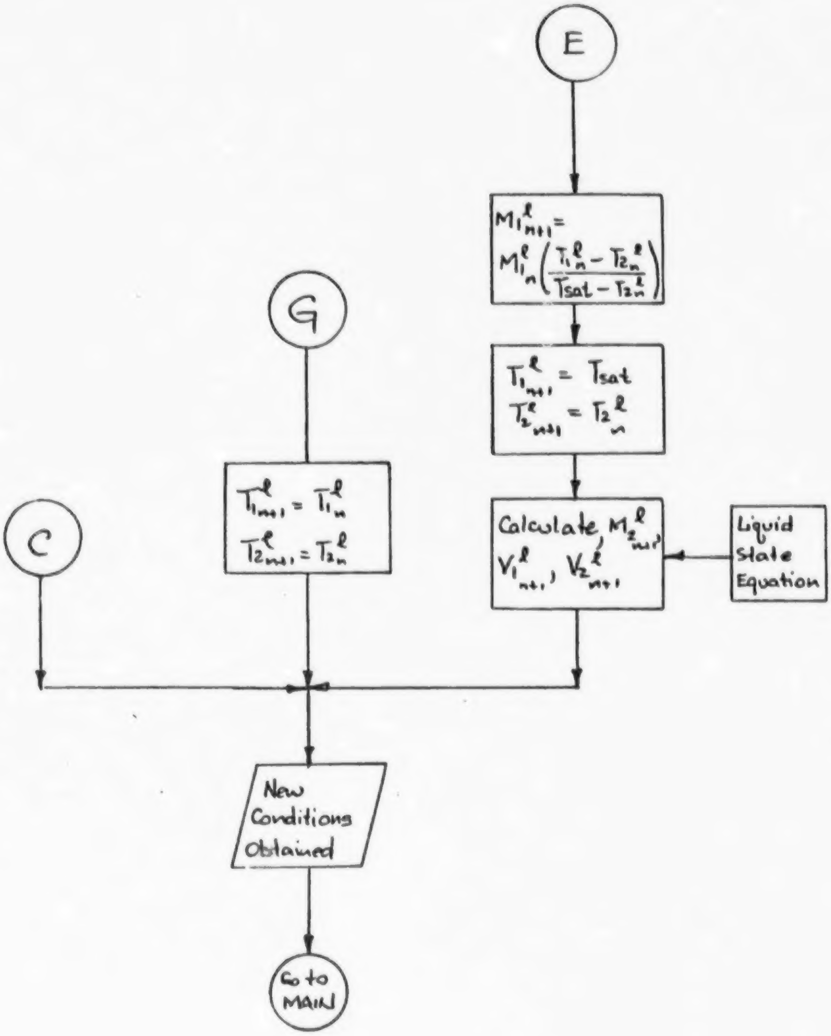
E
$M1^{\ell}_{n+1} = M1^{\ell}_{n}\left(\frac{T1^{\ell}_{n} - T2^{\ell}_{n}}{T_{sat} - T2^{\ell}_{n}}\right)$
G
$T1^{\ell}_{n+1} = T_{sat}$
$T2^{\ell}_{n+1} = T2^{\ell}_{n}$
$T1^{\ell}_{n+1} = T1^{\ell}_{n}$
$T2^{\ell}_{n+1} = T2^{\ell}_{n}$
C
Calculate $M2^{\ell}_{n+1}$, $V1^{\ell}_{n+1}$, $V2^{\ell}_{n+1}$
Liquid State Equation
New Conditions Obtained
Go to MAIN

FIGURE 6.4 (cont'd)

Fluid properties, heat transfer coefficients, and capacitances are based upon the conditions of the previous step, that is, $T^v(j-1)$, $T_1^\ell(j-1)$, $T_2^\ell(j-1)$, and $P(j-1)$, where j is the current time step number. The mixing resistance between the liquid zones is then calculated using the appropriate R_m subroutine discussed in subsequent sections. At this point, the nodal network is completely defined and can be solved for nodal temperatures and heat fluxes. Thus, new values of $T_n^v(j)$, $T1_n^\ell(j)$, and $T2_n^\ell(j)$ are obtained. Subscript n is used as a counter for the number of iterations taken over a given time step.

If the temperature of the subcooled zone exceeds that of the saturated zone, then the liquid zone is taken to be fully saturated. The thermal network is solved again with adjusted masses for the phase temperatures. However, if zone 2 remains subcooled then the simulation proceeds with calculating the new system pressure and phase volumes at the new temperatures. If the valve is closed, the new liquid volume is calculated using the state equation. As temperature affects the liquid expansion much more than does pressure, it is reasonable to include only the thermal expansion of the liquid over the time step to get the new volumes. As the system volume is constant with the PRV closed, using continuity, the vapour volume is obtained. To obtain the new system pressure, a process equation is invoked. With liquid expansion, the vapour becomes compressed. The polytropic exponent used in equation (8) to describe the compression process is the ratio of specific heats, $k = C_p/C_v$, which for propane is approximately equal to 1.13. This assumes isentropic compression over the time step. The new system pressure can be readily obtained from (5) as the vapour volume is known and the conditions of the previous step determines c.

If the valve is open, then the amount of mass which is discharged is calculated using the PRV subroutine and the system pressure as determined in the previous iteration. The new mass of vapour is then known. New vapour conditions, P and V^v are obtained using the process equation, and the gas equation. The polytropic exponent was shown to be a function of temperature (Section 2.3.4). The polytropic exponent subroutine is referenced at this point. Using the two equations, (6) and (8), the two unknowns, P and V^v, can be calculated.

Thus far it has been assumed that no mass is exchanged between phases. However, if the temperature of the liquid phase (zone 1) exceeds the saturation temperature corresponding to the system pressure, then vaporization must occur from this phase to keep the liquid at saturation. Figure 6.5 illustrates the mass transfer attributed to evaporation equation (9). With the temperature of the vapour exceeding that of the saturated liquid, zone condensation will occur. The amount of vapour that condenses is estimated by equation (10).

If no liquid remains in the tank, B = 1, and with new conditions established, program control is transferred to MAIN. Otherwise, mass is distributed between the liquid zones so that: (1) only mass from zone 1 can be vaporized; (2) the mass of zone 1 cannot be less than 5% of the total liquid mass. This means that the sub-cooled liquid region gets progressively smaller with time, until the liquid is fully saturated and can be treated as one zone. As the relief valve spring weakens later into the accident and venting occurs, the remaining liquid becomes sub-cooled, during the rapid pressure variations, but as one body.

With these inter-phase and inter-zone transfers, new vapour conditions can be calculated. A new value of the saturation temperature is determined. If T_1^{ℓ} is close to this value, then the system conditions at the end of the step are obtained and program transfer goes to MAIN. If this tolerance is not achieved, then further mass exchanges are required until this criterion is satisfied.

If the liquid temperature $T_{1n=1}^{\ell}$ is less than the saturation temperature calculated the first time, then mass is transferred from zone 1 into zone 2 and the temperature adjusted so that $T_{1_{n+1}}^{\ell} = T_{sat}$, and $T_{2_{n+1}}^{\ell} = T_{2_n}^{\ell}$, and the total energy in the liquid phase remains the same. Thus new conditions are obtained and program control is returned to MAIN.

CALCULATION OF MASS EXCHANGES BETWEEN PHASES

VAPORIZATION

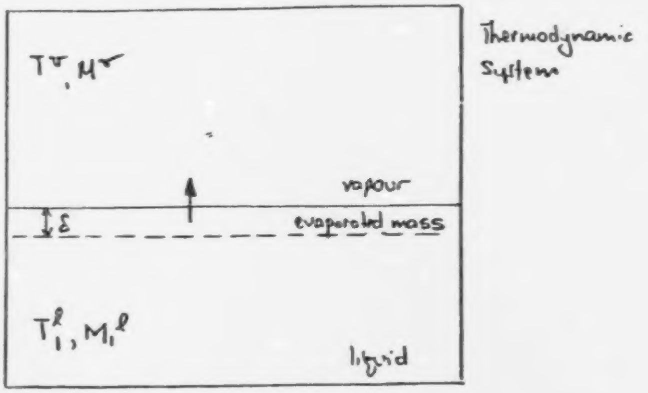
T^v, M^v
Thermodynamic System
vapour
ε
evaporated mass
T_1^l, M_1^l
liquid

$$Q = M_1^l \, Cp^l (T_1^l - T_{sat}) = h_{fg} \Delta M_1^l$$

$$\Delta M_1^l = \frac{M_1^l \, Cp^l (T_1^l - T_{sat})}{h_{fg}} \qquad (9)$$

CONDENSATION

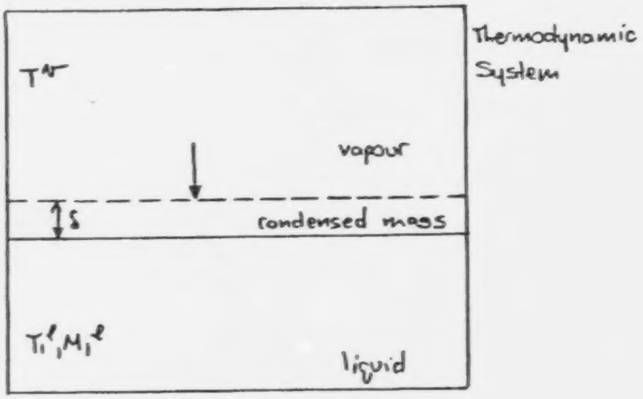
T^v
Thermodynamic System
vapour
δ
condensed mass
T_1^l, M_1^l
liquid

$$\frac{k^l}{\delta}(T^v - T_1^l) = \rho^l h_{fg} \frac{d\delta}{dt}$$

$$\delta = \sqrt{\frac{2k^l (T^v - T_1^l) t}{\rho^l h_{fg}}}$$

$$\Delta M_1^l = \rho^l A_{surface} \, \delta \qquad (10)$$

FIGURE 6.5

6.2.2 Impinging Torch Model

The overall organization of the impinging flame model is presented in Figure 6.6. It can be seen that the model addresses the cases with the impinging flame incident upon the liquid zone or the vapour zone. In the former case, with an intense flame, the steel will fail before the tank pressure reaches the PRV open set point. This means that mass exchange between phases is small and can be neglected. Should the open set point pressure be obtained before failure occurs, the program then goes to an output mode and ends. The role of the vapour throughout this type of event is minor and will not affect the time to failure. This simplifies the formulation of the model considerably as evidenced in the following detailed logic diagram, Figure 6.7.

On the other hand, if the flame impinges upon a wall segment adjacent to the vapour zone, then the simulation process is more complex. With rapid heating of the vapour, the system pressure will build until the PRV opens, discharging vapour. As the pressure falls, the saturation temperature corresponding to this pressure also decreases. At some point, the temperature of the liquid will exceed this saturation temperature and vaporization will occur. Hence, mass and heat transfer occurs between phases with this type of event. This means that the simulation procedure for this case is similar to that described for the engulfing flame model, though the thermal network model is simpler. Though mass exchange between phases is expected, failure will occur before much liquid mass is vapourized.

Figure 6.7 represents the logic diagram for both impinging torch cases. The simulation for the liquid zone case is direct, requiring solution of the thermal network. For the vapour zone case, the network must be solved and mass exchanges must occur before conditions can be established for the next iteration. A discussion of the steps following the solution of the network equations was presented for the engulfing flame model in the previous Section and is similar for this model case.

Reference was made to a number of subroutines in the foregoing discussions. In the subsequent Sections, these model components are described more fully.

OVERALL MODEL ORGANIZATION
Impinging Flame Model
MAIN PROGRAM

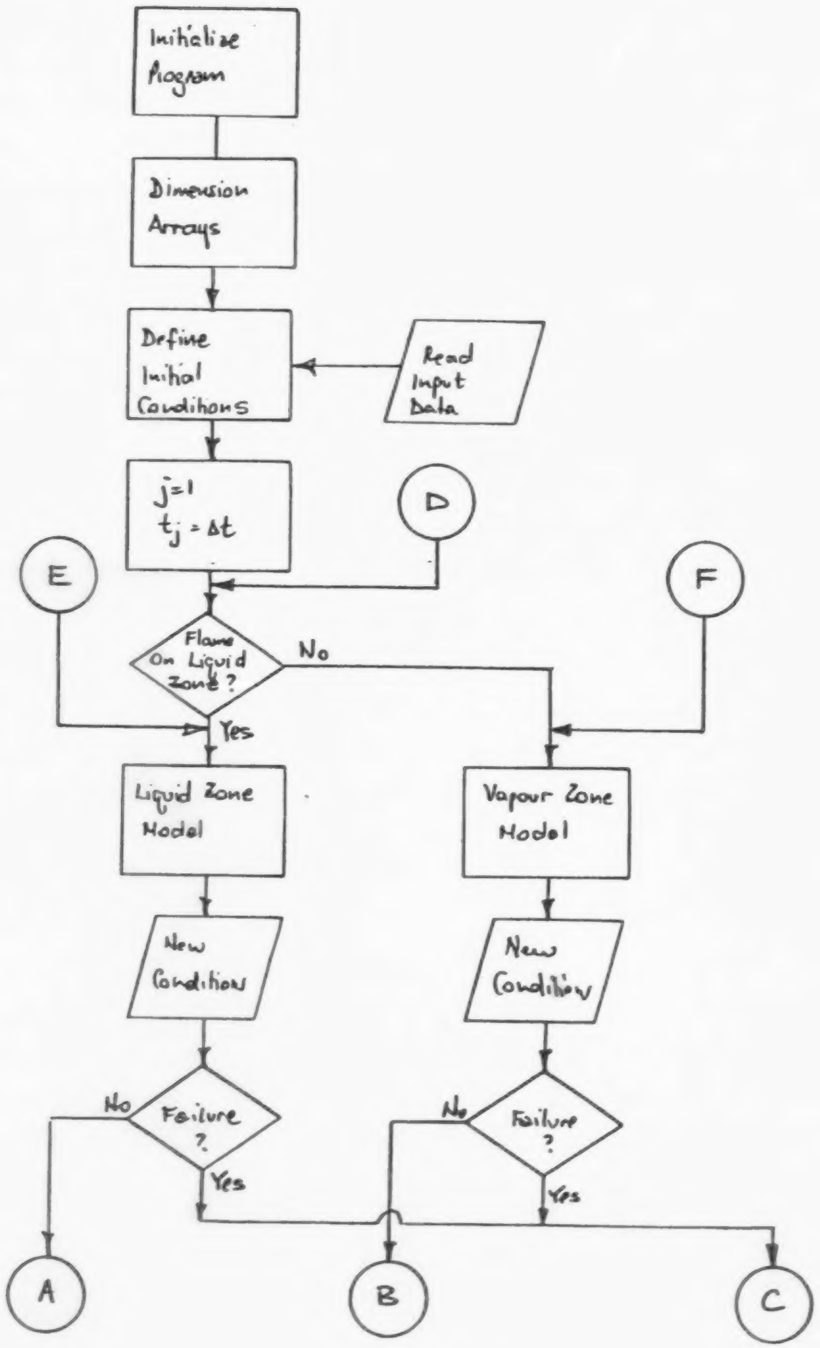
Initialize Program
Dimension Arrays
Define Initial Conditions
Read Input Data
j=1
$t_j = \Delta t$
D
E
F
Flame On Liquid Zone?
No
Yes
Liquid Zone Model
Vapour Zone Model
New Condition
New Condition
Failure?
Failure?
No
Yes
No
Yes
A
B
C

FIGURE 6.6

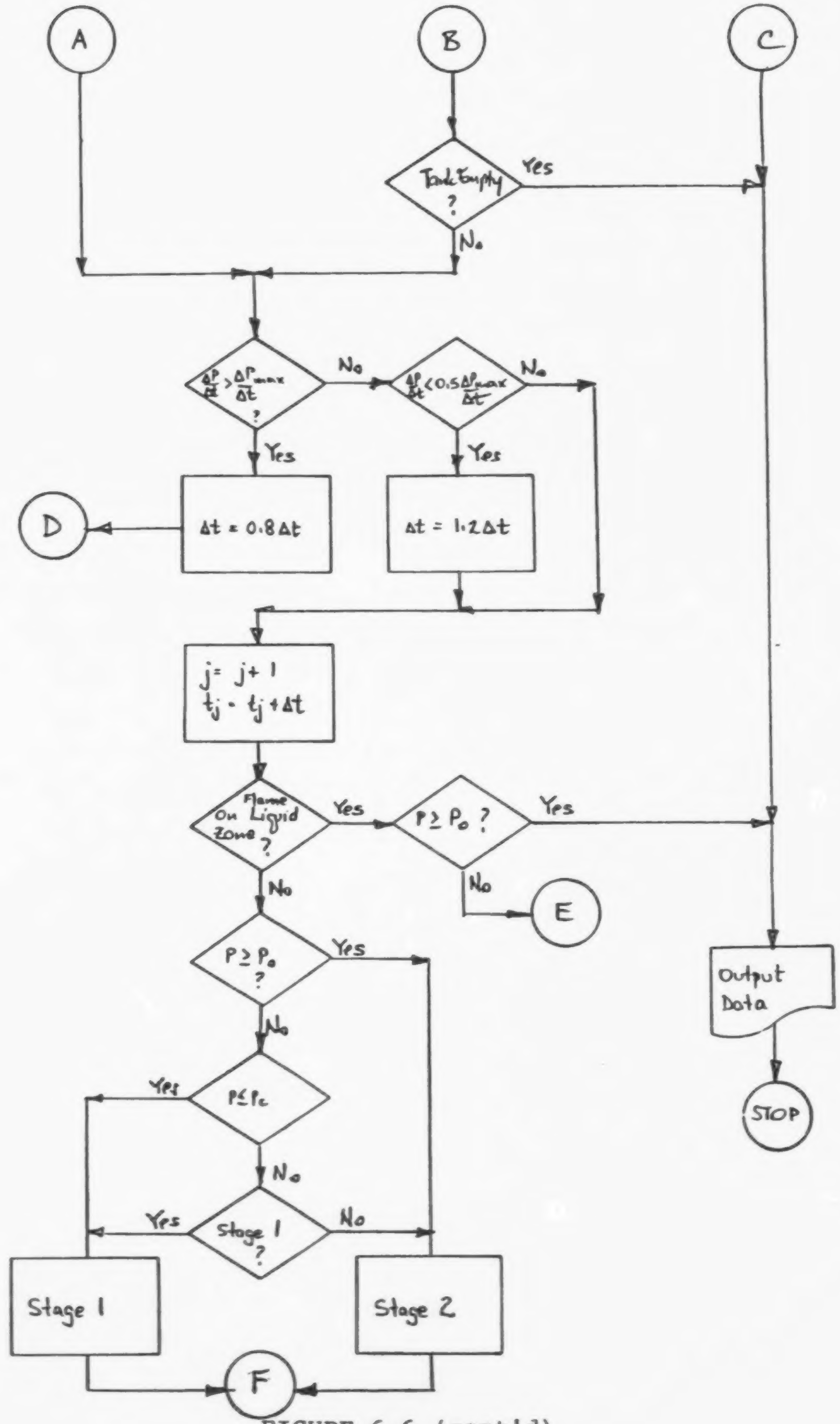
A
B
C
Tank Empty ?
Yes
No
$\frac{\Delta P}{\Delta t} > \frac{\Delta P_{max}}{\Delta t}$?
No
$\frac{\Delta P}{\Delta t} < 0.5 \frac{\Delta P_{max}}{\Delta t}$
No
Yes
Yes
D
$\Delta t = 0.8 \Delta t$
$\Delta t = 1.2 \Delta t$
$j = j + 1$
$t_j = t_j + \Delta t$
Flame On Liquid Zone ?
Yes
$P \geq P_o$?
Yes
No
No
E
Output Data
STOP
$P \geq P_o$?
Yes
No
$P \leq P_c$
Yes
No
Stage 1 ?
Yes
No
Stage 1
Stage 2
F

FIGURE 6.6 (cont'd)

MODEL FORMULATION - Logic Diagram
Impinging Flame Model

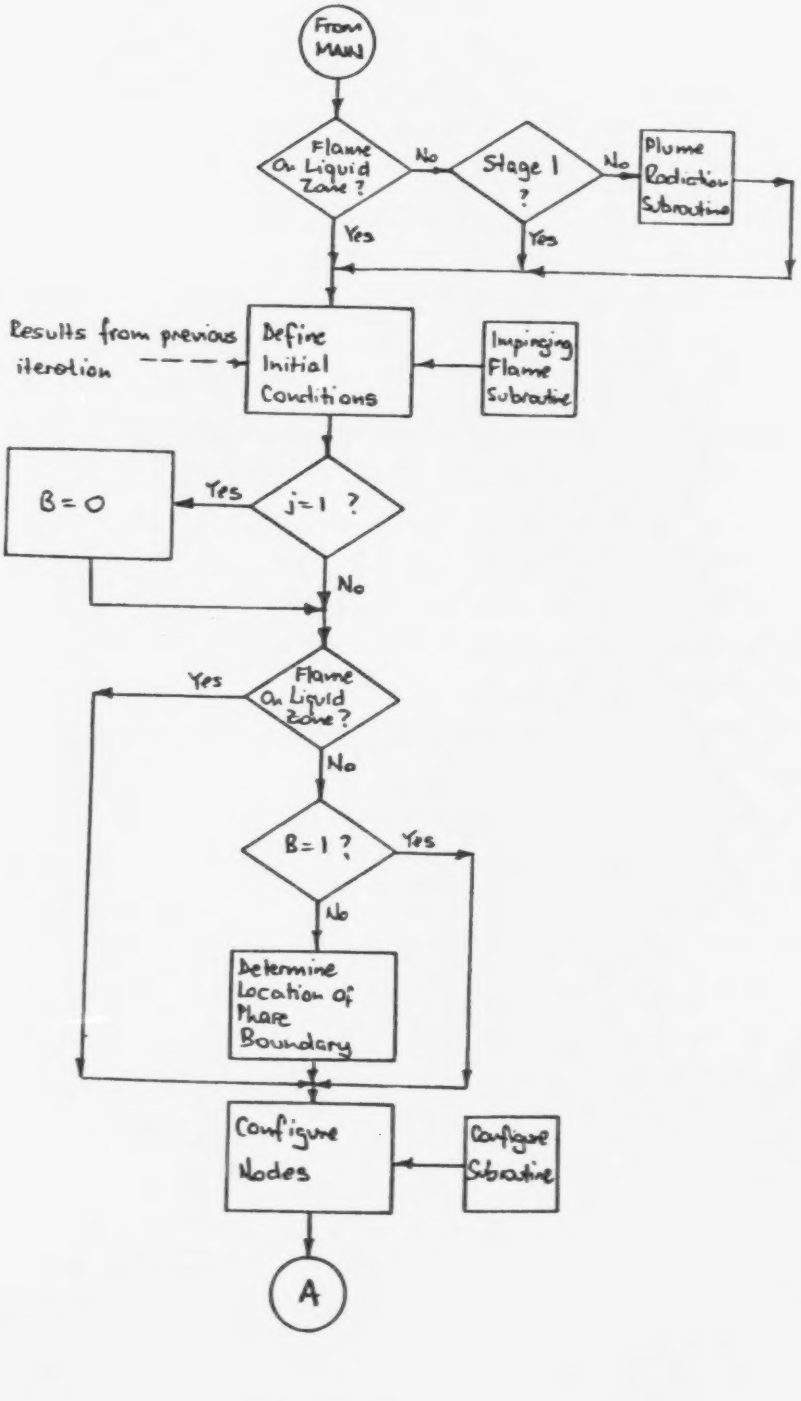
From MAIN
Flame On Liquid Zone ?
No
Stage 1 ?
No
Plume Radiation Subroutine
Yes
Yes
Results from previous iteration
Define Initial Conditions
Impinging Flame Subroutine
B = 0
Yes
j = 1 ?
No
Yes
Flame On Liquid Zone?
No
B = 1 ?
Yes
No
Determine Location of Phase Boundary
Configure Nodes
Configure Subroutine
A

FIGURE 6.7

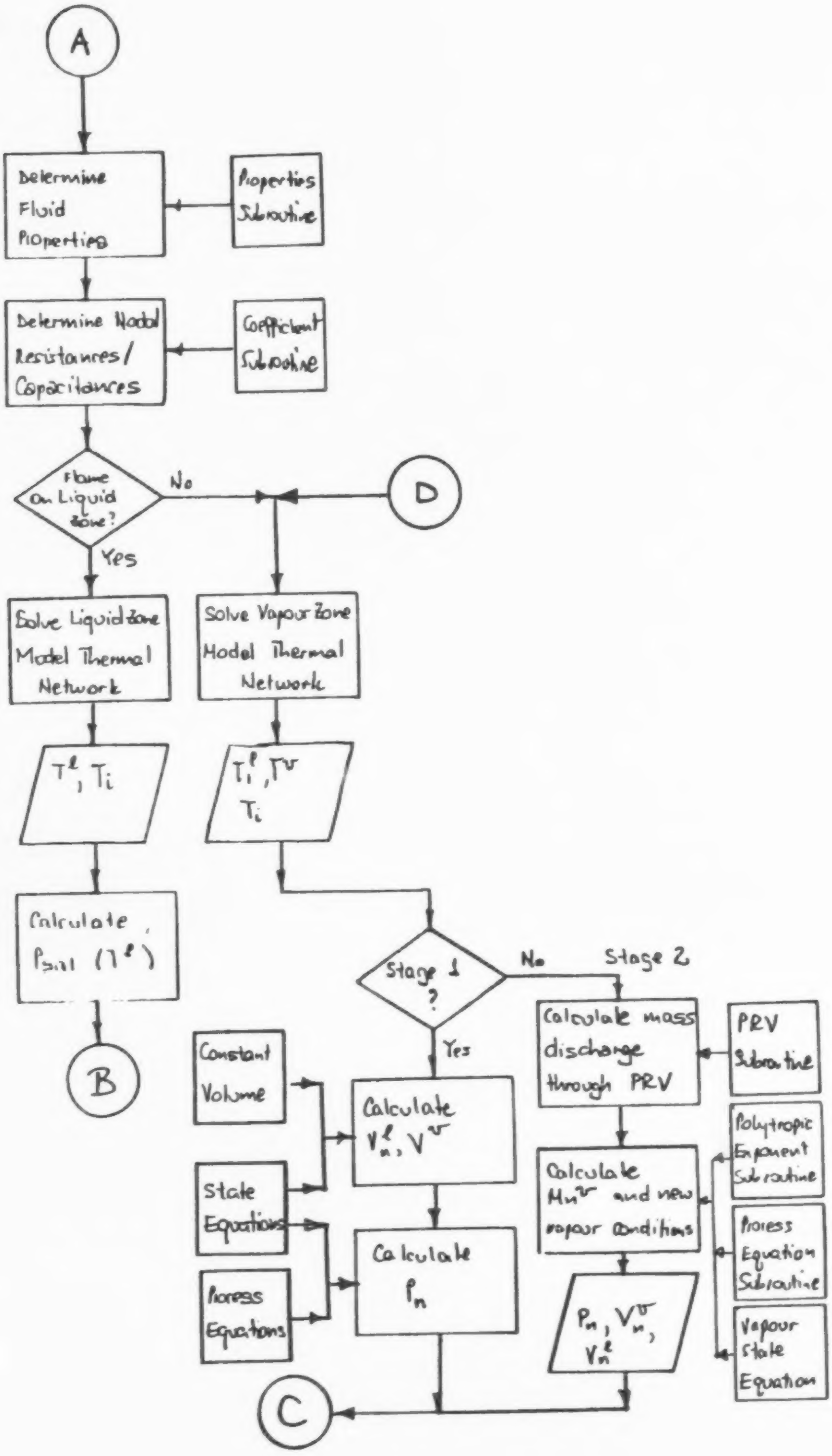
A
Determine Fluid Properties
Properties Subroutine
Determine Nodal Resistances/ Capacitances
Coefficient Subroutine
Flame On Liquid Zone?
No
Yes
D
Solve Liquid Zone Model Thermal Network
Solve Vapour Zone Model Thermal Network
T^l, T_i
T_i^l, T^v T_i
Calculate P_{sat} (T^l)
B
Stage 1 ?
No
Stage 2
Yes
Constant Volume
State Equations
Process Equations
Calculate V_n^l, V^v
Calculate P_n
Calculate mass discharge through PRV
PRV Subroutine
Calculate M_n^v and new vapour conditions
Polytropic Exponent Subroutine
Process Equation Subroutine
Vapour State Equation
P_n, V_n^v, V_n^l
C

FIGURE 6.7 (cont'd)

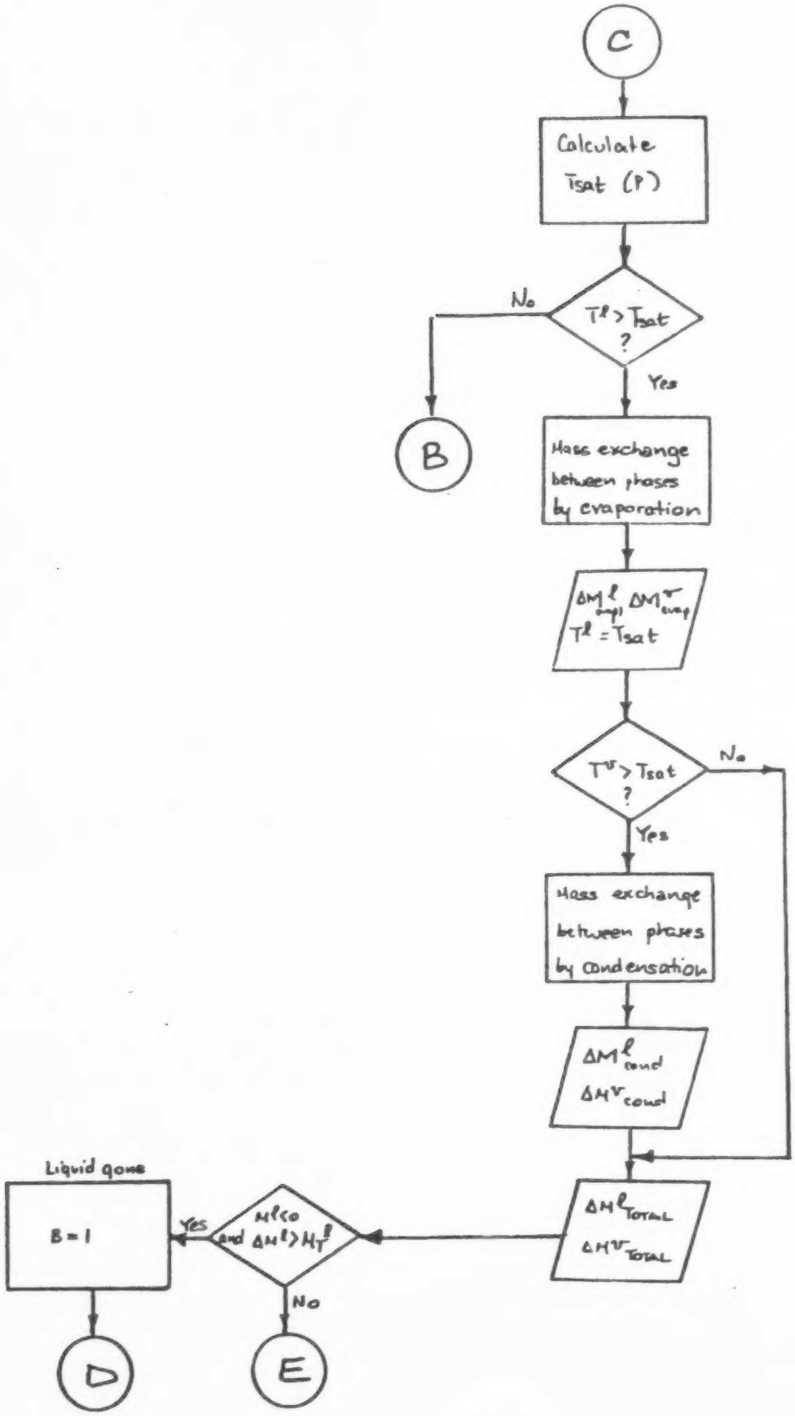
C
Calculate Tsat (P)
No
$T^l >$ Tsat ?
Yes
B
Mass exchange between phases by evaporation
ΔM^l_{evap}, ΔM^v_{evap}
$T^l =$ Tsat
$T^v >$ Tsat ?
No
Yes
Mass exchange between phases by condensation
ΔM^l_{cond}
ΔM^v_{cond}
ΔM^l_{TOTAL}
ΔM^v_{TOTAL}
$M^l < 0$ and $\Delta M^l > M^l_T$
Yes
No
Liquid gone
B = 1
D
E

FIGURE 6.7 (cont'd)

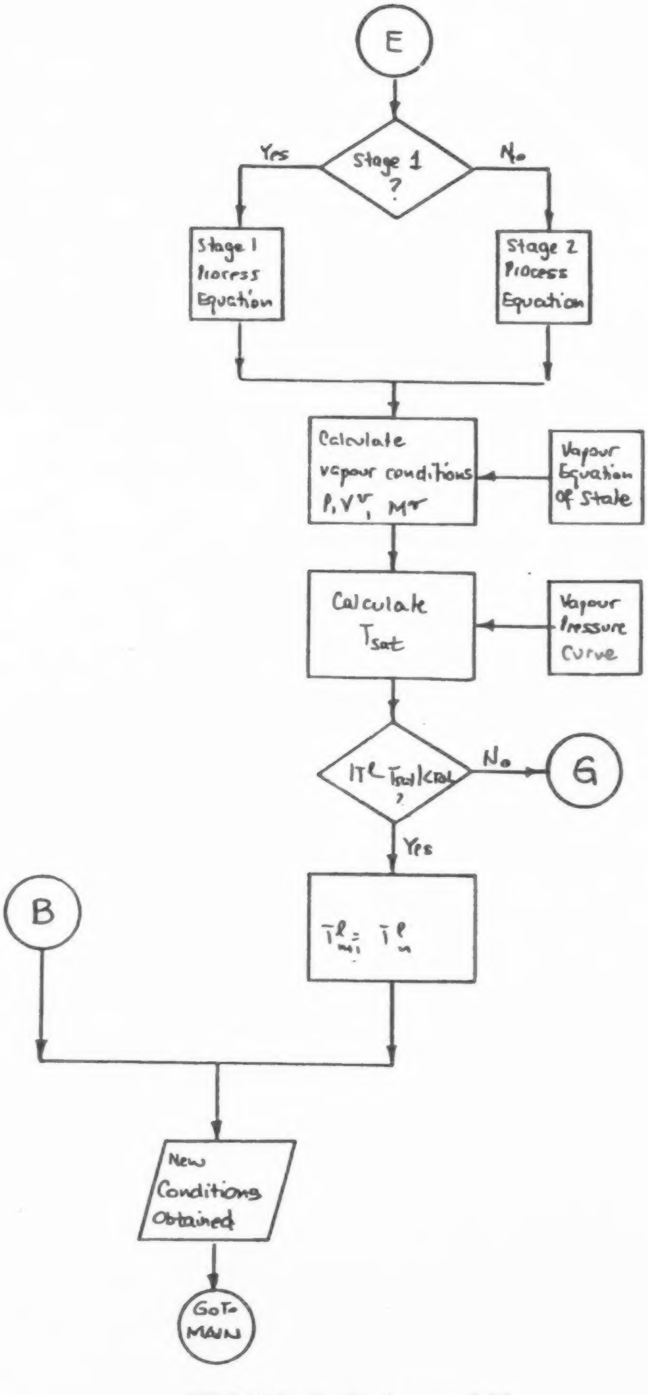
E
Stage 1 ?
Yes
No
Stage 1 Process Equation
Stage 2 Process Equation
Calculate vapour conditions P, V^v, M^v
Vapour Equation of State
Calculate T_sat
Vapour Pressure Curve
|T^l - T_sat| < Tol ?
No
G
Yes
T^l_{n+1} = T^l_n
B
New Conditions Obtained
Go To MAIN

FIGURE 6.7 (cont'd)

NOTES:

Stage 1: PRV closed
Stage 2: PRV open

j = time step number
n = iteration number
Δt = time step
A = liquid saturation flag
B = liquid boildown flag

R_m = mixing resitance between liquid zones

T^v = vapour temperature
T_1^l = saturated liquid zone temperature
T_2^l = subcooled liquid zone temperature

M^v = vapour mass
M_1^l = saturated liquid mass
M_2^l = subcooled liquid mass
M_T^l = total liquid mass
P = system pressure
P_{sat} = saturation pressure
T_{sat} = saturation temperature

V^v = vapour volume
V_1^l = saturated liquid volume
V_2^l = subcooled liquid volume
V_T^l = total liquid volume

P_o = PRV open pressure set point
P_c = PRV close pressure set point

MODEL COMPONENTS

Component Reference No.	Component	Model		
		Engulfing Flame	Impinging Torch	
			Liquid zone	Vapour zone
6.3.1	Location of phase boundaries	1		1
6.3.2	Location of zonal boundaries	1		
6.3.3	Notal configuring	1	2	3
6.3.4	Heat input functions - pool fire	1		
6.3.5	- impinging torch		1	1
6.3.6	- Plume radiation	1		
6.3.7	Fluid Properties subroutine	1	1	1
6.3.8	Steel properties subroutine	1	1	1
6.3.9	Insulation properties subroutine	1	1	1
6.3.10	EXPLOSAFE properties subroutine	1	1	1
6.3.11	Heat transfer coefficients subroutine	1	1	1
6.3.12	Coefficients subroutine	1	2	3
6.3.13	R_m subroutine	1		
6.3.14	Thermal network			
6.3.15	PRV subroutine	1		1
6.3.16	State equations - liquid phase	1		1
6.3.17	- vapour phase	1		1
6.3.18	Process equations - Stage 1	1		1
6.3.19	- Stage 2	1		1
6.3.20	Vapour pressure equation	1	1	1
6.3.21	Mass transfer equations - vaporization	1		1
6.3.22	- condensation	1		1
6.3.23	Failure subroutine	1	2	3
6.3.24	PRV set points	1		1

TABLE 6.1

6.3 MODEL COMPONENT DESCRIPTION

The components which constitute the detailed aspects of the thermodynamic system are listed in Table 6.1. A reference number is associated with each of these components. It should be noted that some subroutines are common to a number of the proposed models; for example, the location of phase boundaries subroutine (6.3 1) is the same for both the engulfing flame and impinging torch (vapour zone) models. On the other hand, the nodal configuring subroutine is different for each of the models and hence is given the following reference numbers 6.3.3.1, 6.3.3.2, and 6.3.3.3 for the engulfing flame, impinging torch (liquid zone), and impinging torch (vapour zone) models, respectively. Each of these subroutines are discussed in detail in the subsections below.

6.3.1 Location of Phase Boundaries

The location of the phase boundaries for both the engulfing flame and impinging torch (vapour zone) models can be determined using the subroutine logic presented in Figure 6.8. The aim of the procedure is to determine the distance to the liquid level from the tank top (x_n), the area of the vapour/liquid boundary ($A_n^{\ell v}$), and the area of the tank wetted by vapour (A_n^v) and liquid (A_n^{ℓ}).

6.3.2 Location of Zonal Boundaries

The boundary between the saturated and sub-cooled liquid zones is determined by their relative volumes, with the latter volume always less than 95% of the total liquid volume. Figure 6.9 presents the logic to be used to determine the geometry of the inner sub-cooled zone. The distance from the liquid level to the tank top, x_{2_n}, is calculated, as are the surface areas.

6.3.3.1 Nodal Configuring - Engulfing Flame Model

In order that the model be flexible, the user specifies the total number of nodes around the tank shell and the program determines internodal spacing, nodal areas, and determines whether the nodes are located adjacent to either the liquid or vapour space as shown in Figure 6.10. This subroutine initializes the heat transfer resistance and thermal capacitance vectors. Internodal connections are defined.

LOCATION OF PHASE BOUNDARIES
(6.3.1.1)

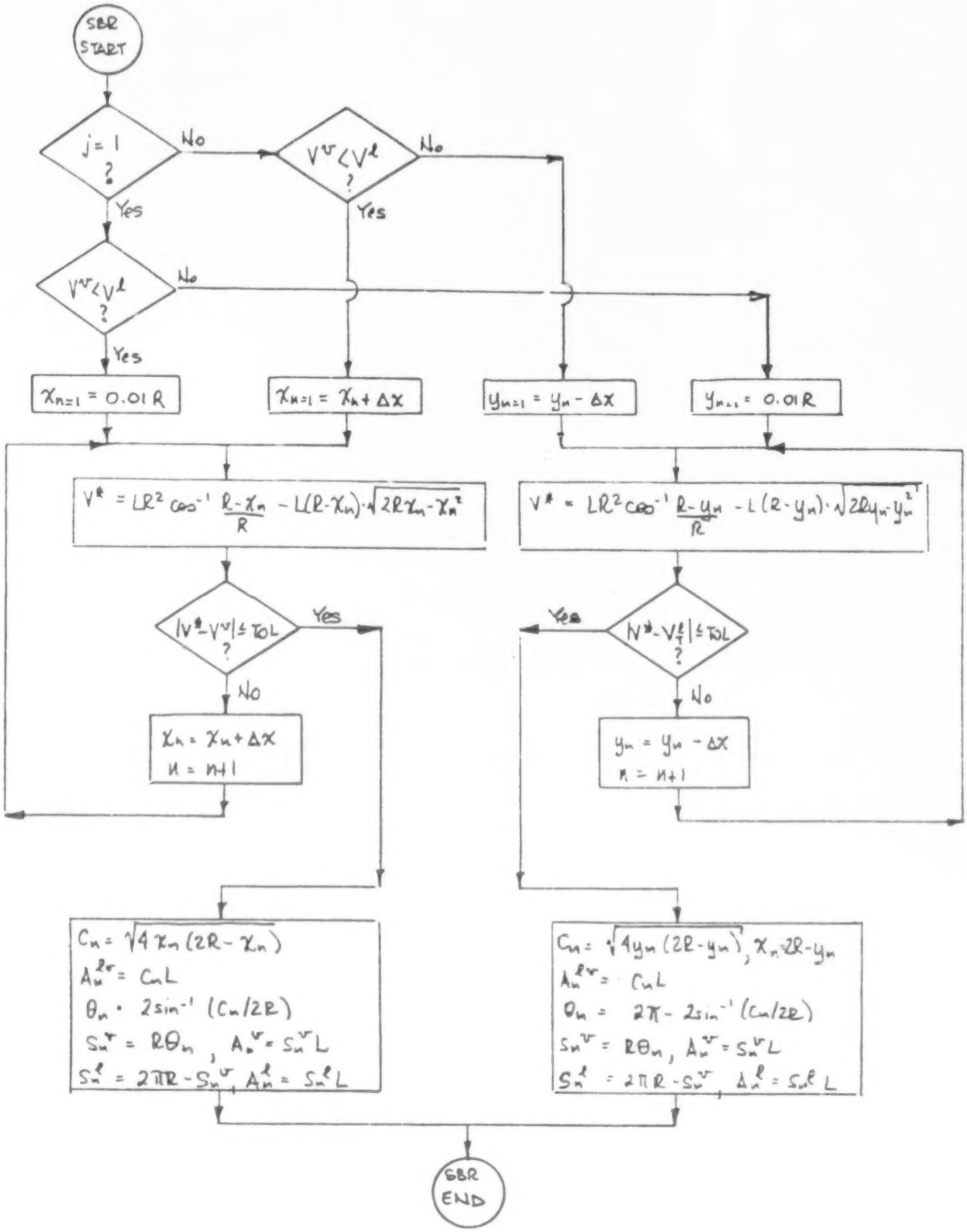
SBR START
$j = 1$?
No
Yes
$V^v < V^l$?
No
Yes
$V^v < V^l$?
No
Yes
$x_{n=1} = 0.01R$
$x_{n=1} = x_n + \Delta x$
$y_{n=1} = y_n - \Delta x$
$y_{n=1} = 0.01R$
$V^* = LR^2 \cos^{-1} \frac{R - x_n}{R} - L(R - x_n) \cdot \sqrt{2Rx_n - x_n^2}$
$V^* = LR^2 \cos^{-1} \frac{R - y_n}{R} - L(R - y_n) \cdot \sqrt{2Ry_n - y_n^2}$
$|V^* - V^v| \leq TOL$?
Yes
No
$|V^* - V_T^l| \leq TOL$?
Yes
No
$x_n = x_n + \Delta x$
$n = n+1$
$y_n = y_n - \Delta x$
$n = n+1$
$C_n = \sqrt{4x_n(2R - x_n)}$
$A_n^{lv} = C_n L$
$\theta_n = 2\sin^{-1}(C_n/2R)$
$S_n^v = R\theta_n$, $A_n^v = S_n^v L$
$S_n^l = 2\pi R - S_n^v$, $A_n^l = S_n^l L$
$C_n = \sqrt{4y_n(2R - y_n)}$, $x_n = 2R - y_n$
$A_n^{lv} = C_n L$
$\theta_n = 2\pi - 2\sin^{-1}(C_n/2R)$
$S_n^v = R\theta_n$, $A_n^v = S_n^v L$
$S_n^l = 2\pi R - S_n^v$, $A_n^l = S_n^l L$
SBR END

FIGURE 6.8

NOTES:

J	time step number
V^v	vapour volume
V_T^l	liquid volume (total)
R	tank radius
L	tank length
x_n	distance from tank top to vapour/liquid interface
y_n	distance from tank bottom to vapour/liquid interface
Δx	incremental distance chosen so that convergence occurs rapidly.
C_n	distance between walls along interface
A_n^{lv}	interface surface area
θ_n	angle
A_n^v	surface area wetted by vapour
A_n^l	surface area wetted by liquid
TOL	tolerance allowed between approximated value of volume, V^*, and actual.
SBR	subroutine

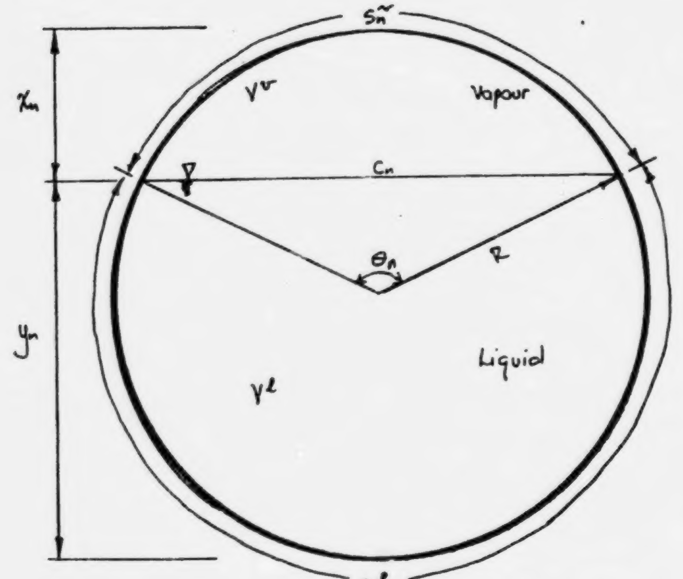

FIGURE 6.8 (cont'd)

LOCATION OF ZONAL BOUNDARIES
(6.3.2.1)

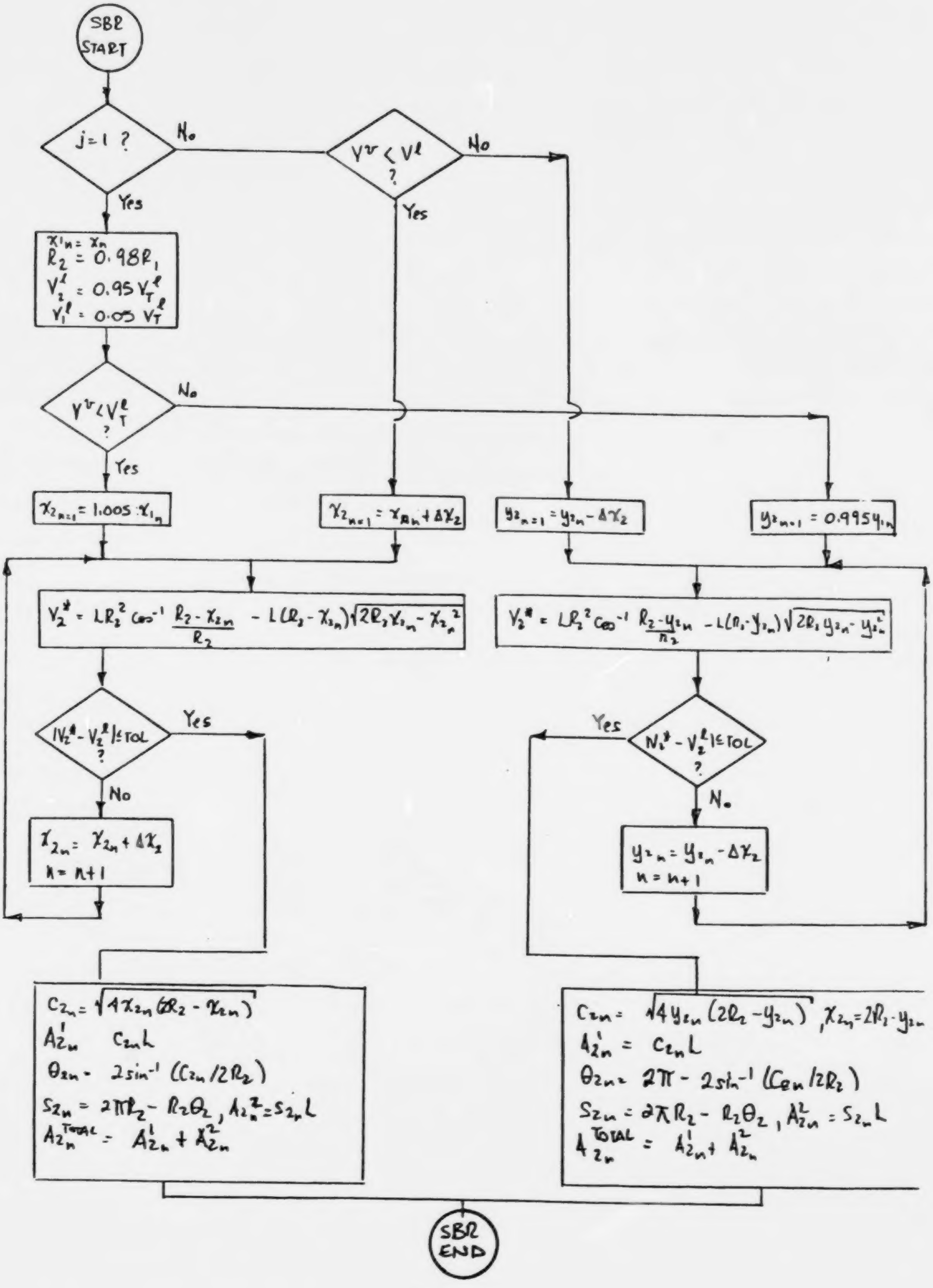
SBR START
j=1 ?
No
Yes
$V^v < V^l$?
No
Yes
$x'_n = x_n$
$R_2 = 0.98R_1$
$V_2^l = 0.95V_T^l$
$V_1^l = 0.05V_T^l$
$V^v < V_T^l$?
No
Yes
$x_{2_{n=1}} = 1.005x_{1_n}$
$x_{2_{n+1}} = x_{2n} + \Delta x_2$
$y_{2_{n=1}} = y_{2n} - \Delta x_2$
$y_{2_{n+1}} = 0.995y_{1n}$
$V_2^* = LR_2^2\cos^{-1}\frac{R_2 - x_{2n}}{R_2} - L(R_2 - x_{2n})\sqrt{2R_2x_{2n} - x_{2n}^2}$
$V_2^* = LR_2^2\cos^{-1}\frac{R_2 - y_{2n}}{R_2} - L(R_2 - y_{2n})\sqrt{2R_2y_{2n} - y_{2n}^2}$
$|V_2^* - V_2^l| \le TOL$?
Yes
No
$x_{2n} = x_{2n} + \Delta x_2$
$n = n+1$
$|V_2^* - V_2^l| \le TOL$?
Yes
No
$y_{2n} = y_{2n} - \Delta x_2$
$n = n+1$
$C_{2n} = \sqrt{4x_{2n}(2R_2 - x_{2n})}$
$A_{2n}^1 = C_{2n}L$
$\theta_{2n} = 2\sin^{-1}(C_{2n}/2R_2)$
$S_{2n} = 2\pi R_2 - R_2\theta_2$, $A_{2n}^2 = S_{2n}L$
$A_{2n}^{TOTAL} = A_{2n}^1 + A_{2n}^2$
$C_{2n} = \sqrt{4y_{2n}(2R_2 - y_{2n})}$, $x_{2n} = 2R_2 - y_{2n}$
$A_{2n}^1 = C_{2n}L$
$\theta_{2n} = 2\pi - 2\sin^{-1}(C_{2n}/2R_2)$
$S_{2n} = 2\pi R_2 - R_2\theta_2$, $A_{2n}^2 = S_{2n}L$
$A_{2n}^{TOTAL} = A_{2n}^1 + A_{2n}^2$
SBR END

FIGURE 6.9

NOTES:

j	time step number
V^v	vapour volume
V_1^l	saturated liquid volume
V_2^l	subcooled liquid volume
R	tank radius
R_2	subcooled zone radius
L	tank length
x_{2n}	distance from tank top to boundary between saturated and liquid zones
y_{2n}	distance from tank bottom to boundary " " " " "
Δx_2	incremental distance
c_{2n}	width of boundary
A^1_{2n}	area of boundary
A^2_{2n}	area of subcooled zone below boundary
TOL	tolerance
SBR	subroutine

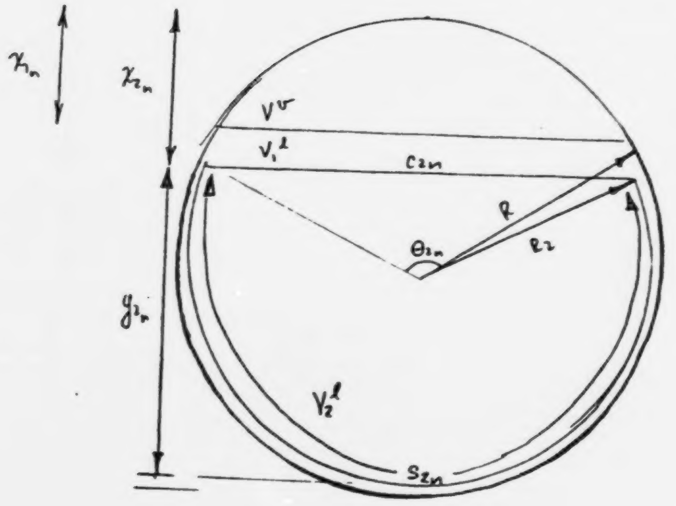

FIGURE 6.9 (cont'd)

NODAL CONFIGURING - Engulfing Flame Model
(6.3.3.1)

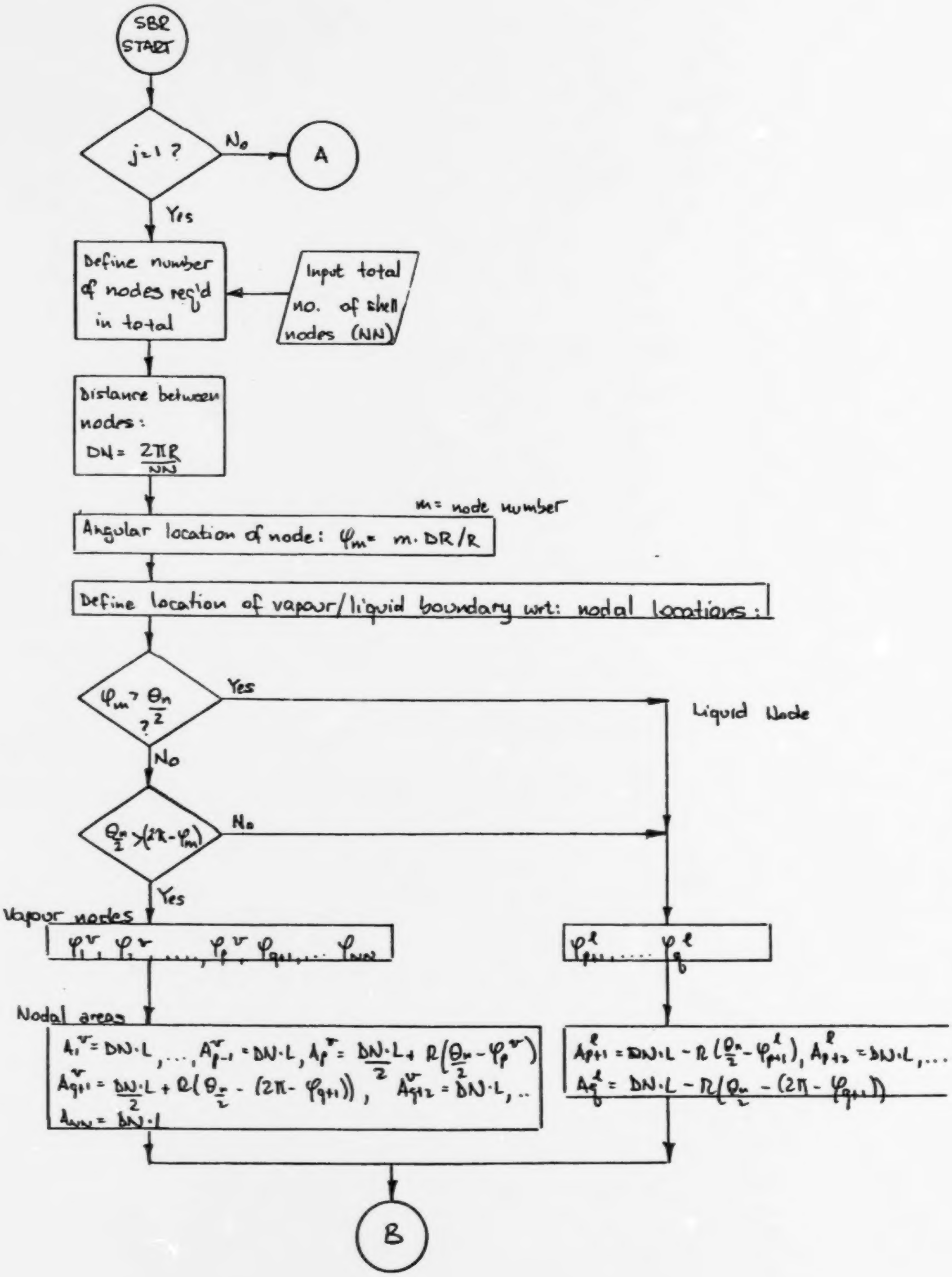
SBR START
j=1 ?
No
A
Yes
Define number of nodes req'd in total
Input total no. of shell nodes (NN)
Distance between nodes: DN = 2πR/NN
m = node number
Angular location of node: φm = m·DR/R
Define location of vapour/liquid boundary wrt: nodal locations:
φm > θn/2 ?
Yes
Liquid Node
No
θn/2 > (2π - φm)
No
Yes
Vapour nodes
φ1v, φ2v, ..., φpv, φq+1, ... φNN
φp+1l, ... φql
Nodal areas
A1v = DN·L, ..., Ap-1v = DN·L, Apv = DN/2·L + R(θn/2 - φpv)
Aq+1v = DN/2·L + R(θn/2 - (2π - φq+1)), Aq+2v = DN·L, ..
ANN = DN·L
Ap+1l = DN·L - R(θn/2 - φp+1l), Ap+2l = DN·L, ...
Aql = DN·L - R(θn/2 - (2π - φq+1))
B

FIGURE 6.10

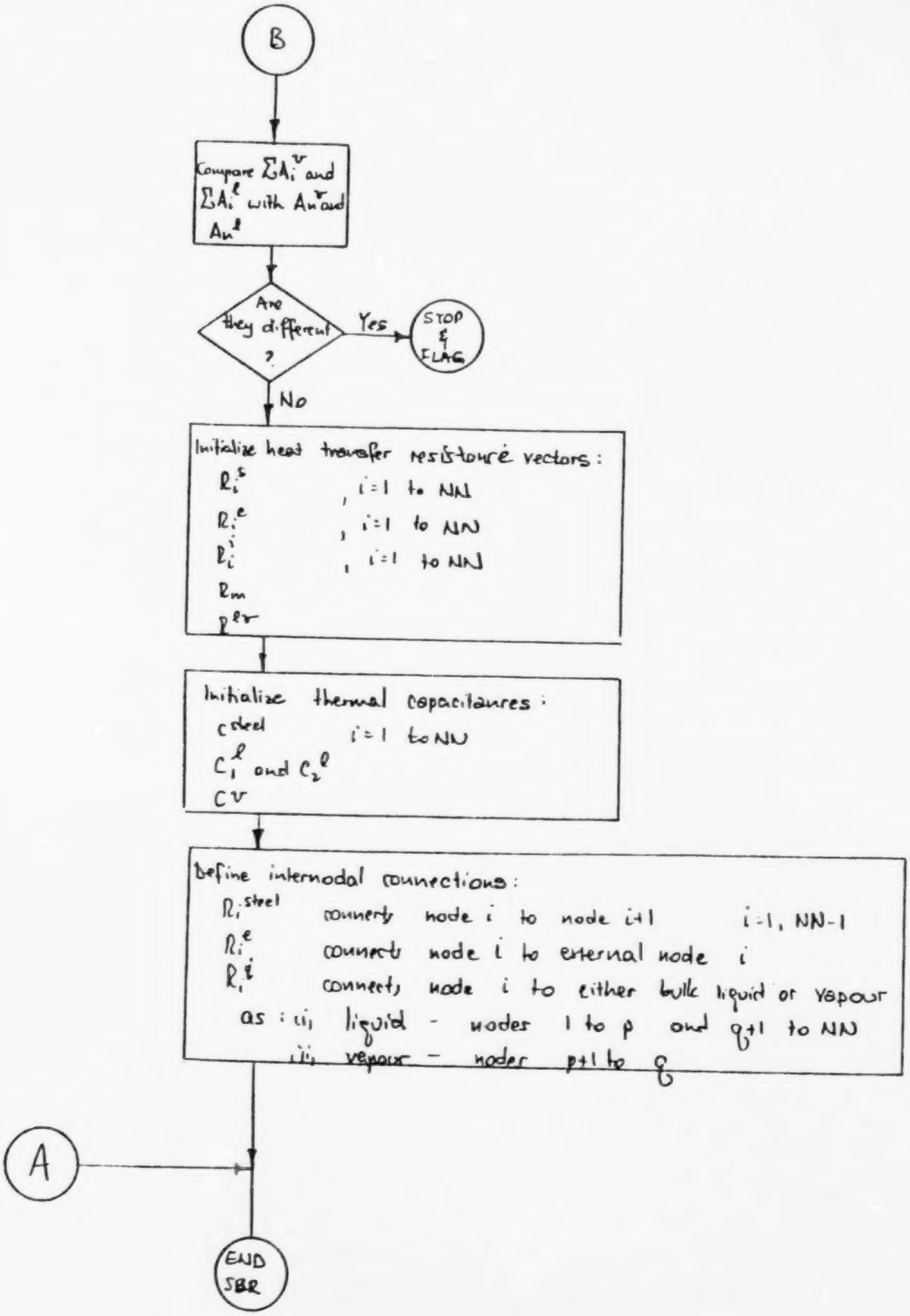
B
Compare $\sum A_i^v$ and $\sum A_i^l$ with A_n^v and A_n^l
Are they different ?
Yes
STOP & FLAG
No
Initialize heat transfer resistance vectors:
R_i^s , i=1 to NN
R_i^e , i=1 to NN
R_i^i , i=1 to NN
R_m
R^{lv}
Initialize thermal capacitances:
C^{steel} i=1 to NN
C_1^l and C_2^l
C^v
Define internodal connections:
R_i^{steel} connects node i to node i+1 i=1, NN-1
R_i^e connects node i to external node i
R_i^i connects node i to either bulk liquid or vapour
as : i) liquid - nodes 1 to p and q+1 to NN
ii) vapour - nodes p+1 to q
A
END SBR

FIGURE 6.10 (cont'd)

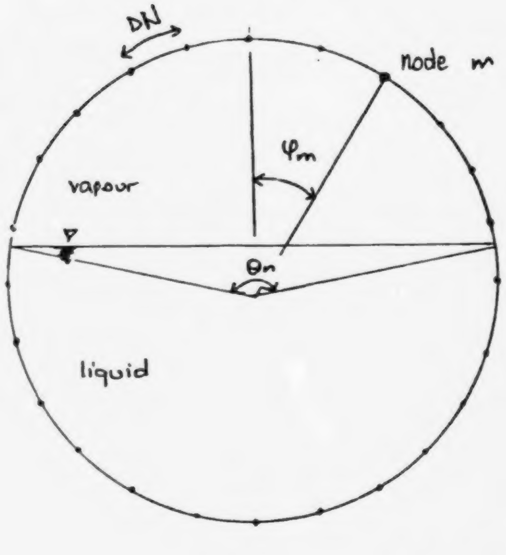
DN
node m
φ_m
vapour
∇
θ_n
liquid

TYPICAL SHELL NODAL CONFIGURATION
Engulfing flame model.

FIGURE 6.10 (cont'd)

6.3.3.2 Nodal Configuring - Impinging Torch Model (vapour zone)

This procedure, Figure 6.11, defines the nodes, the heat transfer resistance and thermal capacitance vectors, and the internodal connections for the impinging torch model, as previously illustrated in Figure 5.6.

6.3.3.3 Nodal Configuring - Impinging Torch Model (liquid zone)

Figure 6.12 presents this subroutine. As with the above-mentioned procedure, nodes are defined, as are the resistance and capacitance vectors, and the connections between nodes.

6.3.4 Heat Input Function - Pool Fire

The flame surrounding the tank represents the system forcing function. That is, the intensity of the fire determines the rate at which the tank pressure rises, the PRV valve opens, the lading boils away, etc.. To describe the conditions external to the tank, both the boundary temperatures and heat transfer coefficients are defined. The coefficients (6.3.11) are taken to be dependent parameters, with the external temperatures being user specified. Figure 6.13 shows two types of flame temperature profiles which can be specified. T_f can be taken to be constant throughout the accident or can be variable with actual or hypothetical data input. Figure 6.14 shows how this procedure is followed by the subroutine.

6.3.5 Heat Input Function - Impinging Torch

For the impinging torch model, the flame is taken to act over the full nodal area at node 4 (Figure 5.6), where DN is this portion of the circumference. One heat transfer coefficient and flame temperature need to be determined. As with the engulfing flame model, the flame temperature is specified by the user as input, see Figure 6.15.

6.3.6 Heat Input Function - Plume Radiation

In most engulfing flame events, such as those in the Suffield trials, the vented propane gas will ignite and burn as a large plume. This plume will not normally

NODAL CONFIGURING - Impinging Torch Model
Liquid Zone
(6.3.3.2)

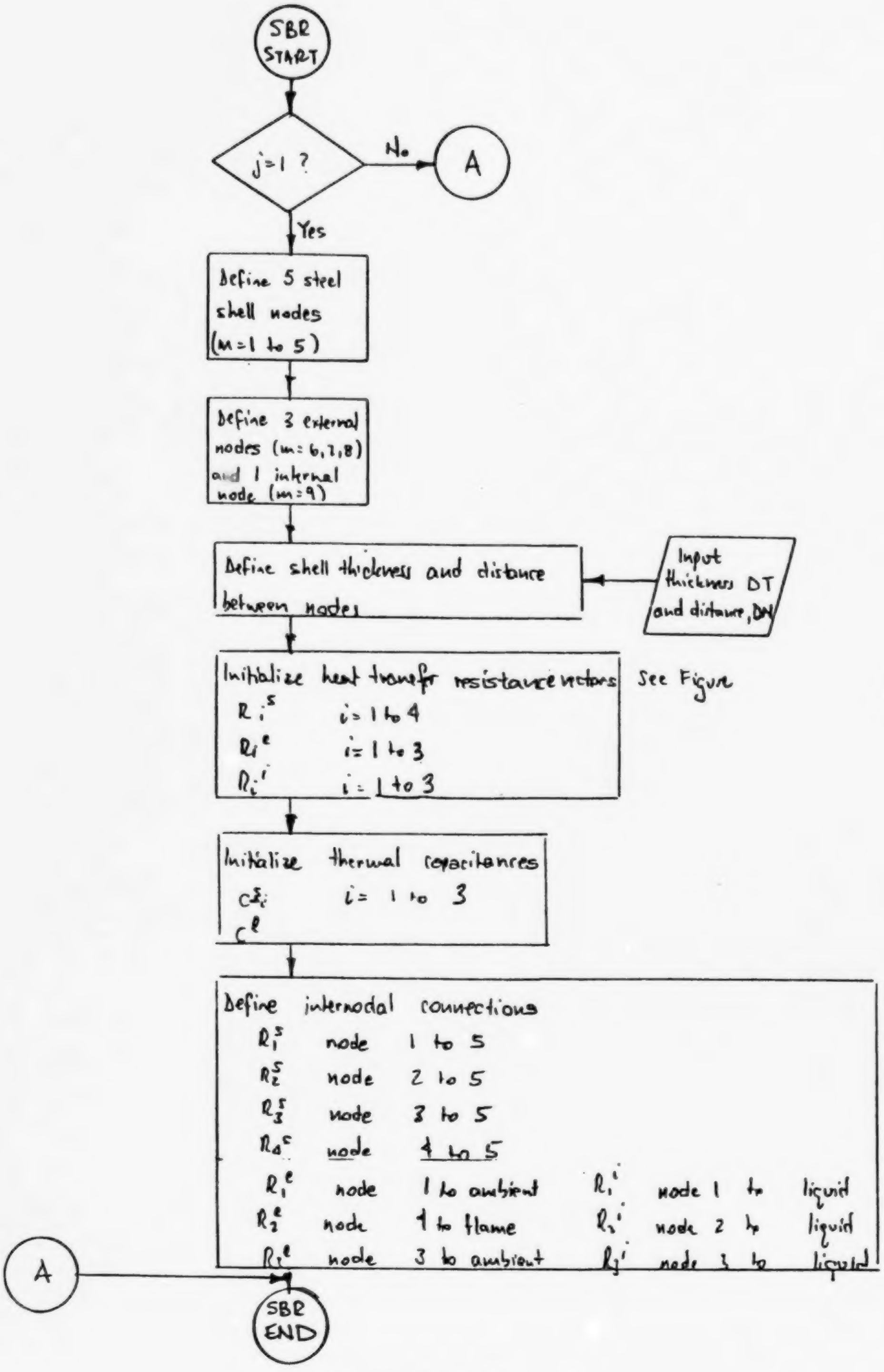
SBR START
j=1 ?
No
A
Yes
Define 5 steel shell nodes (m=1 to 5)
Define 3 external nodes (m=6,7,8) and 1 internal node (m=9)
Define shell thickness and distance between nodes
Input thickness DT and distance, DN
Initialize heat transfr resistance vectors
See Figure
R_i^s i=1 to 4
R_i^e i=1 to 3
R_i^i i=1 to 3
Initialize thermal capacitances
C_i^s i= 1 to 3
C^l
Define internodal connections
R_1^s node 1 to 5
R_2^s node 2 to 5
R_3^s node 3 to 5
R_4^s node 4 to 5
R_1^e node 1 to ambient
R_1^i node 1 to liquid
R_2^e node 4 to flame
R_2^i node 2 to liquid
R_3^e node 3 to ambient
R_3^i node 3 to liquid
A
SBR END

FIGURE 6.11

NODAL CONFIGURING - Impinging Torch Model
Vapour Zone
(5.3.3.3)

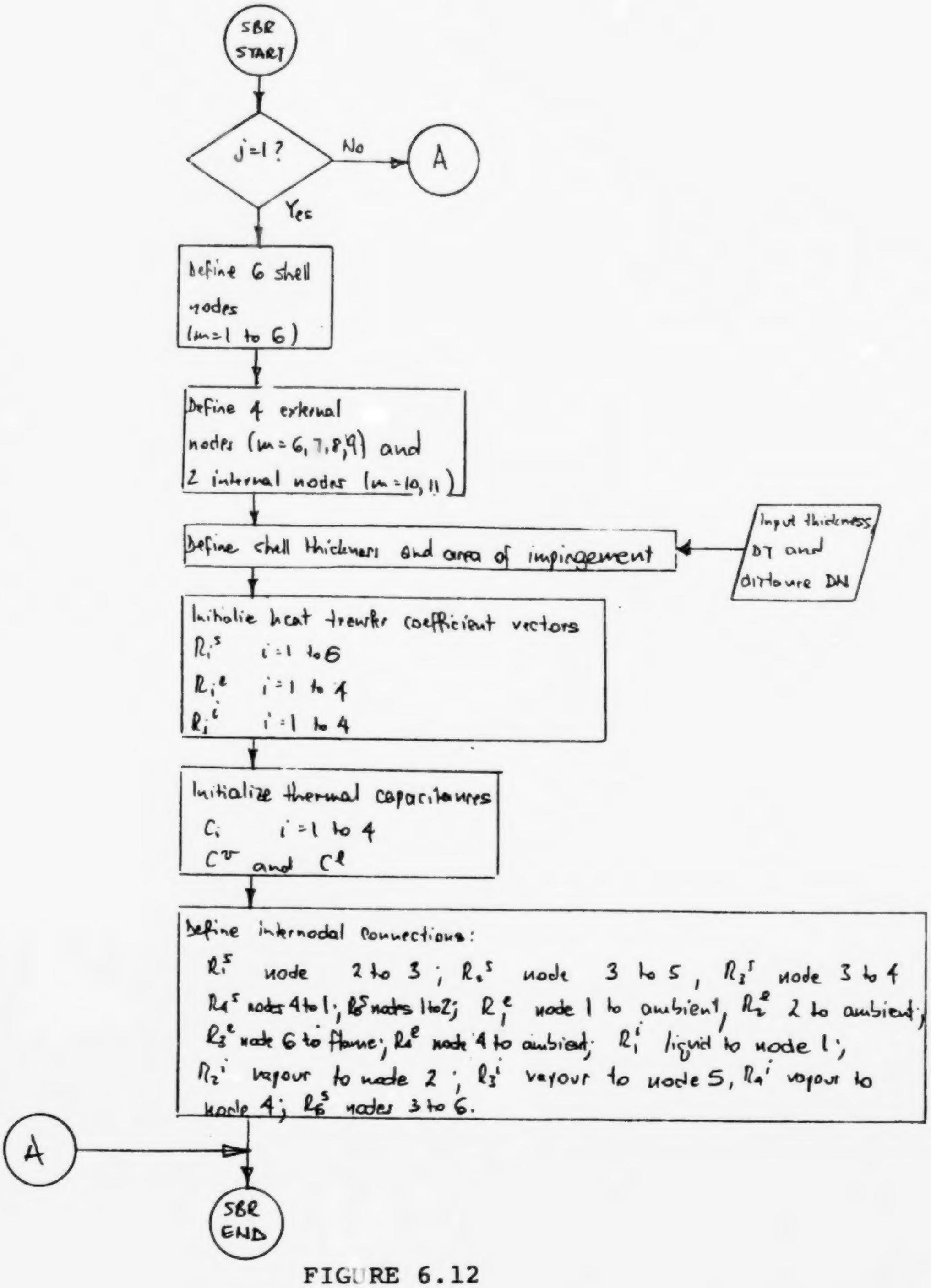
SBR START
j=1 ?
No
A
Yes
Define 6 shell nodes (m=1 to 6)
Define 4 external nodes (m=6, 7, 8, 9) and 2 internal nodes (m=10, 11)
Define shell thickness and area of impingement
Input thickness DT and distance DN
Initialize heat transfer coefficient vectors
R_i^s i=1 to 6
R_i^e i=1 to 4
R_i^i i=1 to 4
Initialize thermal capacitances
C_i i=1 to 4
C^v and C^l
Define internodal connections:
R_1^s node 2 to 3; R_2^s node 3 to 5, R_3^s node 3 to 4
R_4^s nodes 4 to 1; R_5^s nodes 1 to 2; R_1^e node 1 to ambient, R_2^e 2 to ambient;
R_3^e node 6 to flame; R_4^e node 4 to ambient; R_1^i liquid to node 1;
R_2^i vapour to node 2; R_3^i vapour to node 5, R_4^i vapour to node 4; R_6^s nodes 3 to 6.
A
SBR END

FIGURE 6.12

POSSIBLE FLAME TEMPERATURE PROFILES

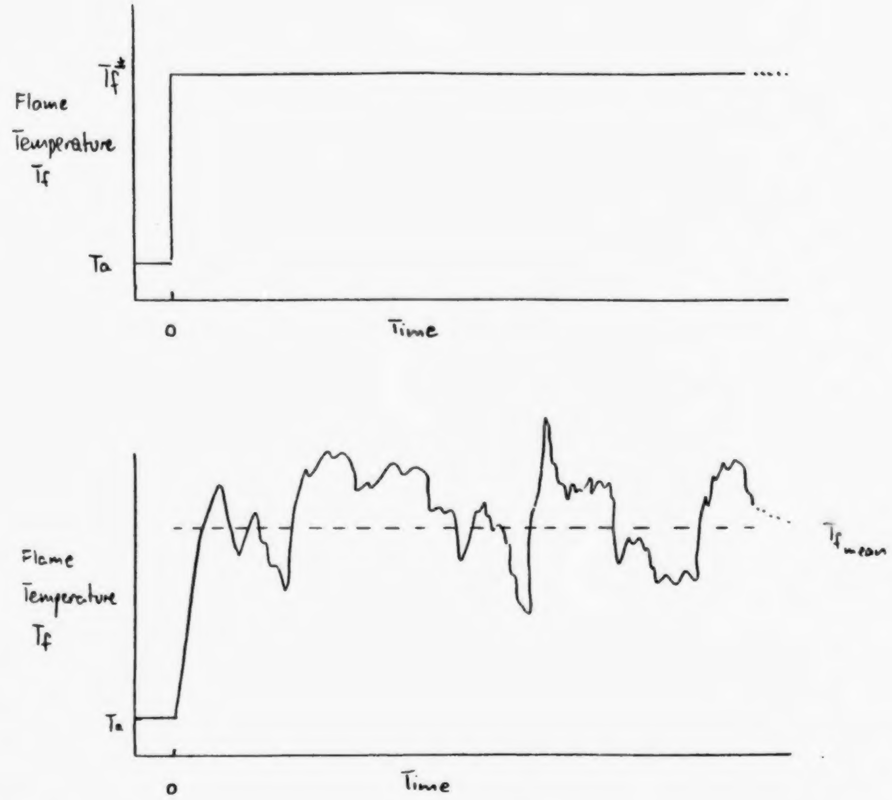

$T_f = T_f(t)$

FIGURE 6.13

HEAT INPUT FUNCTION - Pool Fire
(6.3.4.1)

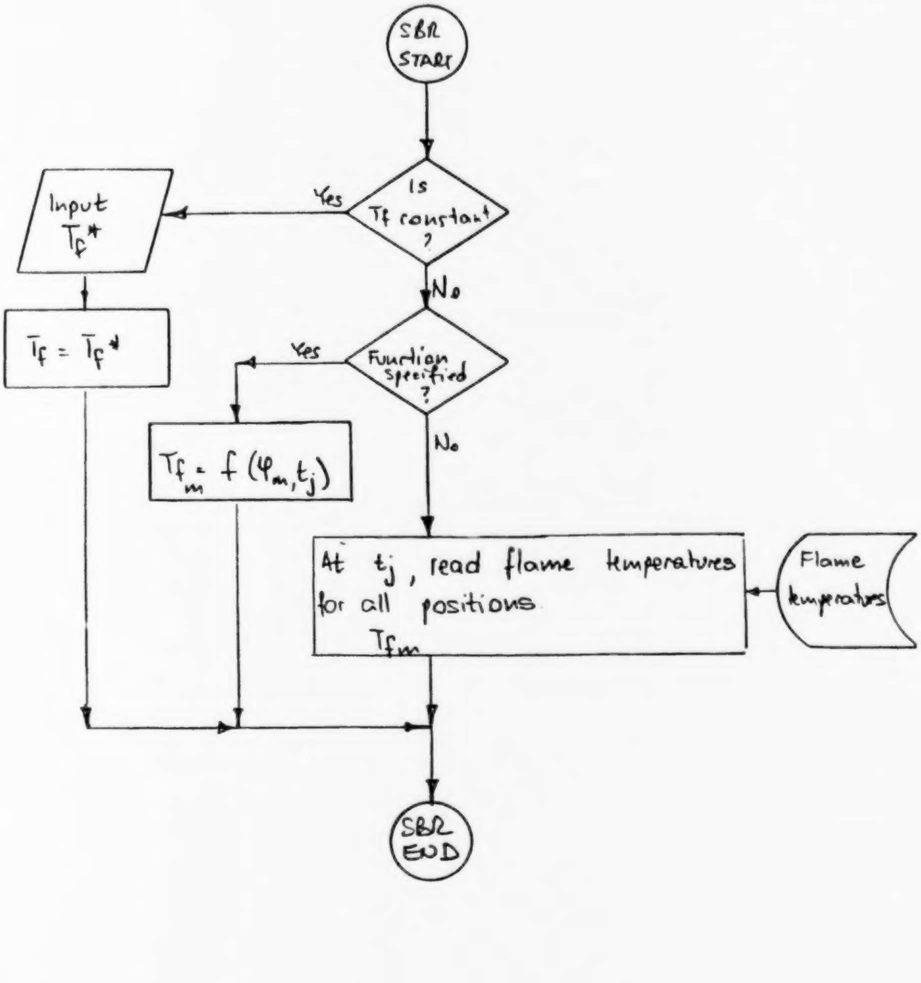
SBR START
Is Tf constant ?
Yes
Input T_f^*
$T_f = T_f^*$
No
Function specified ?
Yes
$T_{f_m} = f(\varphi_m, t_j)$
No
At t_j, read flame temperatures for all positions. T_{fm}
Flame temperatures
SBR END

FIGURE 6.14

HEAT INPUT FUNCTION - Impinging Torch
(6.3.5.1)

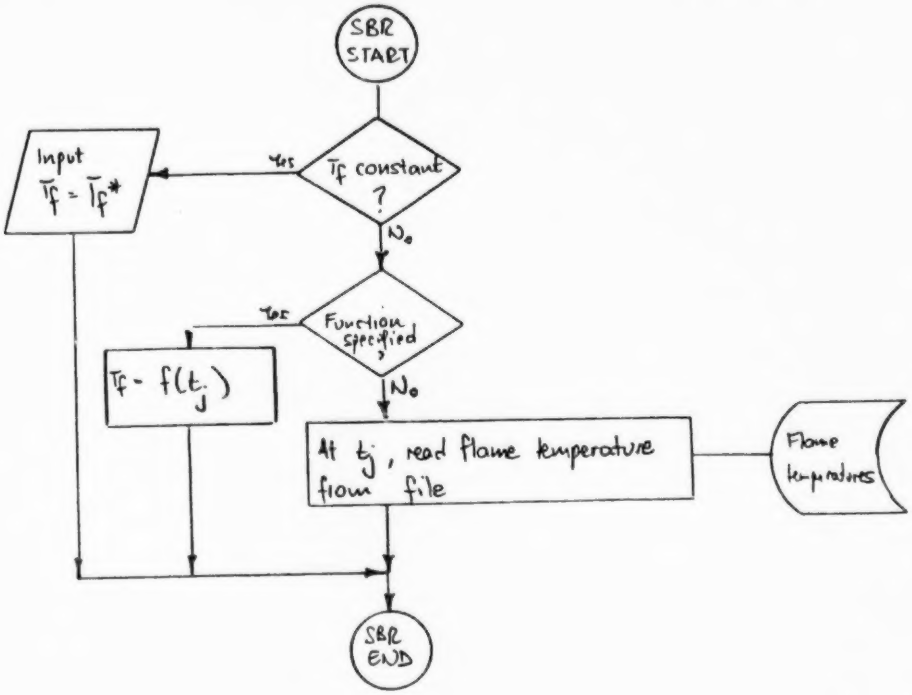
SBR START
Tf constant ?
Yes
Input
Tf = Tf*
No
Function specified ?
Yes
Tf - f(tj)
No
At tj, read flame temperature from file
Flame temperatures
SBR END

FIGURE 6.15

impinge on the tank itself, but a significant amount of thermal radiation from the plume will be intercepted at adjacent parts of the tank surface. If these parts of the tank coincide with the regions of maximum stress/temperature, the additional heating may be critical to the occurrence or location of tank failure.

The radiation from the plume can be estimated if the general dimensions of the visible plume are known, using standard computational techniques for luminous flame emissions and geometric configuration factors appropriate to the case. Although some of the plume radiation would frequently be intercepted by the sooty engulfing flames, the case of maximum concern when both engulfing flames and radiating plume are contributing to the heating can be estimated.

This estimate is made by assuming **that** the propane plume approximates a sphere of gas of radius r_1^* at temperature T_1^*, positioned with its center distance h above the top of the tank. Radiation is considered to impinge upon a disc-shaped area on the top of the tank. The disc is taken to have a radius of r_2^* and be at temperature, T_2^*. The tank diameter is D.

The emissivity of the sphere of gas is estimated on the basis of the CO_2 and the H_2O components of the products of stoichiometric combustion of propane. For any particular tank diameter D, tank surface absorptivity α_T, and surface temperature T_2^*, the heat transfer radiation gain of the tank top can be estimated from the relation,

$$\frac{Q}{A_2} = \frac{4\pi r_1^{*2}}{\pi r_2^{*2}} \cdot F_{12} \cdot \sigma \cdot (e_f\, T_1^{*4} - \alpha_T\, T_2^{*4}) \qquad (11)$$

where $F_{12} = \{1 - (1 - r_2/h)^{-\frac{1}{2}}\}/2$ and

$\alpha_T \sim 0.85$

and e_f is evaluated using Hottel's methods for gases and will be a function of the flame size, temperature, and composition. Assuming chemically correct combustion, with $h=3r_2^*$, $r_1^*=r_2^*$, $r_2^*=D/4$, D= 1.8 m, T_1= 1927 °C, T_2=260 °C., this shows a maximum radiation gain on the tank top during plume combustion of 3800 Btu/hr/ft^2 (11985 W/m^2).

HEAT INPUT FUNCTION - Plume Radiation
(6.3.6.1)

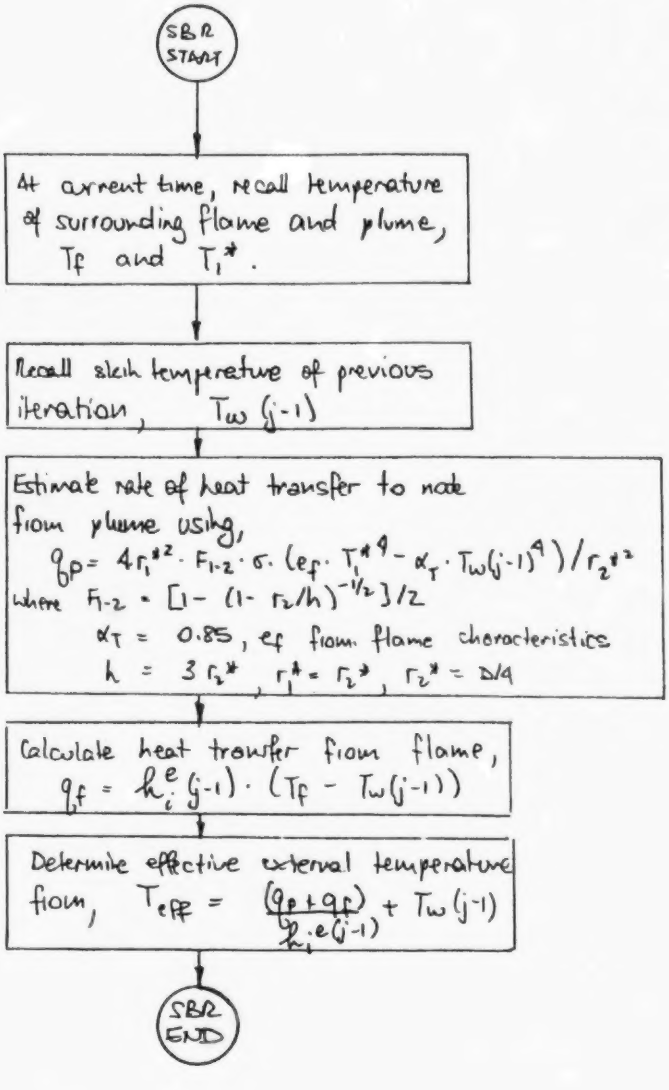

At current time, recall temperature of surrounding flame and plume, T_f and T_1^*.

Recall skin temperature of previous iteration, $T_w(j-1)$

Estimate rate of heat transfer to node from plume using,

$$q_p = 4 r_1^{*2} \cdot F_{1-2} \cdot \sigma \cdot (e_f \cdot T_1^{*4} - \alpha_T \cdot T_w(j-1)^4) / r_2^{*2}$$

where $F_{1-2} = [1 - (1 - r_2/h)^{-1/2}]/2$

$\alpha_T = 0.85$, e_f from flame characteristics

$h = 3 r_2^*$, $r_1^* = r_2^*$, $r_2^* = D/4$

Calculate heat transfer from flame,

$$q_f = h_i^e(j-1) \cdot (T_f - T_w(j-1))$$

Determine effective external temperature from,

$$T_{eff} = \frac{(q_p + q_f)}{h_i^e(j-1)} + T_w(j-1)$$

FIGURE 6.16

It is indeed a complex matter to separate the plume radiation contribution from that of the surrounding flame. However, an effective external nodal temperature is defined using the subroutine logic illustrated in Figure 6.16. This adjusted temperature is then used throughout the calculations for the time step.

6.3.7 Fluid Properties Subroutine

Straightforwardly this subroutine is used to determine the enthalpy, specific vapour volume, latent heat of vaporization, specific heats and thermal conductivities using digitized forms of the thermodynamic property tables, Figure 6.17.

6.3.8 Steel Properties Subroutine

At the current nodal temperature and system pressure, the steel thermal conductivities, capacitances, and allowable stress values are calculated, Figure 6.18.

6.3.9 Insulation Properties Subroutine

Insulation properties are taken to depend upon system pressure and the average temperature of the material. Once these are determined, the thermal conductivity and capacity are obtained from property tables, expressed in a digitized format for the program, Figure 6.19.

6.3.10 EXPLOSAFE Properties Subroutine

In Figure 6.20 the subroutine proposed to establish the mean temperature of the matrix is estimated. Thermal conductivity, heat capacity, density, surface area, and void fraction are obtained by making reference to the digitized properties list.

6.3.11 Heat Transfer Coefficients Subroutine

The coefficients referred to in this procedure describe the unit heat transfer rates between the fluid and the wall, which may or may not be insulated. External coefficients are denoted h^e and may be exposed to either flame or ambient conditions. In the latter case, values for the coefficient are obtained from a function dependent upon the average temperature (between the ambient and the tank skin) and the external pressure (atmospheric). If the external node represents a flame, then radiant transfer dominates. To keep the model workable, the external coefficient in this case is taken

FLUID PROPERTIES SUBROUTINE
(6.3.7.1)

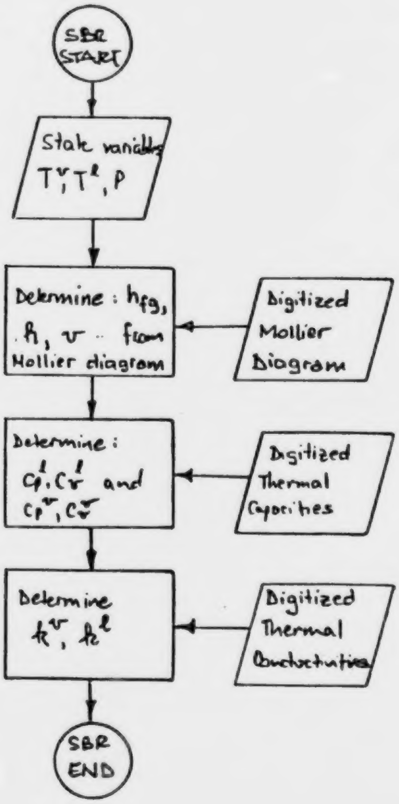
SBR START
State variables
T^v, T^l, P
Determine : h_{fg}, h, v .. from Mollier diagram
Digitized Mollier Diagram
Determine : C_p^l, C_v^l and C_p^v, C_v^v
Digitized Thermal Capacities
Determine k^v, k^l
Digitized Thermal Conductivities
SBR END

FIGURE 6.17

STEEL PROPERTIES SUBROUTINE
(6.3.8.1)

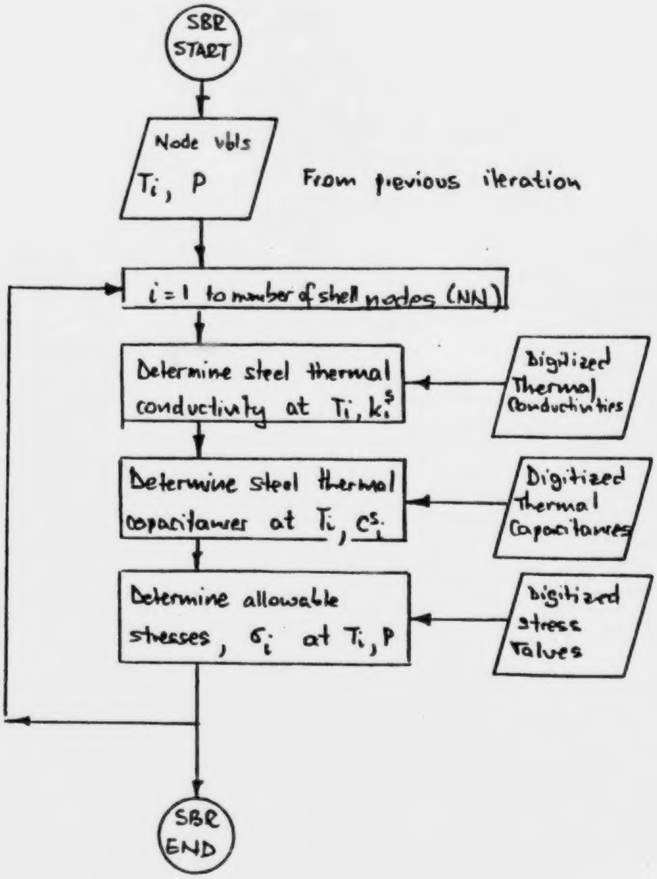

SBR START
Node vbls
T_i, P
From previous iteration
i = 1 to number of shell nodes (NN)
Determine steel thermal conductivity at T_i, k_i^s
Digitized Thermal Conductivities
Determine steel thermal capacitances at T_i, C_i^s
Digitized Thermal Capacitances
Determine allowable stresses, σ_i at T_i, P
Digitized stress Values
SBR END

FIGURE 6.18

INSULATION PROPERTIES SUBROUTINE
(6.3.9.1)

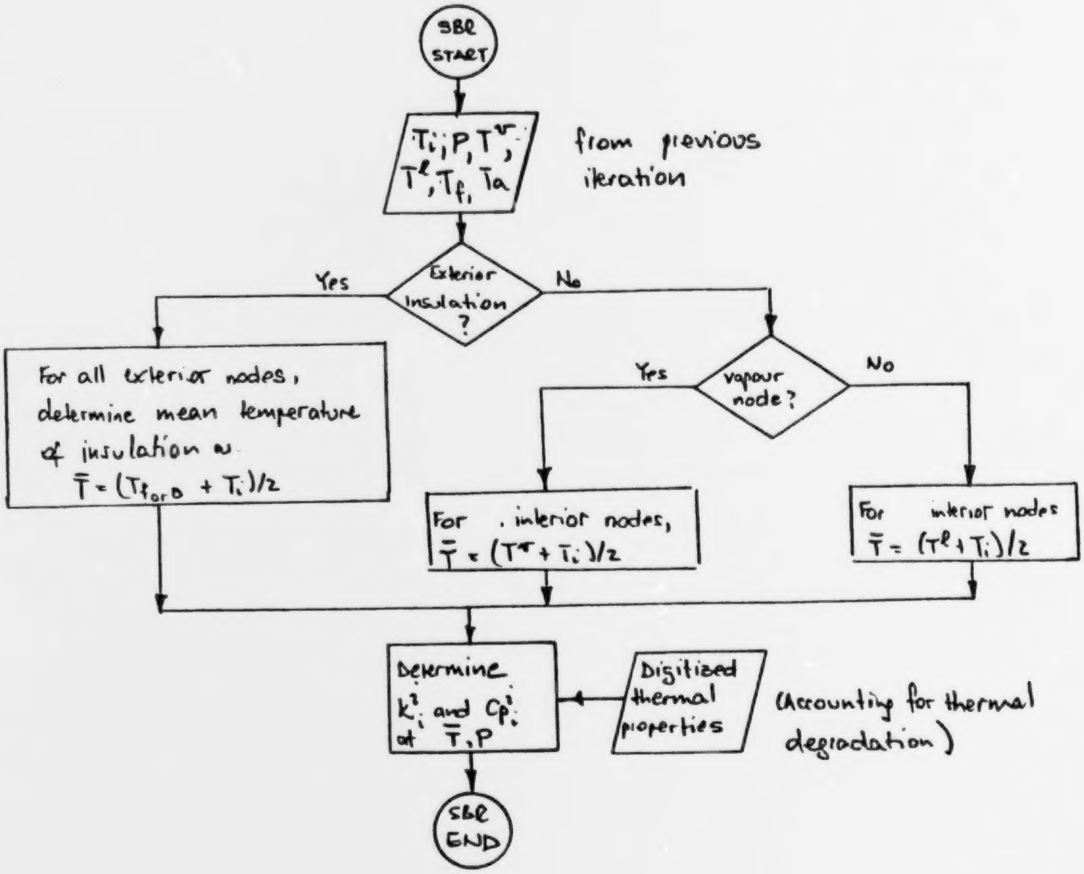
SBR START
$T_i; P, T^v; T^\ell, T_f, T_a$
from previous iteration
Exterior insulation ?
Yes
No
For all exterior nodes, determine mean temperature of insulation as $\bar{T} = (T_{f\,or\,a} + T_i)/2$
Yes
vapour node ?
No
For interior nodes, $\bar{T} = (T^v + T_i)/2$
For interior nodes $\bar{T} = (T^\ell + T_i)/2$
Determine k_i^j and Cp_i^j at $\bar{T}, P$
Digitized thermal properties
(Accounting for thermal degradation)
SBR END

FIGURE 6.19

EXPLOSAFE PROPERTIES SUBROUTINE
(6.3.10.1)

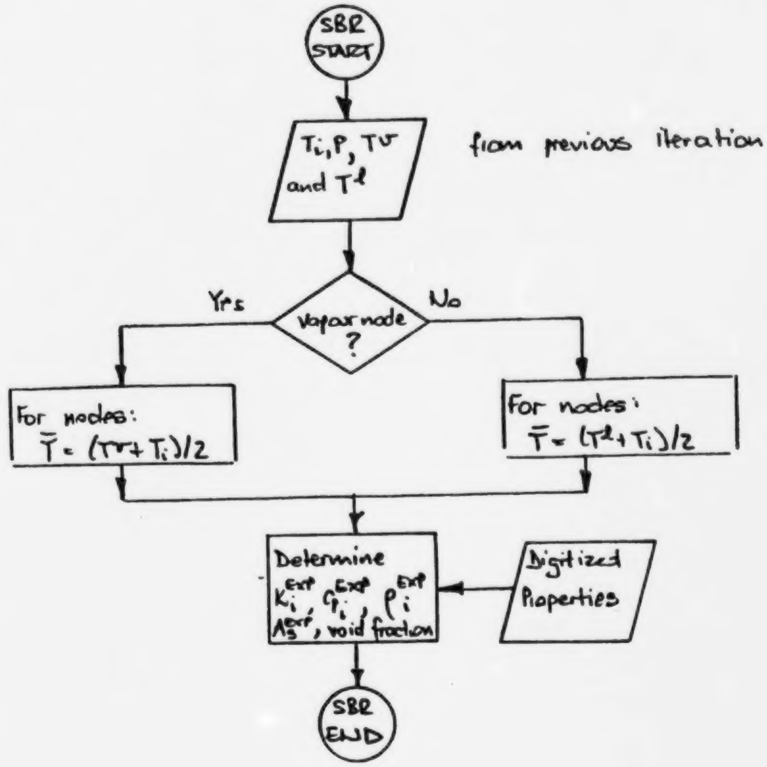
SBR START
T_i, P, T^v and T^l
from previous iteration
Vapor node ?
Yes
No
For nodes: $\bar{T} = (T^v + T_i)/2$
For nodes: $\bar{T} = (T^l + T_i)/2$
Determine K_i^{Exp}, $C_{p_i}^{Exp}$, ρ_i^{Exp}, Λ_s^{Exp}, void fraction
Digitized Properties
SBR END

FIGURE 6.20

HEAT TRANSFER COEFFICIENTS SUBROUTINE
(6.3.11.1)

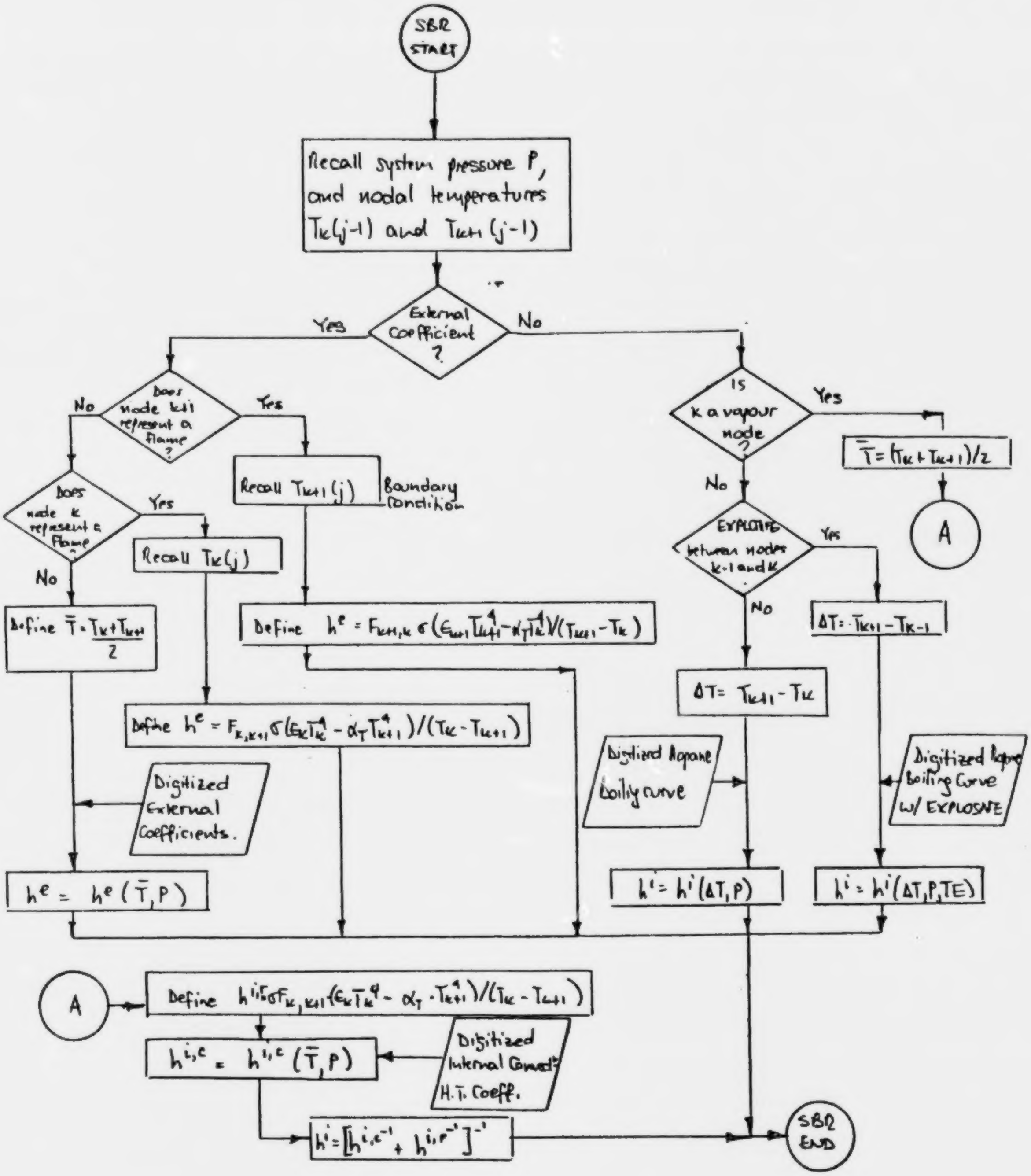
SBR START
Recall system pressure P, and nodal temperatures $T_K(j-1)$ and $T_{K+1}(j-1)$
External Coefficient ?
Yes
No
Does node K+1 represent a flame ?
No
Yes
Recall $T_{K+1}(j)$
Boundary condition
Does node K represent a flame ?
Yes
No
Recall $T_K(j)$
Define $\bar{T} = \frac{T_K + T_{K+1}}{2}$
Define $h^e = F_{K+1,K}\,\sigma(\epsilon_{K+1}T_{K+1}^4 - \alpha_T T_K^4)/(T_{K+1} - T_K)$
Define $h^e = F_{K,K+1}\,\sigma(\epsilon_K T_K^4 - \alpha_T T_{K+1}^4)/(T_K - T_{K+1})$
Digitized External Coefficients.
$h^e = h^e(\bar{T}, P)$
Is K a vapour node ?
Yes
No
$\bar{T} = (T_K + T_{K+1})/2$
A
EXPLOSIVE between nodes K-1 and K ?
Yes
No
$\Delta T = T_{K+1} - T_{K-1}$
$\Delta T = T_{K+1} - T_K$
Digitized Propane Boiling curve
Digitized Propane Boiling Curve w/ EXPLOSIVE
$h^i = h^i(\Delta T, P)$
$h^i = h^i(\Delta T, P, TE)$
A
Define $h^{i,r} = \sigma F_{K,K+1}(\epsilon_K T_K^4 - \alpha_T \cdot T_{K+1}^4)/(T_K - T_{K+1})$
$h^{i,c} = h^{i,c}(\bar{T}, P)$
Digitized Internal Convect. H.T. Coeff.
$h^i = [h^{i,c^{-1}} + h^{i,r^{-1}}]^{-1}$
SBR END

FIGURE 6.21

to depend upon the new flame temperature and the previous value of the tank skin temperature. This is justified in that the skin exhibits considerable thermal capacity and hence skin temperature changes, as well as coefficient changes, are small over a given time step. This permits coefficient calculation directly. Otherwise, an iterative procedure would be necessary, requiring the skin temperature to be determined through solution of the thermal network. This would be a time-consuming procedure. The one proposed is considered efficient and workable, Figure 6.21.

If the coefficient required is internal to the tank, then two cases are considered; the heat transfer path originates either with a vapour or a liquid node.
In the former instance, heat transfer occurs by both radiative and convective mechanisms. Radiative internal exchange is significant in cars without EXPLOSAFE when the inner wall reaches temperatures exceeding 540 °C, as the propane gas absorption spectrum is opaque over a number of critical wavelength bands (eg.3 to $4_{\mu m}$ and 6 to $7.5_{\mu m}$), Figure 6.22. This means that radiation emitted from the tank surface will be absorbed by the vapour and to some extent, the liquid surface. A convective component is added inversely to the radiative coefficient to produce an effective total skin to fluid coefficient.

If the node originates with a liquid node, then the internal coefficient is determined from the appropriate digitized boiling curve, with or without EXPLOSAFE. Procedures to obtain these curves are discussed in Section 9.2.

6.3.12.1 Coefficients Subroutine - Engulfing Flame Model

Using the subroutines described in the previous Section, overall resistance values are obtained as shown in Figure 6.23. Values are assigned to each of the links in the thermal network model. For example, resistance $R_{i,}^{e}$ represents the resistance to heat flow through the insulation externally applied to the tank, whereas $R_{i,2}^{e}$ represents the resistance between the insulation and the ambient air, at note i. Internal resistances at node i are devoted R_i^{i}. The mass of each node is determined using geometric relations. The total nodal capacitance is weighted with respect to the masses and capacitances of the components at each node. The resistance to heat flow across the liquid/vapour interface is determined from a selected value of $h^{\ell v}$, the heat transfer coefficient supplied as input.

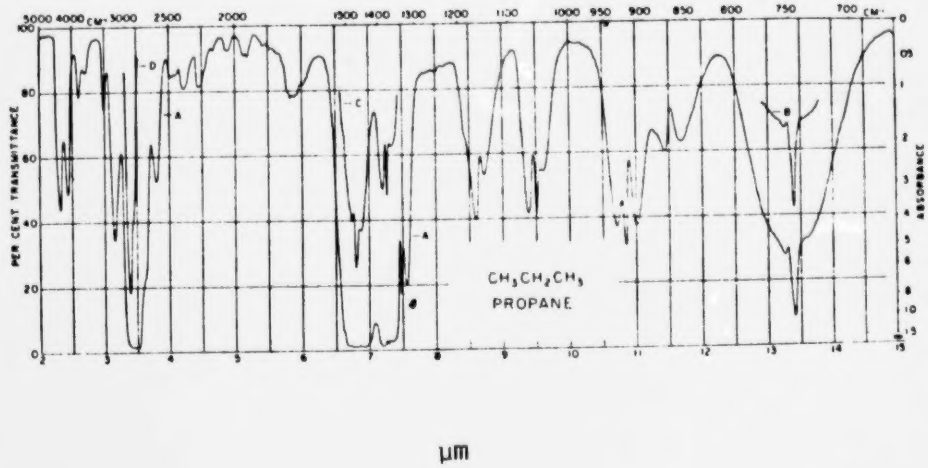

Figure 6.22 Infrared spectrum of gaseous propane; 10-cm path length cell, with NaCl windows; cell pressure: curve A: 94.526 kN/m^2 (709 mmHg); curve B: 28.131 kN/m^2 (211 mmHg); curve C: 12.532 kN/m^2 (94 mmHg); curve D: 2.000 kN/m^2 (15 mmHg)(16).

From Matheson Gas Products Handbook, Propane (31)

COEFFICIENTS SUBROUTINE - Engulfing Flame Model (6.3.12.1)

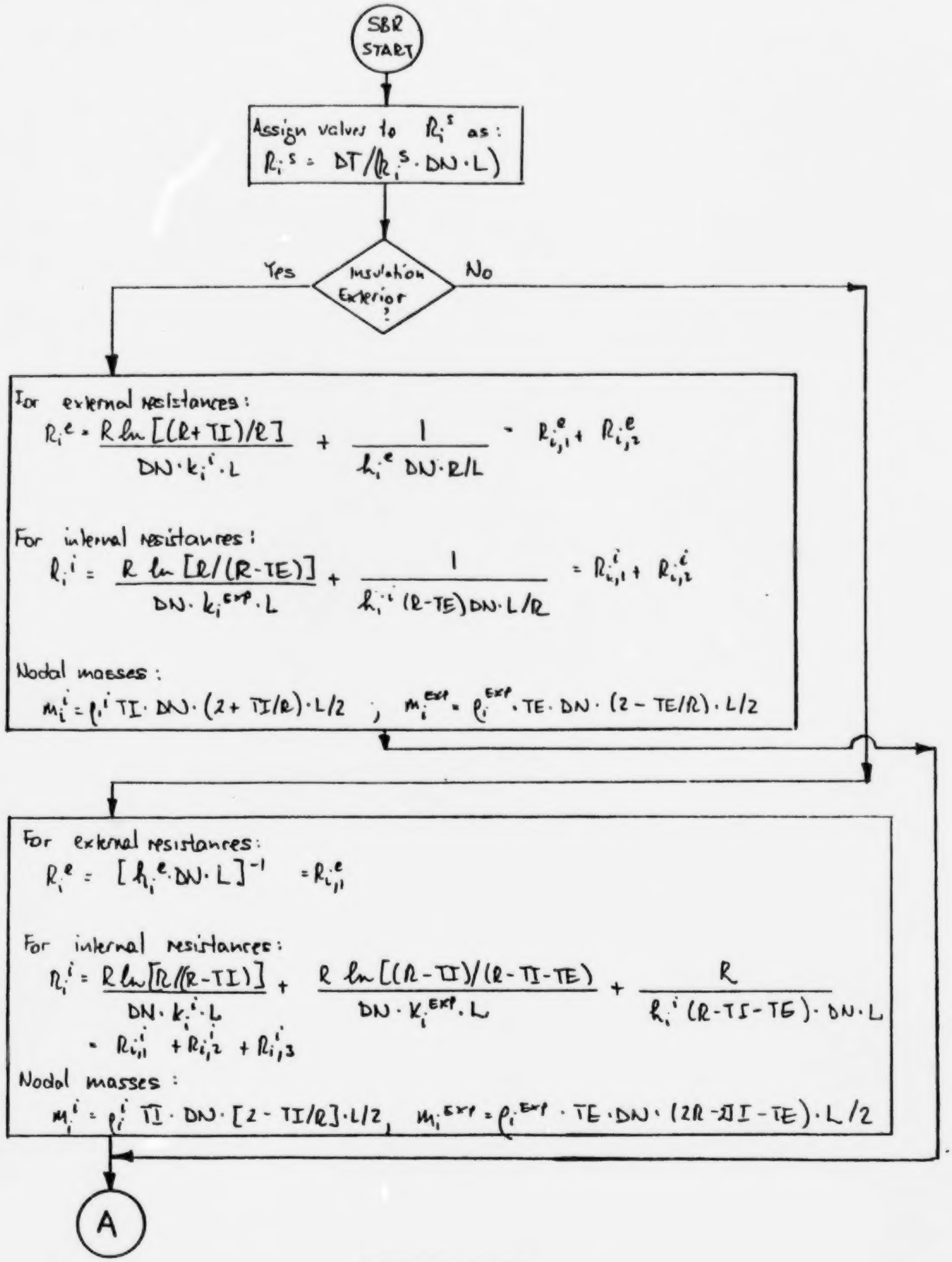
SBR START
Assign values to R_i^s as:
$R_i^s = DT/(k_i^s \cdot DN \cdot L)$
Yes
Insulation Exterior ?
No
For external resistances:
$R_i^e = \frac{R \ln[(R+TI)/R]}{DN \cdot k_i^i \cdot L} + \frac{1}{h_i^e DN \cdot R/L} = R_{i,1}^e + R_{i,2}^e$
For internal resistances:
$R_i^i = \frac{R \ln[R/(R-TE)]}{DN \cdot k_i^{EXP} \cdot L} + \frac{1}{h_i^i (R-TE) DN \cdot L/R} = R_{i,1}^i + R_{i,2}^i$
Nodal masses:
$m_i^i = \rho_i^i TI \cdot DN \cdot (2+TI/R) \cdot L/2$, $m_i^{EXP} = \rho_i^{EXP} \cdot TE \cdot DN \cdot (2-TE/R) \cdot L/2$
For external resistances:
$R_i^e = [h_i^e \cdot DN \cdot L]^{-1} = R_{i,1}^e$
For internal resistances:
$R_i^i = \frac{R \ln[R/(R-TI)]}{DN \cdot k_i^i \cdot L} + \frac{R \ln[(R-TI)/(R-TI-TE)}{DN \cdot K_i^{EXP} \cdot L} + \frac{R}{h_i^i (R-TI-TE) \cdot DN \cdot L}$
$= R_{i,1}^i + R_{i,2}^i + R_{i,3}^i$
Nodal masses:
$m_i^i = \rho_i^i TI \cdot DN \cdot [2-TI/R] \cdot L/2$, $m_i^{EXP} = \rho_i^{EXP} \cdot TE \cdot DN \cdot (2R-2TI-TE) \cdot L/2$
A

FIGURE 6.23

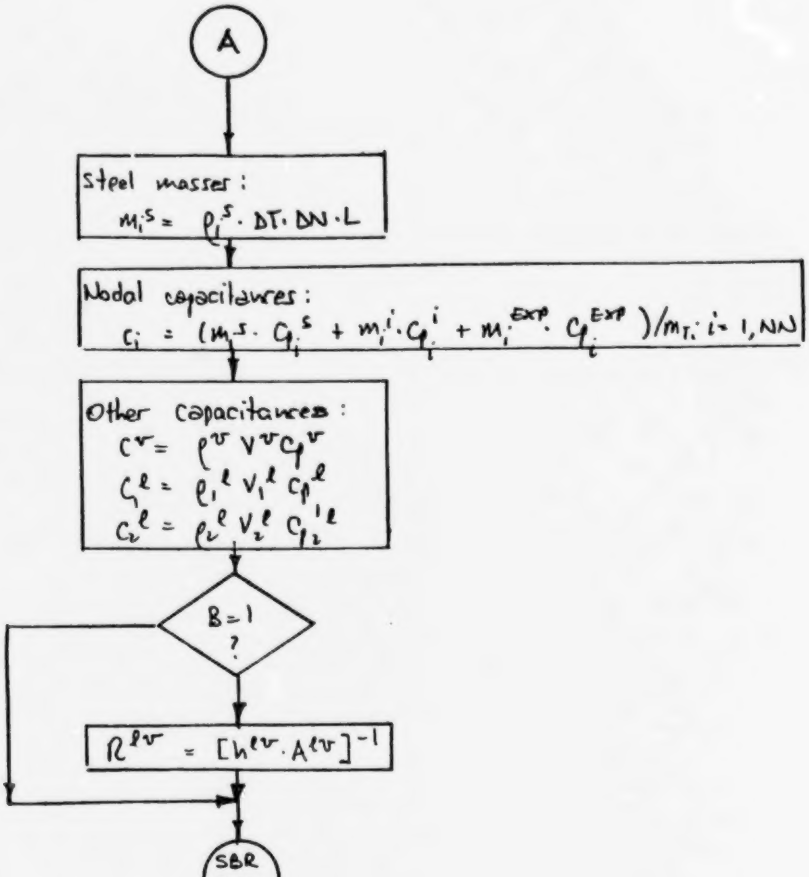
A
Steel masses :
$m_i^S = \rho_i^S \cdot DT \cdot DN \cdot L$
Nodal capacitances :
$c_i = (m_i^S \cdot c_{p_i}^S + m_i^i \cdot c_{p_i}^i + m_i^{EXP} \cdot c_{p_i}^{EXP}) / m_{T_i} \; i = 1, NN$
Other capacitances :
$C^v = \rho^v V^v c_p^v$
$C_1^l = \rho_1^l V_1^l c_p^l$
$C_2^l = \rho_2^l V_2^l c_{p_2}'^l$
B = 1 ?
$R^{lv} = [h^{lv} \cdot A^{lv}]^{-1}$
SBR END

FIGURE 6.23 (cont'd)

NOTES:

TI - insulation thickness
TE = Explosafe thickness

h_i^e = external heat transfer coefficient at node i
h_i^i = internal heat transfer coefficient at node i
h^{lv} - heat transfer coefficient across vapour liquid interface

m_i^s = mass of shell node i (steel)
m_i^i = mass of insulation (node i)
m_i^{EXP} = mass of EXPLOSAFE (node i)
m_{T_i} = total mass at node i.
c_i = total nodal heat capacitance.

COEFFICIENTS SUBROUTINE - Impinging Torch Model
(Liquid Zone)
(6.3.12.2)

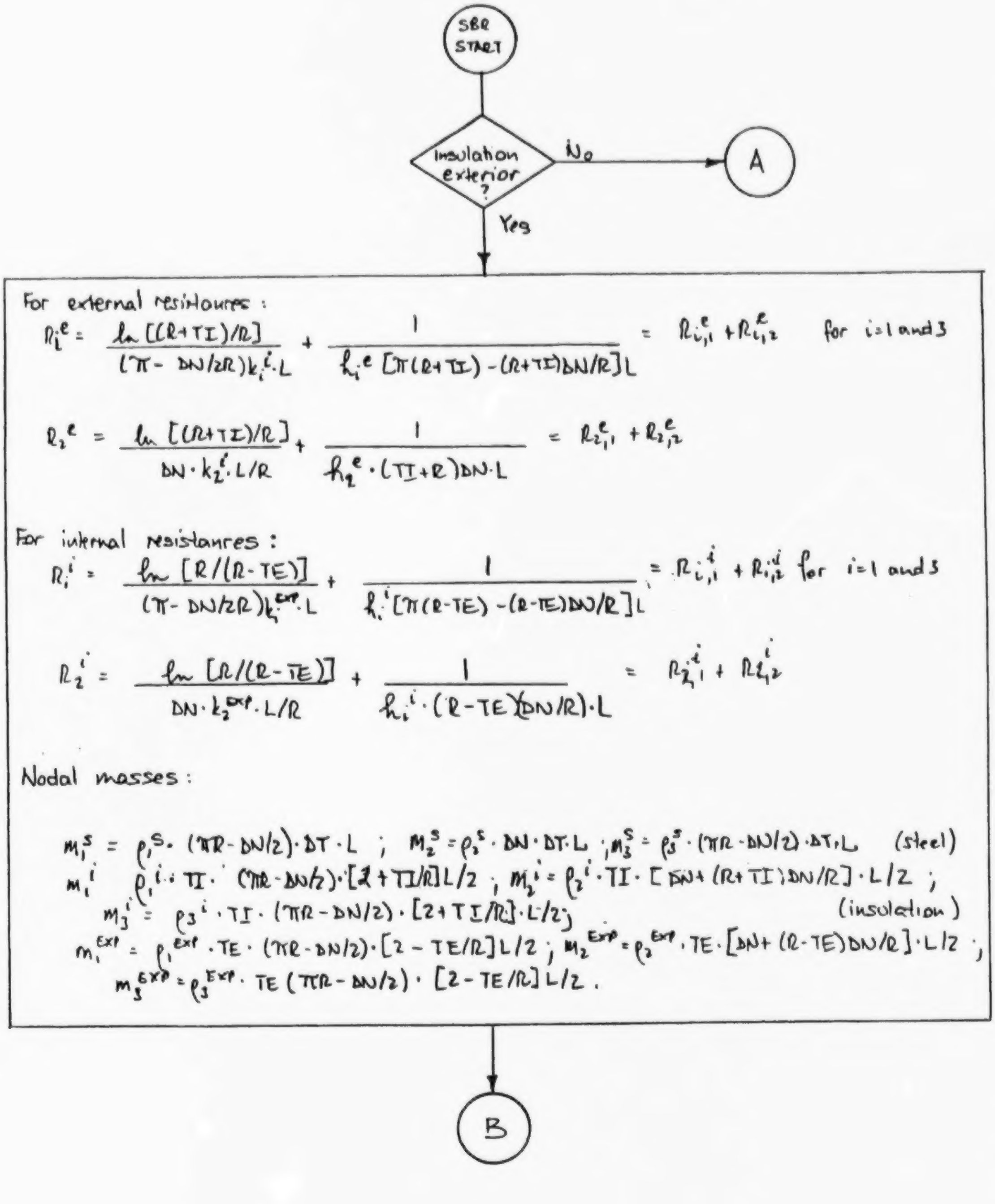

For external resistances :

$$R_i^e = \frac{\ln[(R+TI)/R]}{(\pi - DN/2R)k_i^i \cdot L} + \frac{1}{h_i^e[\pi(R+TI)-(R+TI)DN/R]L} = R^e_{i,1} + R^e_{i,2} \quad \text{for } i=1 \text{ and } 3$$

$$R_2^e = \frac{\ln[(R+TI)/R]}{DN\cdot k_2^i \cdot L/R} + \frac{1}{h_2^e\cdot(TI+R)DN\cdot L} = R^e_{2,1} + R^e_{2,2}$$

For internal resistances :

$$R_i^i = \frac{\ln[R/(R-TE)]}{(\pi - DN/2R)k_i^{exp}\cdot L} + \frac{1}{h_i^i[\pi(R-TE)-(R-TE)DN/R]L} = R^i_{i,1} + R^i_{i,2} \quad \text{for } i=1 \text{ and } 3$$

$$R_2^i = \frac{\ln[R/(R-TE)]}{DN\cdot k_2^{exp}\cdot L/R} + \frac{1}{h_i^i\cdot(R-TE)(DN/R)\cdot L} = R^i_{2,1} + R^i_{2,2}$$

Nodal masses :

$m_1^s = \rho_1^s\cdot(\pi R - DN/2)\cdot DT\cdot L$; $M_2^s = \rho_2^s\cdot DN\cdot DT\cdot L$; $m_3^s = \rho_3^s\cdot(\pi R - DN/2)\cdot DT\cdot L$ (steel)

$m_1^i \quad \rho_1^i\cdot TI\cdot(\pi R - DN/2)\cdot[2+TI/R]L/2$; $m_2^i = \rho_2^i\cdot TI\cdot[DN+(R+TI)DN/R]\cdot L/2$;

$m_3^i = \rho_3^i\cdot TI\cdot(\pi R - DN/2)\cdot[2+TI/R]\cdot L/2$; (insulation)

$m_1^{EXP} = \rho_1^{exp}\cdot TE\cdot(\pi R - DN/2)\cdot[2-TE/R]L/2$; $M_2^{Exp} = \rho_2^{Exp}\cdot TE\cdot[DN+(R-TE)DN/R]\cdot L/2$;

$m_3^{EXP} = \rho_3^{Exp}\cdot TE(\pi R - DN/2)\cdot[2-TE/R]L/2$.

FIGURE 6.24

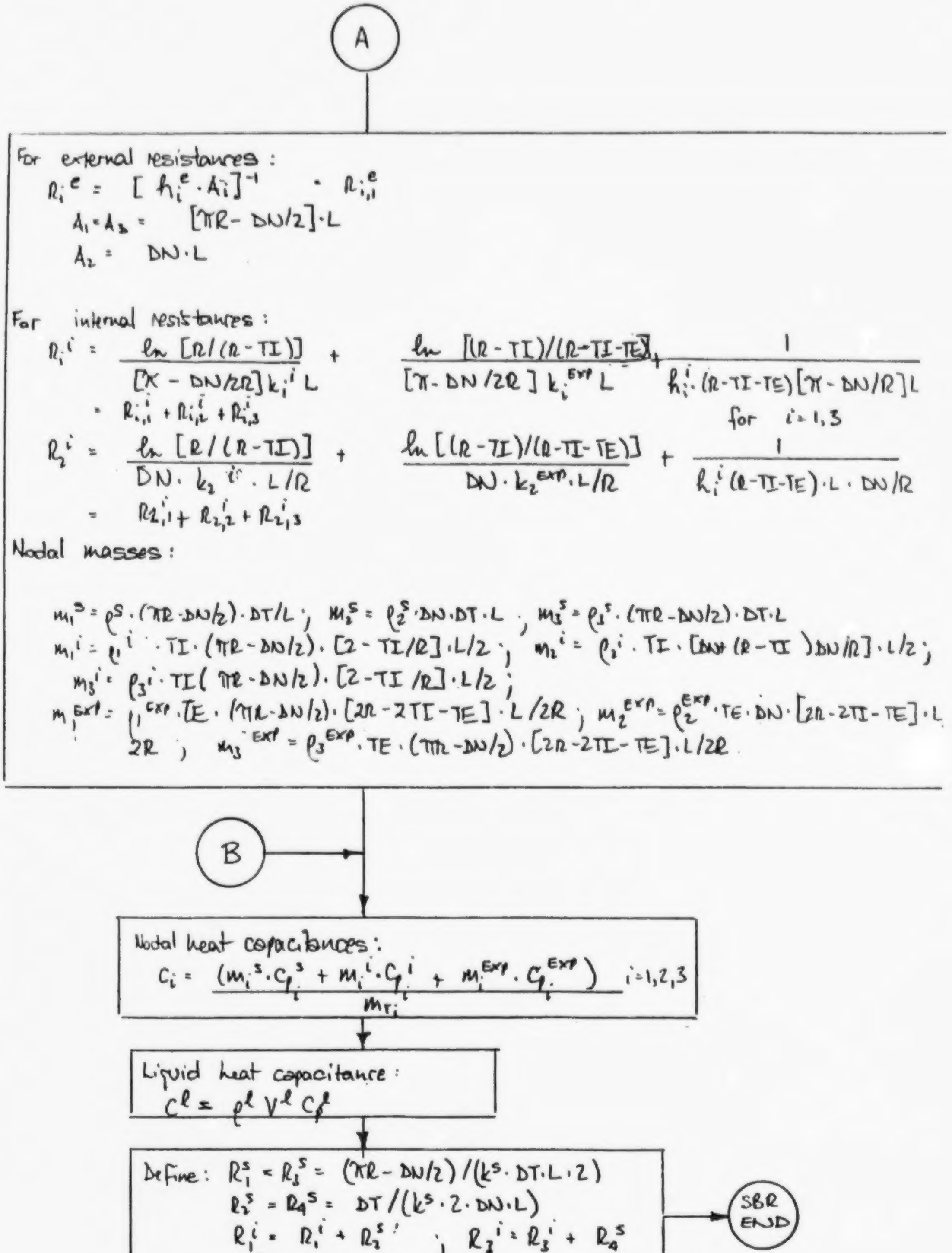

For external resistances:

$$R_i^e = [h_i^e \cdot A_i]^{-1} = R_{i,1}^e$$

$$A_1 = A_3 = [\pi R - DN/2] \cdot L$$

$$A_2 = DN \cdot L$$

For internal resistances:

$$R_i^i = \frac{\ln[R/(R-TI)]}{[\pi - DN/2R]k_i^i L} + \frac{\ln[(R-TI)/(R-TI-TE)]}{[\pi - DN/2R]k_i^{EXP} L} + \frac{1}{h_i^i \cdot (R-TI-TE)[\pi - DN/R]L}$$

$$= R_{i,1}^i + R_{i,2}^i + R_{i,3}^i \qquad \text{for } i = 1,3$$

$$R_2^i = \frac{\ln[R/(R-TI)]}{DN \cdot k_2^i \cdot L/R} + \frac{\ln[(R-TI)/(R-TI-TE)]}{DN \cdot k_2^{EXP} \cdot L/R} + \frac{1}{h_i^i (R-TI-TE) \cdot L \cdot DN/R}$$

$$= R_{2,1}^i + R_{2,2}^i + R_{2,3}^i$$

Nodal masses:

$m_1^s = \rho^s \cdot (\pi R - DN/2) \cdot DT/L$; $m_2^s = \rho_2^s \cdot DN \cdot DT \cdot L$; $m_3^s = \rho_3^s \cdot (\pi R - DN/2) \cdot DT \cdot L$

$m_1^i = \rho_1^i \cdot TI \cdot (\pi R - DN/2) \cdot [2 - TI/R] \cdot L/2$; $m_2^i = \rho_2^i \cdot TI \cdot [DN + (R - TI)DN/R] \cdot L/2$;

$m_3^i = \rho_3^i \cdot TI(\pi R - DN/2) \cdot [2 - TI/R] \cdot L/2$;

$m_1^{EXP} = \rho_1^{EXP} \cdot TE \cdot (\pi R - DN/2) \cdot [2R - 2TI - TE] \cdot L/2R$; $m_2^{EXP} = \rho_2^{EXP} \cdot TE \cdot DN \cdot [2R - 2TI - TE] \cdot L / 2R$; $m_3^{EXP} = \rho_3^{EXP} \cdot TE \cdot (\pi R - DN/2) \cdot [2R - 2TI - TE] \cdot L/2R$

Nodal heat capacitances:

$$C_i = \frac{(m_i^s \cdot C_{p_i}^s + m_i^i \cdot C_{p_i}^i + m_i^{EXP} \cdot C_{p_i}^{EXP})}{m_{T_i}} \qquad i = 1,2,3$$

Liquid heat capacitance:

$$C^l = \rho^l V^l C_p^l$$

Define: $R_1^s = R_3^s = (\pi R - DN/2)/(k^s \cdot DT \cdot L \cdot 2)$

$R_2^s = R_4^s = DT/(k^s \cdot 2 \cdot DN \cdot L)$

$R_1^i = R_1^i + R_2^s$; $R_3^i = R_3^i + R_4^s$

$R_1^e = R_1^e + R_2^s$; $R_3^e = R_3^e + R_4^s$

FIGURE 6.24 (cont'd)

COEFFICIENTS SUBROUTINE - Impinging Torch Model
(Vapour Zone)
(6.3.12.3)

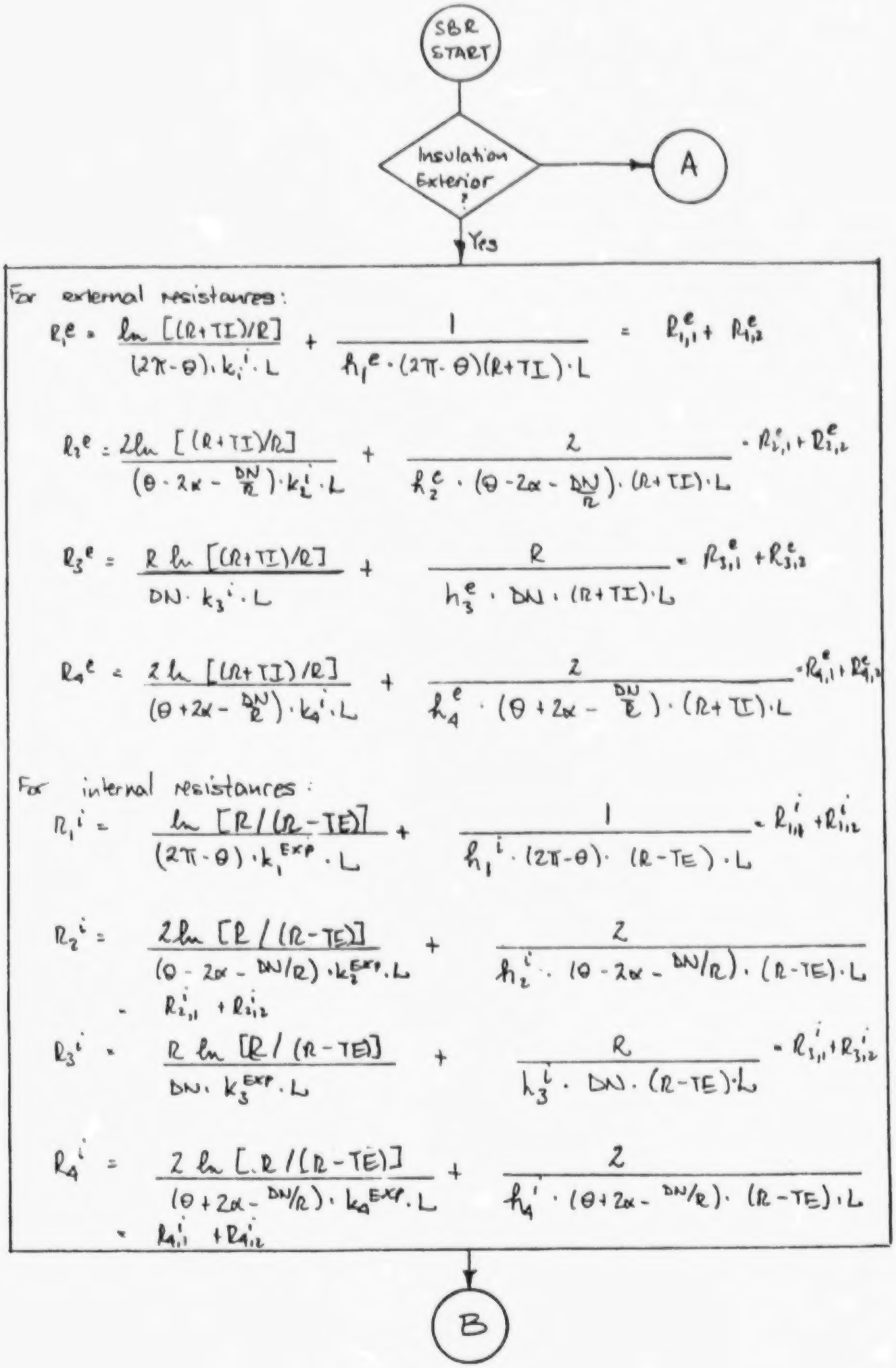

For external resistances:

$$R_1^e = \frac{\ln[(R+TI)/R]}{(2\pi-\theta)\cdot k_1^i\cdot L} + \frac{1}{h_1^e\cdot(2\pi-\theta)(R+TI)\cdot L} = R_{1,1}^e + R_{1,2}^e$$

$$R_2^e = \frac{2\ln[(R+TI)/R]}{(\theta-2\alpha-\frac{DN}{R})\cdot k_2^i\cdot L} + \frac{2}{h_2^e\cdot(\theta-2\alpha-\frac{DN}{R})\cdot(R+TI)\cdot L} = R_{2,1}^e + R_{2,2}^e$$

$$R_3^e = \frac{R\ln[(R+TI)/R]}{DN\cdot k_3^i\cdot L} + \frac{R}{h_3^e\cdot DN\cdot(R+TI)\cdot L} = R_{3,1}^e + R_{3,2}^e$$

$$R_4^e = \frac{2\ln[(R+TI)/R]}{(\theta+2\alpha-\frac{DN}{R})\cdot k_4^i\cdot L} + \frac{2}{h_4^e\cdot(\theta+2\alpha-\frac{DN}{R})\cdot(R+TI)\cdot L} = R_{4,1}^e + R_{4,2}^e$$

For internal resistances:

$$R_1^i = \frac{\ln[R/(R-TE)]}{(2\pi-\theta)\cdot k_1^{EXP}\cdot L} + \frac{1}{h_1^i\cdot(2\pi-\theta)\cdot(R-TE)\cdot L} = R_{1,1}^i + R_{1,2}^i$$

$$R_2^i = \frac{2\ln[R/(R-TE)]}{(\theta-2\alpha-DN/R)\cdot k_2^{EXP}\cdot L} + \frac{2}{h_2^i\cdot(\theta-2\alpha-DN/R)\cdot(R-TE)\cdot L} = R_{2,1}^i + R_{2,2}^i$$

$$R_3^i = \frac{R\ln[R/(R-TE)]}{DN\cdot k_3^{EXP}\cdot L} + \frac{R}{h_3^i\cdot DN\cdot(R-TE)\cdot L} = R_{3,1}^i + R_{3,2}^i$$

$$R_4^i = \frac{2\ln[R/(R-TE)]}{(\theta+2\alpha-DN/R)\cdot k_4^{EXP}\cdot L} + \frac{2}{h_4^i\cdot(\theta+2\alpha-DN/R)\cdot(R-TE)\cdot L} = R_{4,1}^i + R_{4,2}^i$$

FIGURE 6.25

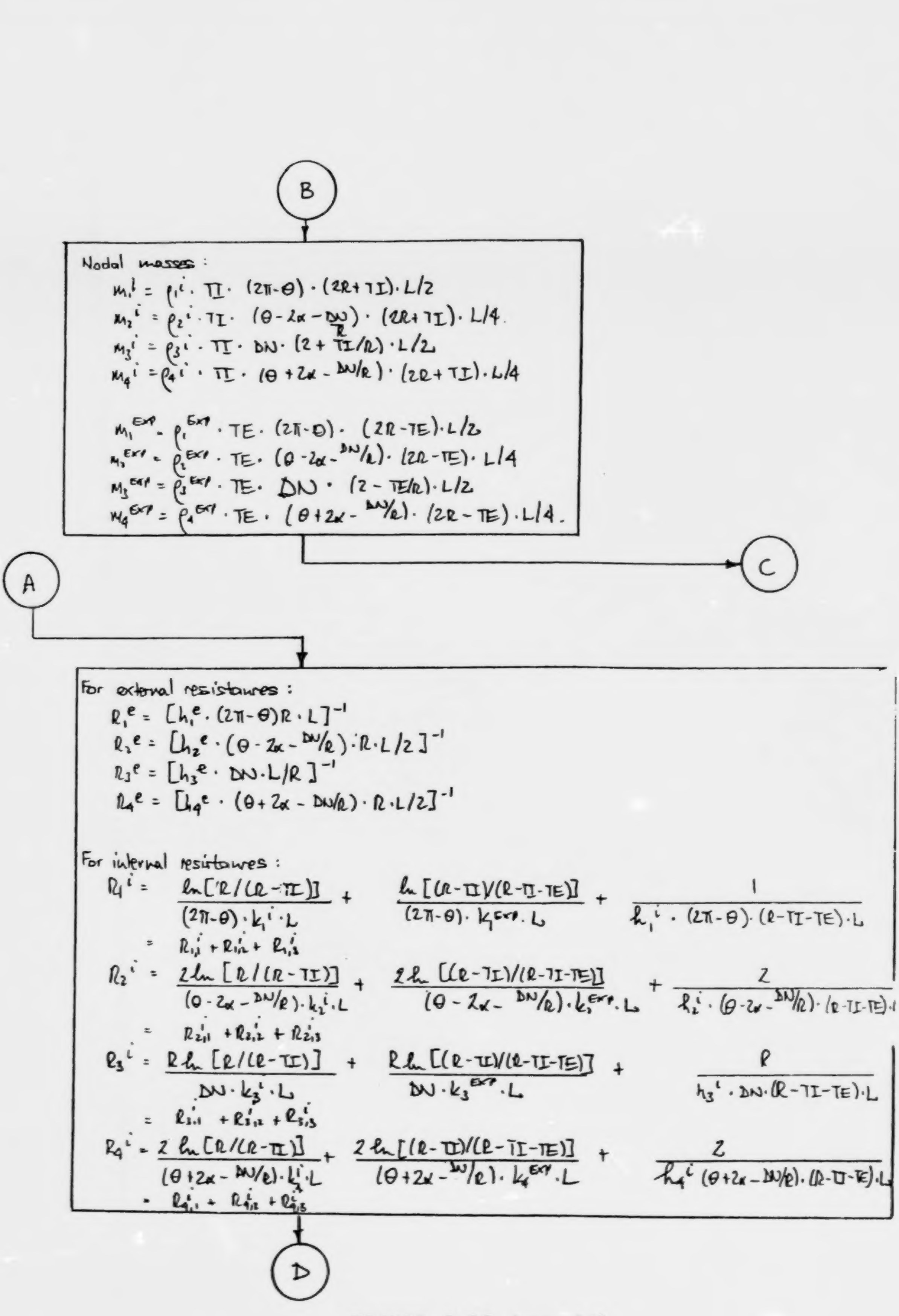

Nodal masses :

$$m_1^i = \rho_1^i \cdot TI \cdot (2\pi-\theta) \cdot (2R+TI) \cdot L/2$$
$$m_2^i = \rho_2^i \cdot TI \cdot (\theta - 2\alpha - \frac{DN}{R}) \cdot (2R+TI) \cdot L/4.$$
$$m_3^i = \rho_3^i \cdot TI \cdot DN \cdot (2 + TI/R) \cdot L/2$$
$$m_4^i = \rho_4^i \cdot TI \cdot (\theta + 2\alpha - DN/R) \cdot (2R+TI) \cdot L/4$$

$$m_1^{EXP} = \rho_1^{EXP} \cdot TE \cdot (2\pi-\theta) \cdot (2R-TE) \cdot L/2$$
$$m_2^{EXP} = \rho_2^{EXP} \cdot TE \cdot (\theta - 2\alpha - DN/R) \cdot (2R-TE) \cdot L/4$$
$$m_3^{EXP} = \rho_3^{EXP} \cdot TE \cdot DN \cdot (2 - TE/R) \cdot L/2$$
$$m_4^{EXP} = \rho_4^{EXP} \cdot TE \cdot (\theta + 2\alpha - DN/R) \cdot (2R-TE) \cdot L/4.$$

For external resistances :

$$R_1^e = [h_1^e \cdot (2\pi-\theta) R \cdot L]^{-1}$$
$$R_2^e = [h_2^e \cdot (\theta - 2\alpha - DN/R) \cdot R \cdot L/2]^{-1}$$
$$R_3^e = [h_3^e \cdot DN \cdot L/R]^{-1}$$
$$R_4^e = [h_4^e \cdot (\theta + 2\alpha - DN/R) \cdot R \cdot L/2]^{-1}$$

For internal resistances :

$$R_1^i = \frac{\ln[R/(R-TI)]}{(2\pi-\theta) \cdot k_1^i \cdot L} + \frac{\ln[(R-TI)/(R-TI-TE)]}{(2\pi-\theta) \cdot k_1^{EXP} \cdot L} + \frac{1}{h_1^i \cdot (2\pi-\theta) \cdot (R-TI-TE) \cdot L}$$
$$= R_{1,1}^i + R_{1,2}^i + R_{1,3}^i$$
$$R_2^i = \frac{2\ln[R/(R-TI)]}{(\theta - 2\alpha - DN/R) \cdot k_2^i \cdot L} + \frac{2\ln[(R-TI)/(R-TI-TE)]}{(\theta - 2\alpha - DN/R) \cdot k_2^{EXP} \cdot L} + \frac{2}{h_2^i \cdot (\theta - 2\alpha - DN/R) \cdot (R-TI-TE) \cdot}$$
$$= R_{2,1}^i + R_{2,2}^i + R_{2,3}^i$$
$$R_3^i = \frac{R\ln[R/(R-TI)]}{DN \cdot k_3^i \cdot L} + \frac{R\ln[(R-TI)/(R-TI-TE)]}{DN \cdot k_3^{EXP} \cdot L} + \frac{R}{h_3^i \cdot DN \cdot (R-TI-TE) \cdot L}$$
$$= R_{3,1}^i + R_{3,2}^i + R_{3,3}^i$$
$$R_4^i = \frac{2\ln[R/(R-TI)]}{(\theta + 2\alpha - DN/R) \cdot k_4^i \cdot L} + \frac{2\ln[(R-TI)/(R-TI-TE)]}{(\theta + 2\alpha - DN/R) \cdot k_4^{EXP} \cdot L} + \frac{2}{h_4^i (\theta + 2\alpha - DN/R) \cdot (R-TI-TE) \cdot L}$$
$$= R_{4,1}^i + R_{4,2}^i + R_{4,3}^i$$

FIGURE 6.25 (cont'd)

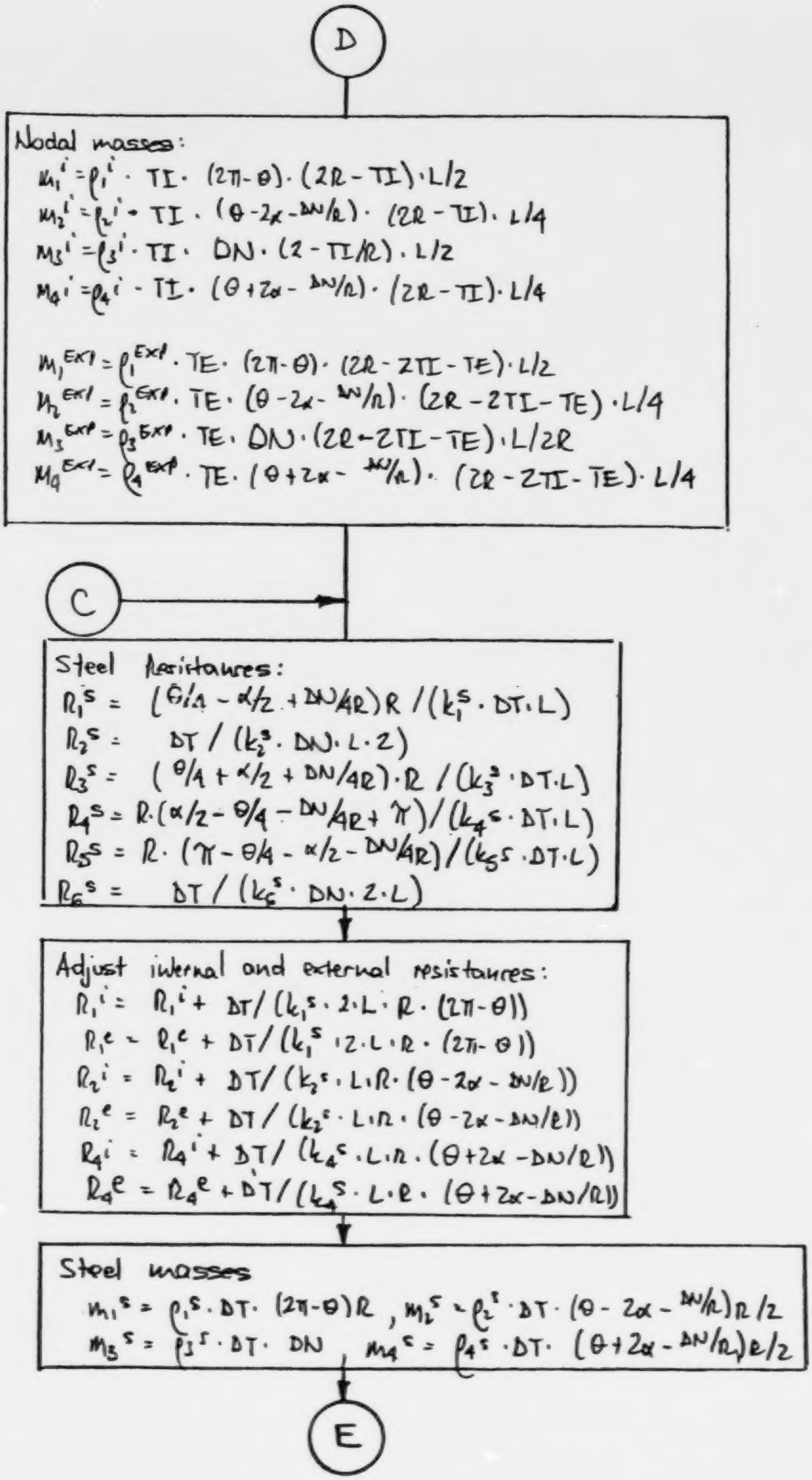

Nodal masses:

$$m_1^i = \rho_1^i \cdot TI \cdot (2\pi - \theta) \cdot (2R - TI) \cdot L/2$$
$$m_2^i = \rho_2^i \cdot TI \cdot (\theta - 2\alpha - DN/R) \cdot (2R - TI) \cdot L/4$$
$$m_3^i = \rho_3^i \cdot TI \cdot DN \cdot (2 - TI/R) \cdot L/2$$
$$m_4^i = \rho_4^i \cdot TI \cdot (\theta + 2\alpha - DN/R) \cdot (2R - TI) \cdot L/4$$

$$m_1^{EXT} = \rho_1^{EXT} \cdot TE \cdot (2\pi - \theta) \cdot (2R - 2TI - TE) \cdot L/2$$
$$m_2^{EXT} = \rho_2^{EXT} \cdot TE \cdot (\theta - 2\alpha - DN/R) \cdot (2R - 2TI - TE) \cdot L/4$$
$$m_3^{EXT} = \rho_3^{EXT} \cdot TE \cdot DN \cdot (2R - 2TI - TE) \cdot L/2R$$
$$m_4^{EXT} = \rho_4^{EXT} \cdot TE \cdot (\theta + 2\alpha - DN/R) \cdot (2R - 2TI - TE) \cdot L/4$$

Steel Resistances:

$$R_1^s = (\theta/4 - \alpha/2 + DN/4R)R / (k_1^s \cdot DT \cdot L)$$
$$R_2^s = DT / (k_2^s \cdot DN \cdot L \cdot 2)$$
$$R_3^s = (\theta/4 + \alpha/2 + DN/4R) \cdot R / (k_3^s \cdot DT \cdot L)$$
$$R_4^s = R \cdot (\alpha/2 - \theta/4 - DN/4R + \pi) / (k_4^s \cdot DT \cdot L)$$
$$R_5^s = R \cdot (\pi - \theta/4 - \alpha/2 - DN/4R) / (k_5^s \cdot DT \cdot L)$$
$$R_6^s = DT / (k_6^s \cdot DN \cdot 2 \cdot L)$$

Adjust internal and external resistances:

$$R_1^i = R_1^i + DT / (k_1^s \cdot 2 \cdot L \cdot R \cdot (2\pi - \theta))$$
$$R_1^e = R_1^e + DT / (k_1^s \cdot 2 \cdot L \cdot R \cdot (2\pi - \theta))$$
$$R_2^i = R_2^i + DT / (k_2^s \cdot L \cdot R \cdot (\theta - 2\alpha - DN/R))$$
$$R_2^e = R_2^e + DT / (k_2^s \cdot L \cdot R \cdot (\theta - 2\alpha - DN/R))$$
$$R_4^i = R_4^i + DT / (k_4^s \cdot L \cdot R \cdot (\theta + 2\alpha - DN/R))$$
$$R_4^e = R_4^e + DT / (k_4^s \cdot L \cdot R \cdot (\theta + 2\alpha - DN/R))$$

Steel masses

$$m_1^s = \rho_1^s \cdot DT \cdot (2\pi - \theta) R, \quad m_2^s = \rho_2^s \cdot DT \cdot (\theta - 2\alpha - DN/R) R/2$$
$$m_3^s = \rho_3^s \cdot DT \cdot DN, \quad m_4^s = \rho_4^s \cdot DT \cdot (\theta + 2\alpha - DN/R) R/2$$

FIGURE 6.25 (cont'd)

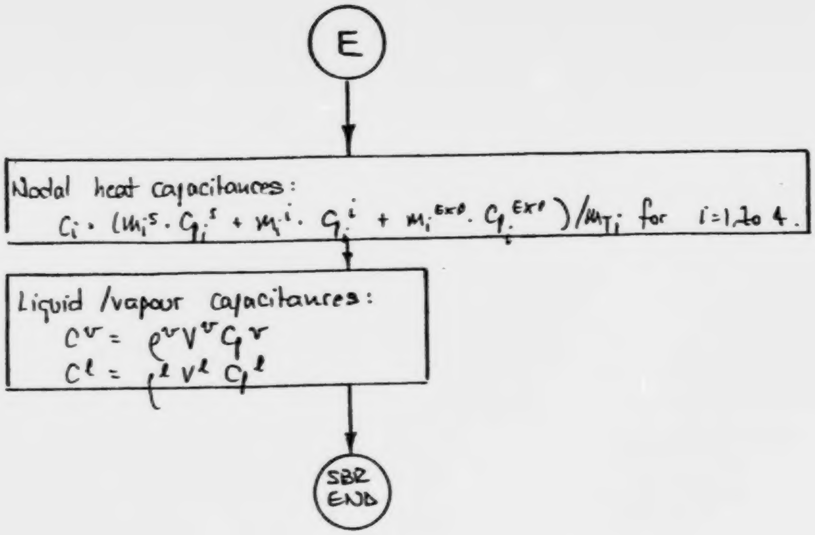
E
Nodal heat capacitances:
$C_i = (m_i^s \cdot c_{p_i}^s + m_i^i \cdot c_{p_i}^i + m_i^{Exp} \cdot c_{p_i}^{Exp})/m_{T_i}$ for $i=1$ to 4.
Liquid /vapour capacitances:
$C^v = \rho^v V^v c_p^v$
$C^l = \rho^l V^l c_p^l$
SBR END

Note: θ = angle describing location of vapour/liquid boundary at $j=1$ (initially).

FIGURE 6.25 (cont'd)

R_m SUBROUTINE
(6.3.13.1)

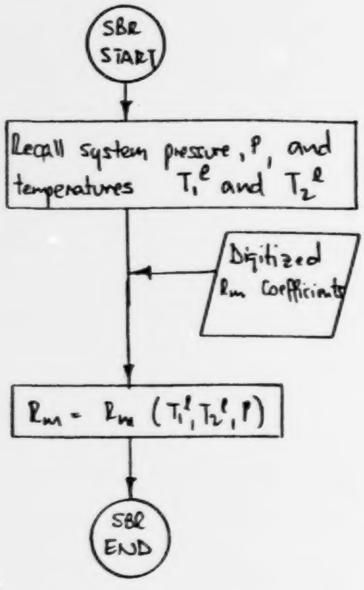
SBR START
Recall system pressure, P, and temperatures T_1^l and T_2^l
Digitized R_m Coefficients
$R_m = R_m(T_1^l, T_2^l, P)$
SBR END

FIGURE 6.26

6.3.12.2 Coefficients Subroutine - Impinging Torch Model (liquid zone)

For this model, as the nodal spacing is different for the central node than for the surrounding nodes, two types of resistances need to be defined for external and internal cases as shown in Figure 6.24. Steel resistances are defined for each of the nodal linkages in the steel shell.

6.3.13.3 Coefficients Subroutine - Impinging Torch Model (vapour zone)

Four steel nodes are defined each with different nodal areas. Figure 6.25 describes the procedure to determine the link resistances from the heat transfer coefficients and thermal conductivities of the materials between the links.

6.3.13 R_m Subroutine

From a digitized function describing the relationship between T_1^{ℓ}, T_2^{ℓ}, P, and the mixing coefficient, R_m, it will be possible to determine the heat transfer from the saturated zone to the sub-cooled zone. As recommended in further sections, determination of this functional relationship should be left to experiment. Figure 6.26 shows how the coefficient can be determined from this function.

6.3.14 Thermal Network

At the center of the thermodynamic model is the network solution for the heat transfer equations. The physical model is represented by modes and links that have variable properties. The network configuration depends upon the particular model of interest. However, the method of solution discussed in this Section is general to all model variations.

The variation in temperature of the modes constituting the network is a function of the thermal capacity, linkage resistances, and heat flows. In its most general form, this is expressed in matrix notation as,

$$\{C\}\cdot[\dot{T}(j)] + \{K\}\cdot[T(j)] = [Q(j)] \qquad (12)$$

Where $\{\ \}$ denote a matrix quantity and
$[\ ]$ a vector,
$\{C\}$ is the heat capacity matrix
$\{K\}$ is the heat conductivity matrix, formed from the individual link resistances
$[Q(j)]$ is the vector of nodal heat inputs
$[T(j)]$ is the vector of nodal temperatures
$[\dot{T}(j)]$ is the vector of time derivatives of nodal temperatures.

A solution to this general equation is obtained when all temperatures and fluxes can be specified. Boundary temperatures and initial heat fluxes "drive" the system and a consistent set of equations and unknowns can be defined. The solution algorithm is described in Figure 6.27 and is described below.

The temperature time derivative can be adequately approximated by the following relation, should the time step be sufficiently small,

$$[\dot{T}(j)]\cong([T(j)-[T(j-1)]])/\Delta t \qquad (13)$$

Let the conductivity matrix be expressed as two matrices,

$$\{K\} = \{K^*\} + \{\Delta K^*\} \qquad (14)$$

Where $\{K^*\}$ is taken to be temperature independent, whereas $\{\Delta K^*\}$ is a temperature dependent matrix. The general equation can be re-arranged as,

$$\left(\frac{1}{\Delta t}\cdot\{C\}+\{K^*\}\right)\cdot[T(j)] = [Q(j)]+\frac{1}{\Delta t}\cdot\{C\}\cdot[T(j-1)]-\Delta Q^* \qquad (15)$$

Where $\Delta Q^* \equiv \{K^*\}\cdot[T(j-1)]$
Define, $\{A\}= \frac{1}{\Delta t}\cdot\{C\}+ \{K^*\}$
and solve for $[T(j)]$. Therefore,

$$[T(j)] = \{A\}^{-1}\cdot \left([Q(j)] + \frac{1}{\Delta t}\cdot\{C\}\cdot[T(j-1)] - \Delta Q^*\right) \qquad (16)$$

This now forms a consistent set of equations which can be solved for $[T(j)]$. To adjust the heat transfer coefficients accounting for

THERMAL NETWORK

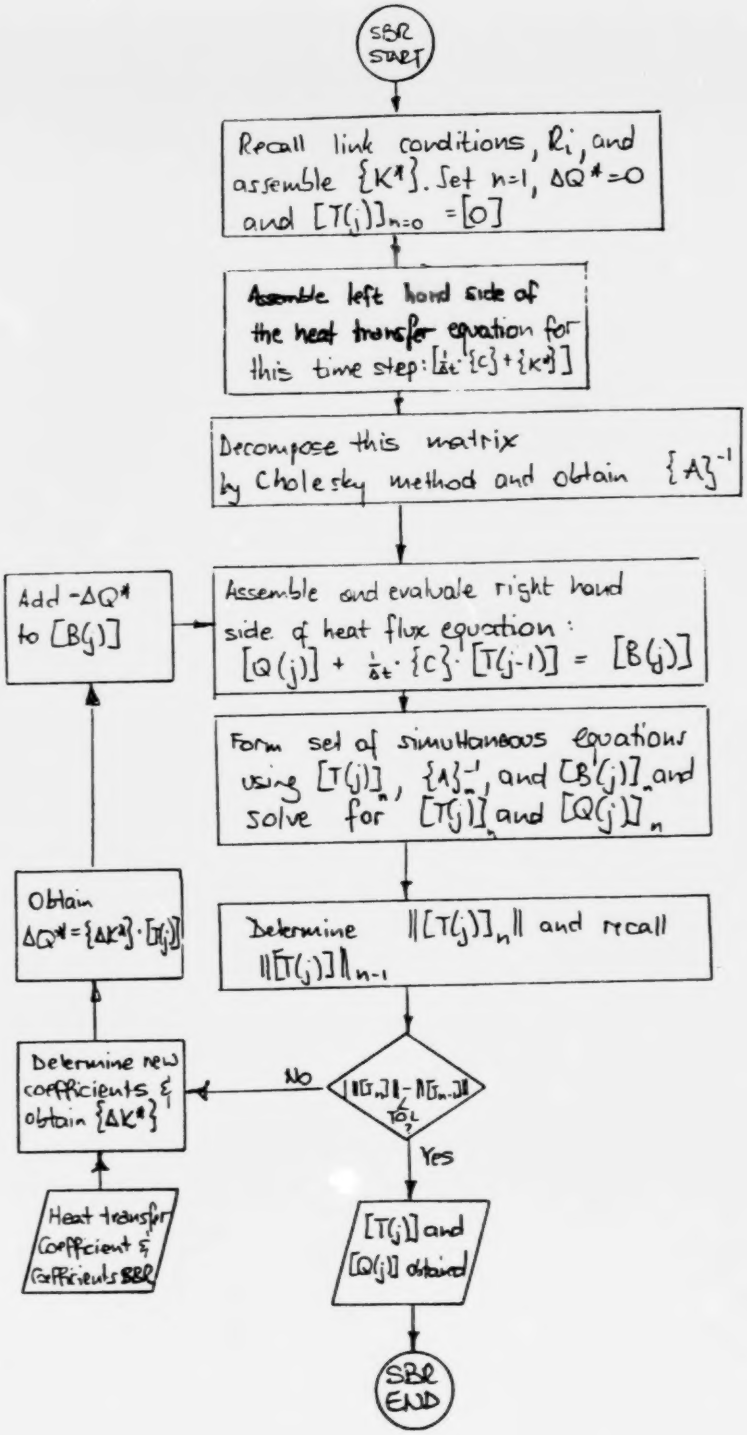
SBR START
Recall link conditions, R_i, and assemble $\{K^*\}$. Set $n=1$, $\Delta Q^*=0$ and $[T(j)]_{n=0} = [0]$
Assemble left hand side of the heat transfer equation for this time step: $[\frac{1}{\Delta t}\cdot\{C\}+\{K^*\}]$
Decompose this matrix by Cholesky method and obtain $\{A\}^{-1}$
Assemble and evaluate right hand side of heat flux equation: $[Q(j)] + \frac{1}{\Delta t}\cdot\{C\}\cdot[T(j-1)] = [B(j)]$
Add $-\Delta Q^*$ to $[B(j)]$
Form set of simultaneous equations using $[T(j)]_n$, $\{A\}_n^{-1}$, and $[B'(j)]_n$ and solve for $[T(j)]_n$ and $[Q(j)]_n$
Obtain $\Delta Q^* = \{\Delta K^*\}\cdot[T(j)]$
Determine $\|[T(j)]_n\|$ and recall $\|[T(j)]\|_{n-1}$
$\|[T_n]\| - \|[T_{n-1}]\| < TOL$?
No
Yes
Determine new coefficients & obtain $\{\Delta K^*\}$
Heat transfer Coefficient & Coefficients SBR
$[T(j)]$ and $[Q(j)]$ obtained
SBR END

FIGURE 6.27

their variation with temperature, the ΔQ^* will be modified. That is, initially $n = 1$ and $\Delta Q^* = 0$. New temperatures, $[T(j)]_n$, are obtained using (16) and serve as the basis to calculate the new heat transfer coefficients as represented by $\{\Delta K^*\}$. That is,

$$\{\Delta K^*\}_n \equiv \{K(j)\}_n - \{K(j)\}_{n=1} \tag{17}$$

Adjustment are made to the new temperatures by adding the correction factor $\{\Delta Q^*\}$. This process is repeated until the nodal temperatures converge to a value set by an overall tolerance. Under some circumstances, the convergence of the above iteration may required a damping factor to be introduced into the iteration to prevent undesirable oscillations which could result in divergence.

$$T_i(j)_n = T_i(j)_{n-1} + D_f \cdot (T_i(j)_n - T_i(j)_{n-1}) \tag{18}$$

Where D_f can be varied by the user according to the rate of convergence.

PRV SUBROUTINE
(6.3.15.1)

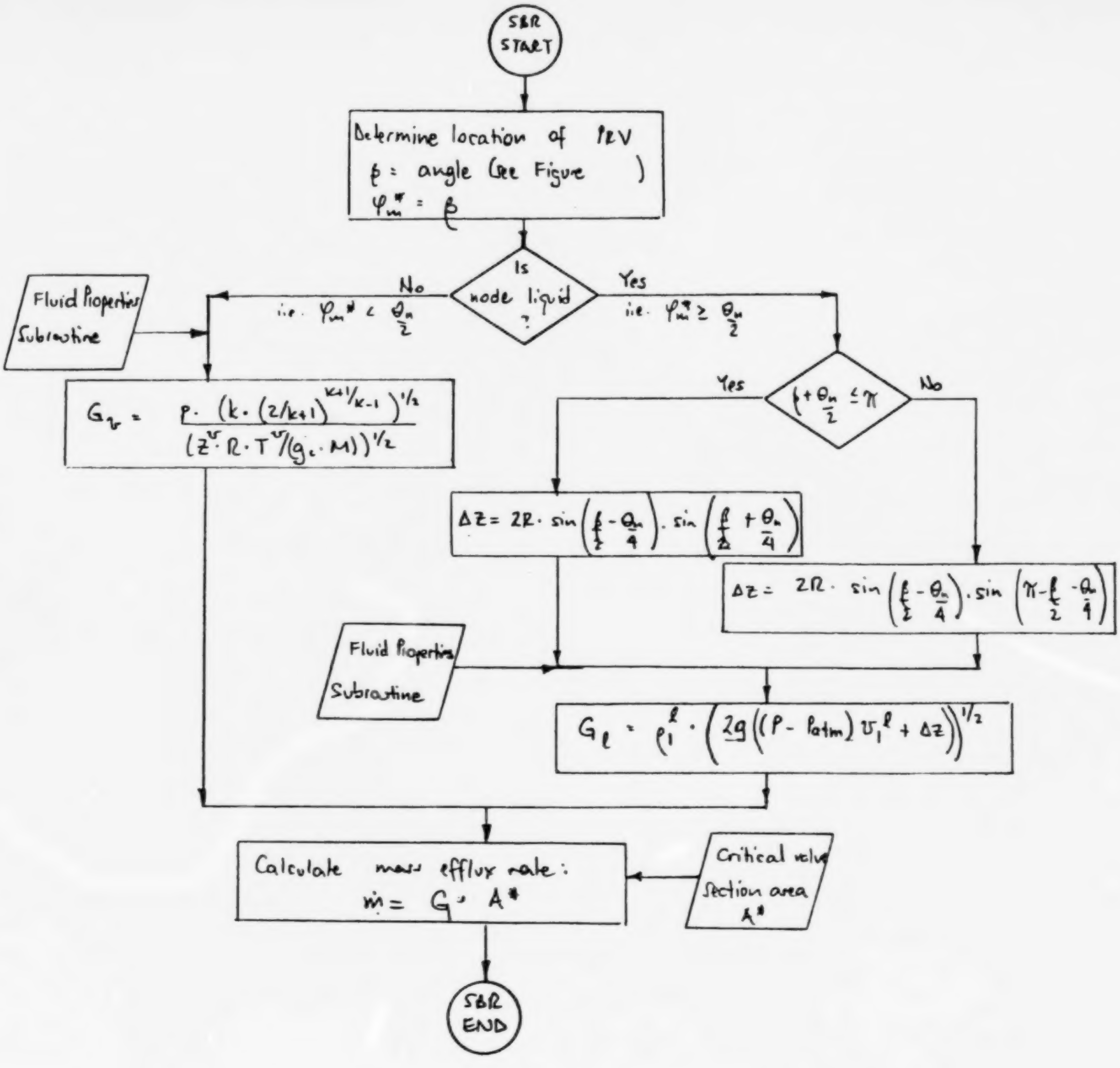
SBR START
Determine location of PRV
β = angle (see Figure)
φm* = β
Is node liquid ?
No
i.e. φm* < θn/2
Yes
i.e. φm* ≥ θn/2
Fluid Properties Subroutine
Gv = p·(k·(2/k+1)^(k+1/k-1))^1/2 / (Z^v·R·T^v/(gc·M))^1/2
Yes
β + θn/2 ≤ π
No
ΔZ = 2R·sin(β/2 − θn/4)·sin(β/2 + θn/4)
ΔZ = 2R·sin(β/2 − θn/4)·sin(π − β/2 − θn/4)
Fluid Properties Subroutine
Gl = ρ1^l·(2g((P − Patm)v1^l + ΔZ))^1/2
Calculate mass efflux rate:
ṁ = G·A*
Critical valve section area A*
SBR END

FIGURE 6.28

6.3.15 PRV Subroutine - Engulfing Flame Model

The purpose of this subroutine is to determine the mass efflux rate from the system given the system temperatures and pressure, liquid level, and PRV location. As discussed in Section 4, this rate will depend upon the quality of the fluid being discharged. Using the two body model concept (liquid and vapour), we have taken the flow to be either fully liquid or fully vapour, depending upon the location of the valve with respect to the phase boundary. Using equation (1) (Section 4.1), the mass flux can be obtained if vapour is discharged. Equation (2) is used to calculate the liquid discharge rate through the critical valve area A*, as shown in the logic diagram, Figure 6.28. The static head on the valve, ΔZ, depends upon the valve and liquid level locations, defined by the angles β and θ_n, respectively and the tank radius, see Figure 6.29.

6.3.16 State Equations - Liquid Phase

The liquid state equation used to determine the specific volume of this phase is given in Figure 6.30. The thermal expansion coefficient, α_T, can be obtained from a digitized thermal properties table. This function is defined as,

$$\alpha_T = \frac{1}{v} \cdot \left(\frac{\partial v}{\partial T} \right)_p \qquad (17)$$

similarly, the isothermal compressibility can be obtained from such a table, as this coefficient is defined as,

$$K_T = \frac{1}{v} \cdot \left(\frac{\partial v}{\partial p} \right)_T \qquad (18)$$

The conditions (T_0, P_0) refer to reference liquid states near to the current state (T,P) which allows for reasonably accurate determination of the coefficients through differentiation of the tabular values.

STATIC LIQUID LEVEL ON PRV (ΔZ)

$$\beta + \frac{\theta_n}{2} > \pi$$

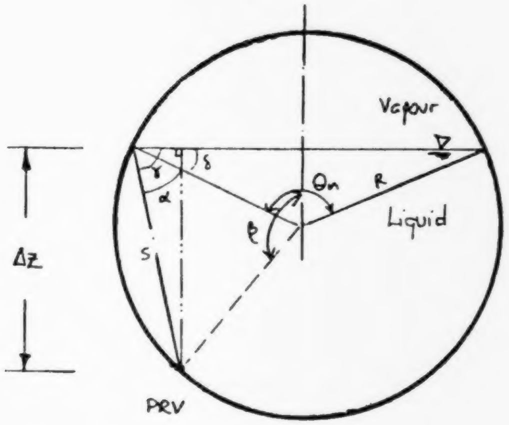
Vapour
∇
δ
γ
α
θ_n
R
Liquid
β
s
Δz
PRV

$$s = 2R \sin \left(\frac{\beta - \theta_n/2}{2}\right)$$

$$\delta = (\pi - \theta_n)/2$$

$$\alpha = (\pi - \beta + \theta_n/2)/2$$

$$\gamma = \pi - \beta/2 - \theta_n/4$$

$$\Delta z = 2R \cdot \sin\left(\frac{\beta - \theta_n/2}{2}\right) \cdot \sin\left(\pi - \frac{\beta}{2} - \frac{\theta_n}{4}\right)$$

$$\beta + \frac{\theta_n}{2} \leq \pi$$

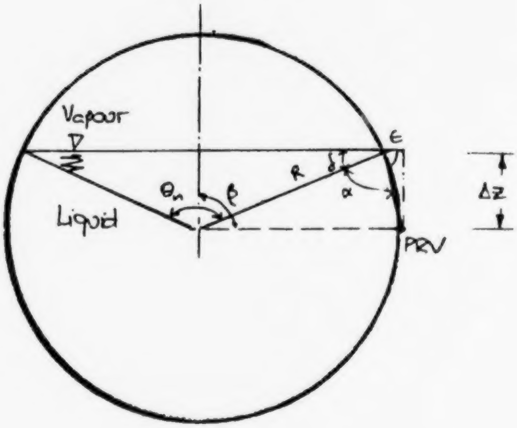
Vapour
∇
ε
δ
R
θ_n
β
α
Liquid
Δz
PRV

$$s = 2R \sin \left(\frac{\beta - \theta_n/2}{2}\right)$$

$$\epsilon = (\beta + \theta_n/2)/2$$

$$\alpha = (\pi - \beta + \theta_n/2)/2$$

$$\Delta z = 2R \cdot \sin\left(\frac{\beta - \theta_n/2}{2}\right) \cdot \sin\left(\frac{\beta + \theta_n/2}{2}\right)$$

FIGURE 6.29

STATE EQUATIONS - (Liquid Phase)
(6.3.16.1)

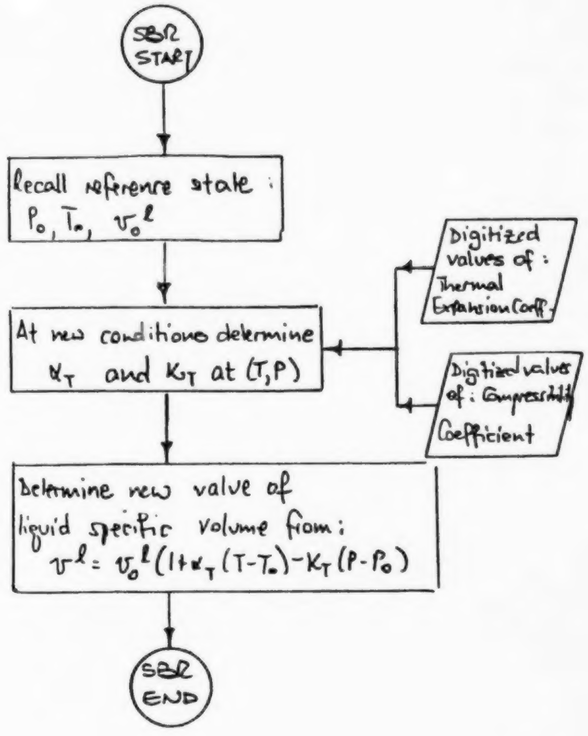
SBR START
Recall reference state : P₀, T₀, v₀ˡ
Digitized values of : Thermal Expansion Coeff.
At new conditions determine αT and KT at (T,P)
Digitized values of : Compressibility Coefficient
Determine new value of liquid specific volume from :
vˡ = v₀ˡ(1+αT(T-T₀)-KT(P-P₀)
SBR END

FIGURE 6.30

STATE EQUATIONS - Vapour Phase
(6.3.17.1)

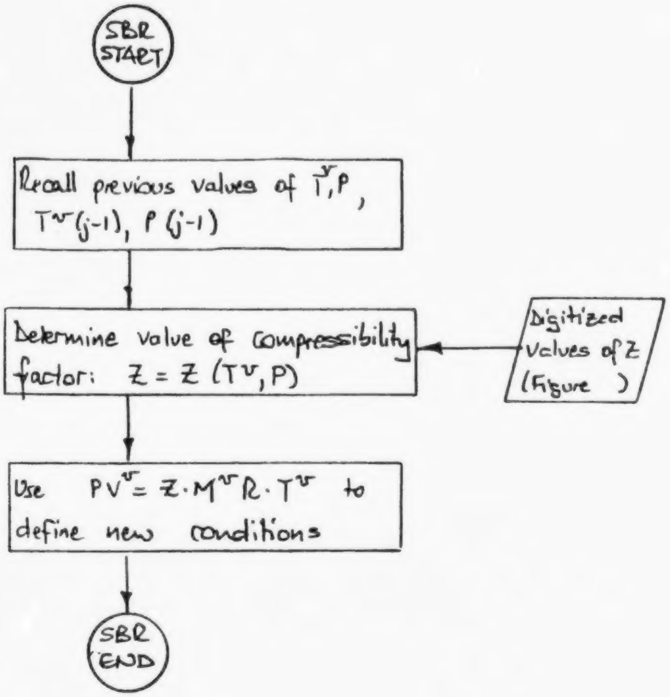
SBR START
Recall previous values of T^v, P, $T^v(j-1)$, $P(j-1)$
Determine value of compressibility factor: $Z = Z(T^v, P)$
Digitized values of Z (Figure)
Use $PV^v = Z \cdot M^v R \cdot T^v$ to define new conditions
SBR END

FIGURE 6.31

6.3.17 State Equations - Vapour Phase

Figure 6.31 makes reference to values of the compressibility factor Z which are required to modify ideal gas law predictions of vapour state parameters. Figure 6.32, from reference (24), presents Z over a wide range of propane vapour pressure and temperatures. This figure would be suitable to digitize for use in this subroutine.

6.3.18 Process Equations - Stage 1

As described in previous Sections, the vapour under heating conditions with the valve closed (Stage 1) undergoes what appears to be isentropic compression during the initial few pressure peaks. During this time, the bulk of the liquid comes to a saturated condition and the rate of thermal expansion of the liquid is reduced. However, during the very first excursion to PRV venting, the process appears to be one of neither constant entropy nor volume. It is proposed that the polytropic exponent describing this process, $n > k$, be determined as part of Phase II, with model predictions fitted to experimental results over the initial periods. Without the model to determine which value of n would most appropriate for this first pressure rise, it will be assumed that $n=k$.

Following the achievement of saturation conditions in the liquid and before the liquid is converted completely to vapour, it appears that the Stage 1 process is one of constant specific volume. This has been incorporated into the logic diagram for the subroutine presented in Figure 6.33.

6.3.19 Process Equation - Stage 2

During periods of rapid system depressurization, the polytropic process is described by $P.v^n = c$, where the exponent n is a function of the temperature, see Section (2.0). When the liquid has come to saturation (B=1) and before the liquid has been converted entirely into vapour (A=1), and when the valve is open, the process approximates to one corresponding to constant specific vapour volume, as described in Figure 6.34.

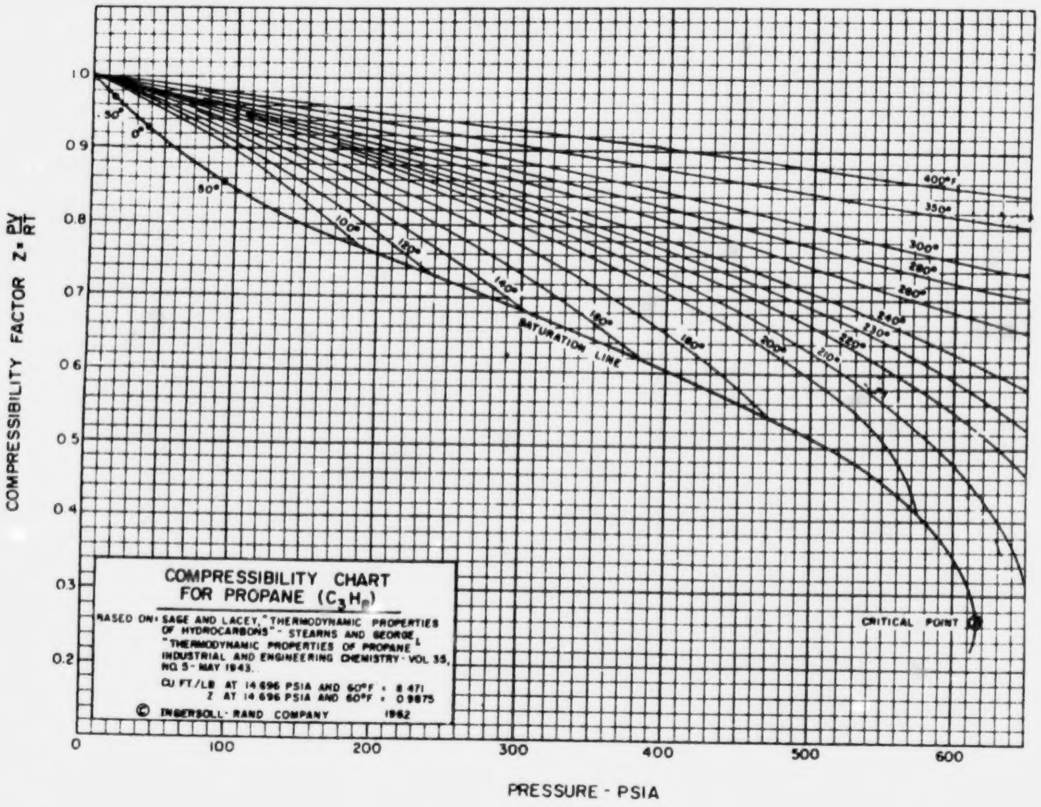

Figure 6. 32 Compressibility chart for propane (Z)
From reference (24)

PROCESS EQUATIONS - Stage 1
(6.3.18.1)

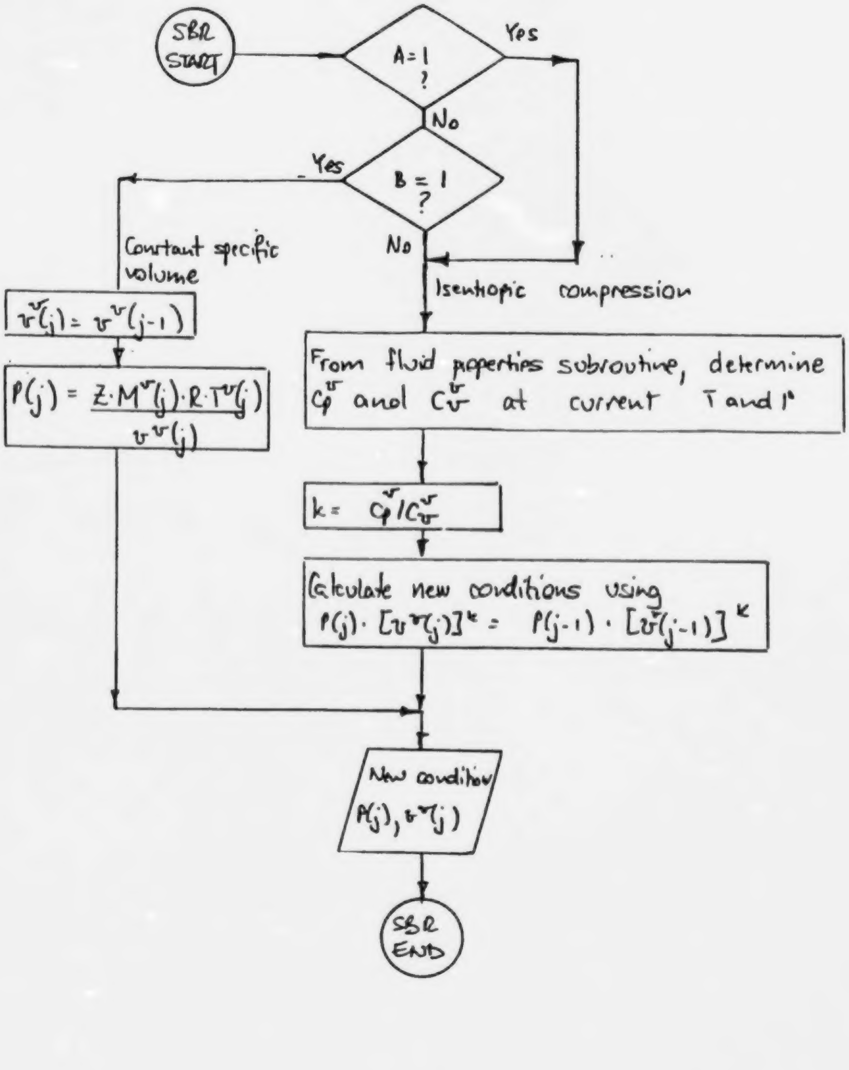
SBR START
A = 1 ?
Yes
No
B = 1 ?
Yes
No
Constant specific volume
$v^v(j) = v^v(j-1)$
$P(j) = \frac{Z \cdot M^v(j) \cdot R \cdot T^v(j)}{v^v(j)}$
Isentropic compression
From fluid properties subroutine, determine C_p^v and C_v^v at current T and P
$k = C_p^v / C_v^v$
Calculate new conditions using $P(j) \cdot [v^v(j)]^k = P(j-1) \cdot [v^v(j-1)]^k$
New condition $P(j), v^v(j)$
SBR END

FIGURE 6.33

PROCESS EQUATION - Stage 2
(6.3.19.1)

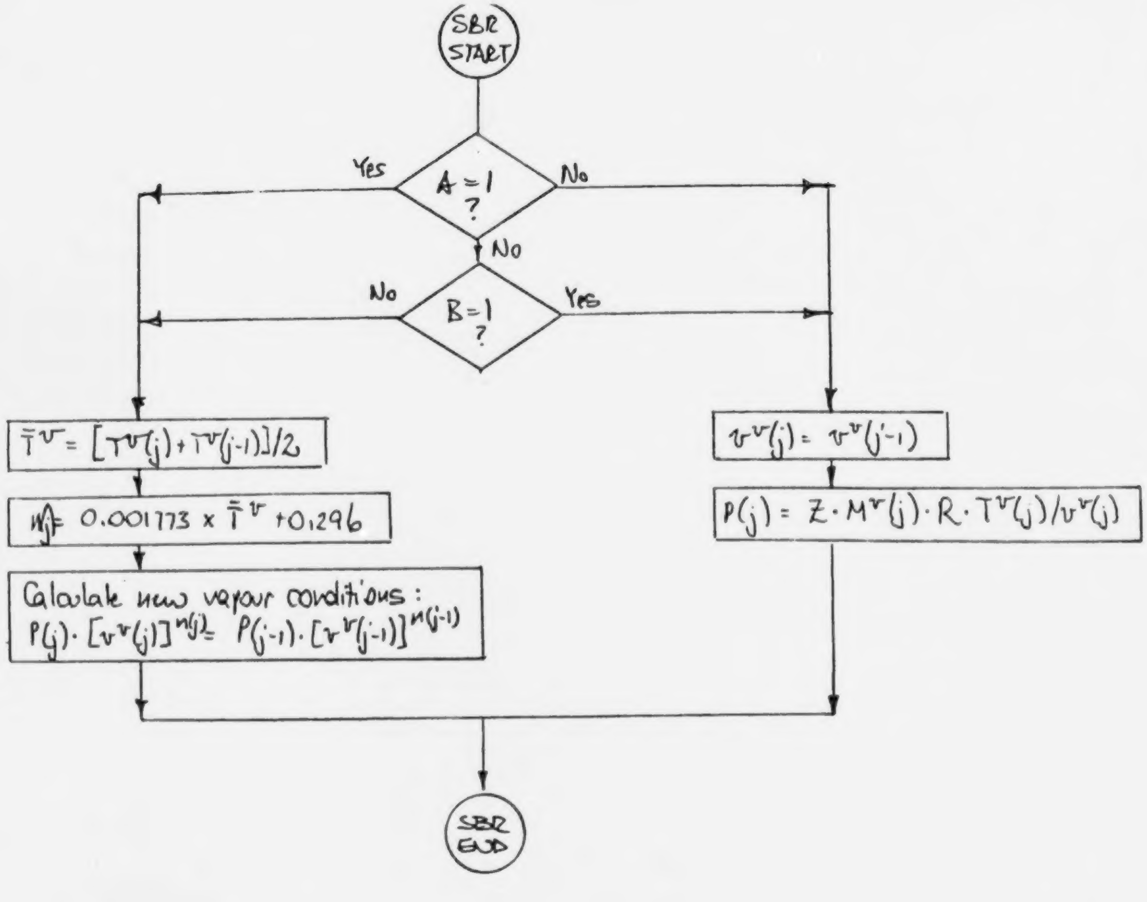
SBR START
Yes
A = 1 ?
No
No
No
B = 1 ?
Yes
$\bar{\bar{T}}^v = [T^v(j) + T^v(j-1)]/2$
$n(j) = 0.001773 \times \bar{\bar{T}}^v + 0,296$
Calculate new vapour conditions:
$P(j) \cdot [v^v(j)]^{n(j)} = P(j-1) \cdot [v^v(j-1)]^{n(j-1)}$
$v^v(j) = v^v(j-1)$
$P(j) = Z \cdot M^v(j) \cdot R \cdot T^v(j)/v^v(j)$
SBR END

FIGURE 6.34

VAPOUR PRESSURE EQUATION
(6.3.20.1)

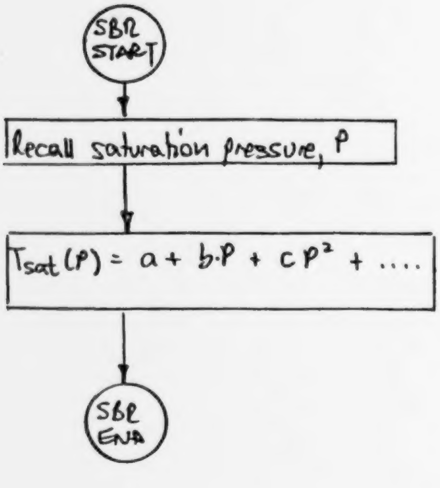
SBR START
Recall saturation pressure, P
$T_{sat}(P) = a + b \cdot P + cP^2 + \ldots.$
SBR END

digitized vapour pressure equation.

FIGURE 6.35

MASS TRANSFER EQUATIONS - Vaporization
(6.3.21.1)

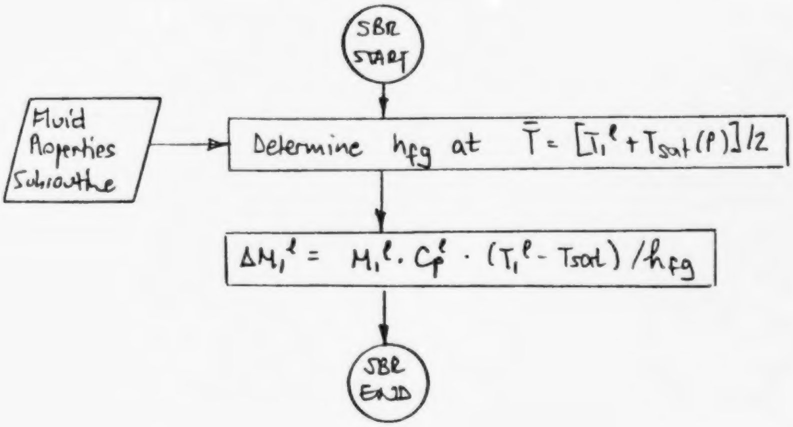
SBR START
Fluid Properties Subroutine
Determine h_{fg} at $\bar{T} = [T_1^{\ell} + T_{sat}(P)]/2$
$\Delta M_1^{\ell} = M_1^{\ell} \cdot C_p^{\ell} \cdot (T_1^{\ell} - T_{sat}) / h_{fg}$
SBR END

FIGURE 6.36

6.3.20 Vapour Pressure Equation

A digitized version of the vapour pressure equation is used to determine the saturation temperature, T_{sat}, as a function of the system pressure, Figure 6.35.

6.3.21 Mass Transfer Equations - Vaporization

The procedure to determine the mass transfered across the phase boundary is described in Figure 6.36. The value of mass exchanged is obtained by performing a heat balance as shown in Figure 6.35.

6.3.22 Mass Transfer Equations - Condensation

As shown in the previous illustration, the condensation rate is determined from a simple heat balance. The mass exchange is derived from this relation and incorporated into the subroutine described in Figure 6.37.

6.3.23 Failure Subroutine

A simple relationship for the tank failure criterion is taken. The ultimate material strength varies with temperature and a σ - T curve will be stored in digital form for this subroutine, Figure 6.38. The particular failure stress will be found by interpolation. The mean shell stress due to pressure and the imposed temperature gradient may be calculated at each time step and failure flagged when this stress exceeds the ultimate stress.

6.3.24 PRV Set Points

To determine the state of the PRV during the accident, system pressure, time, and nodal temperatures are used to define the current set points as discussed in Section 4.2. Further analysis is required to determine the functional relationship, $P_O = P_O(T,P,t)$ and $P_C = P_C(T,P,t)$ for the cases when the valve is in the vapour or liquid space. However, Figure 6.39 provides the structure of the subroutine used to determine these set points for the program.

MASS TRANSFER EQUATIONS - Condensation
(6.3.22.1)

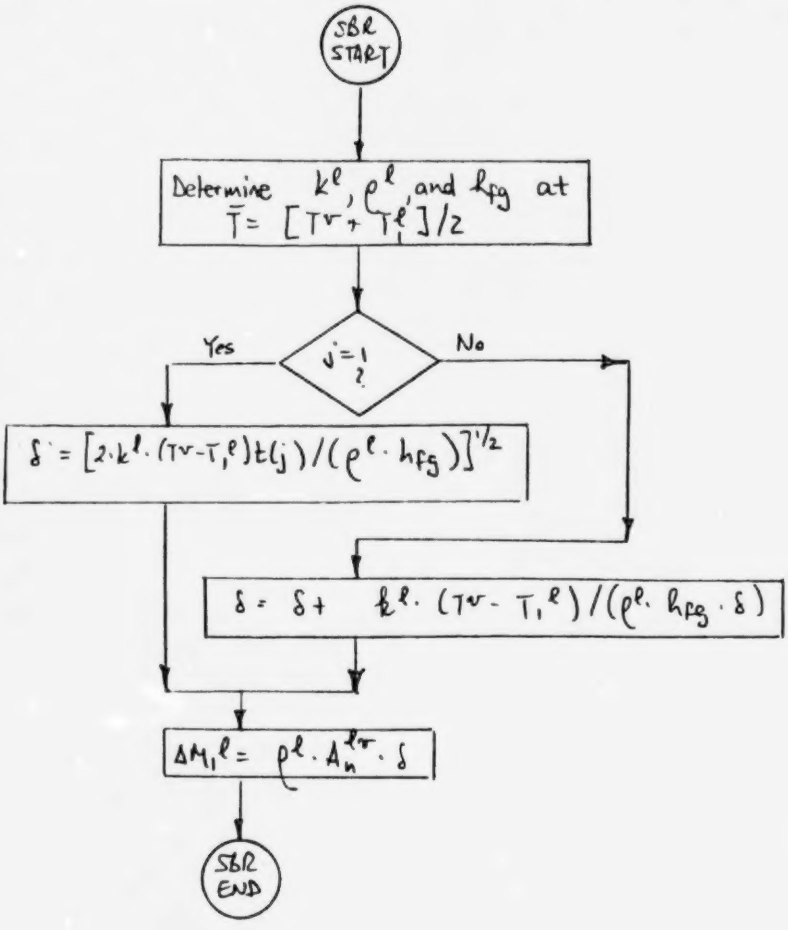
SBR START
Determine k^l, ρ^l, and h_{fg} at $\bar{T} = [T^v + T_1^l]/2$
$j = 1$?
Yes
No
$\delta = [2 \cdot k^l \cdot (T^v - T_1^l) t(j) / (\rho^l \cdot h_{fg})]^{1/2}$
$\delta = \delta + k^l \cdot (T^v - T_1^l) / (\rho^l \cdot h_{fg} \cdot \delta)$
$\Delta M_1^l = \rho^l \cdot A_n^{lv} \cdot \delta$
SBR END

FIGURE 6.37

FAILURE SUBROUTINE

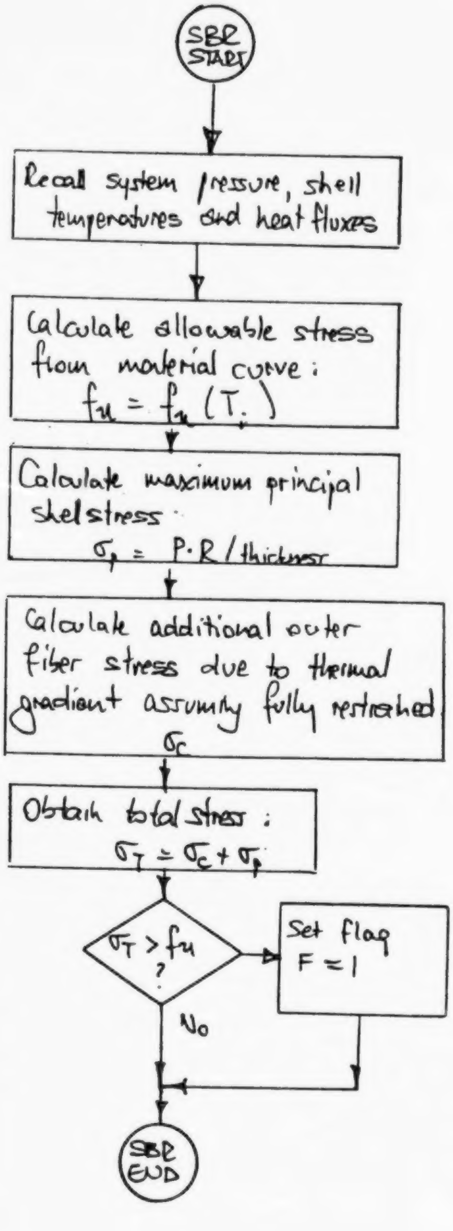
SBR START
Recall system pressure, shell temperatures and heat fluxes
Calculate allowable stress from material curve: $f_u = f_u(T_i)$
Calculate maximum principal shelstress: $\sigma_p = P \cdot R / \text{thickness}$
Calculate additional outer fiber stress due to thermal gradient assuming fully restrained σ_c
Obtain total stress: $\sigma_T = \sigma_c + \sigma_p$
$\sigma_T > f_u$?
Set flag F = 1
No
SBR END

FIGURE 6.38

PRV SET POINTS

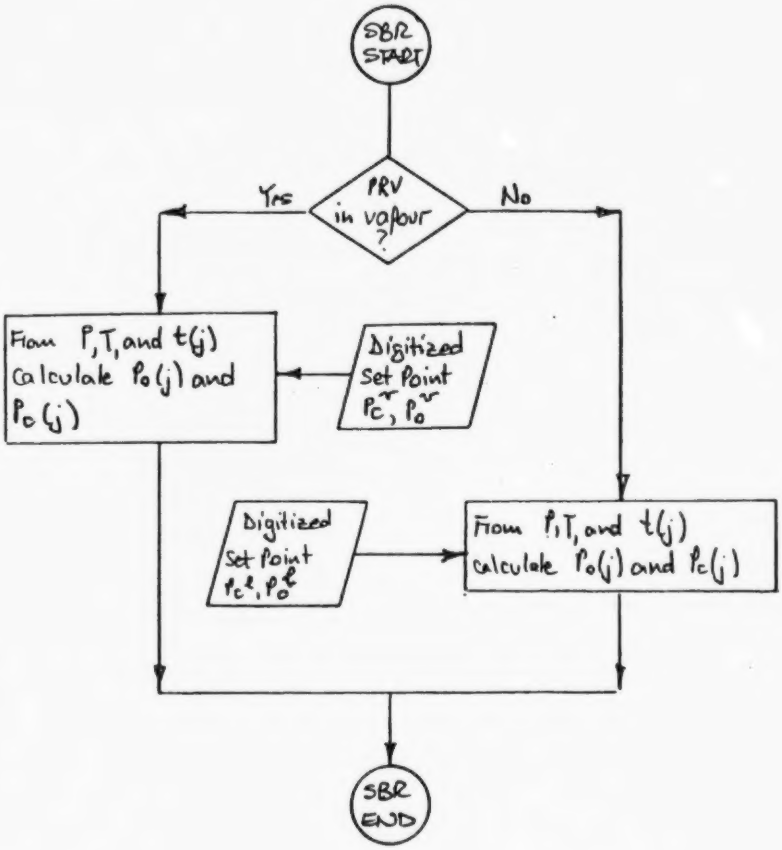
SBR START
PRV in vapour ?
Yes
No
From P, T, and t(j) calculate Po(j) and Pc(j)
Digitized Set Point Pc^v, Po^v
Digitized Set Point Pc^l, Po^l
From P, T, and t(j) calculate Po(j) and Pc(j)
SBR END

FIGURE 6.39

7.0 STRUCTURAL CONSIDERATIONS AND THE FAILURE CRITERIA

7.1 PRESSURE INDUCED STRESSES

The structural failure of the cylindrical pressure vessels typical of those used in the rail tank car must be understood before a prediction of future failures can be made. Some investigation was made of the vessels used in the Suffield tests (3) however, no comprehensive analysis has been made to establish what the failure criteria should be.

The maximum principal stress can be readily calculated for the simple cylindrical vessel from

$$\sigma_{max} = \frac{pR}{t}$$

where p is the internal pressure
R is the radius of the shell
t is the wall thickness

Secondary bending stresses due to pressure are superimposed on this mean stress level wherever there are discontinuities such as at the nozzle intersection, saddle supports and head to cylinder intersection. The values of these additional stresses depend on the nature of the structural design and are minimized by the choice of appropriate material thicknesses and additional material stiffening. Locally however such discontinuities may raise the maximum outer fiber stress in the steel plate by a factor of 1.5 or more. Finite element or similar analysis may be used to determine the nature of these stresses for a particular design and pressure. However, such analysis is relatively costly and could only be justified if it was felt a complex condition caused a maximum stress beyond that predicted by a simple analysis. For example the stresses caused by a thermal variation around the circumference of the tank could not readily be calculated by hand and would require a computer based analysis. H.G. Engineering have a broad experience of computer based structural analysis and in particular have provided analytical solutions to a number of manufacturers of rail cars and also road tankers. Figure 7.1 shows two typical finite element models used to evaluate stress concentrations at the head of a B-train tanker.

TWO TYPICAL STRUCTURAL MODELS OF A TANK CAR

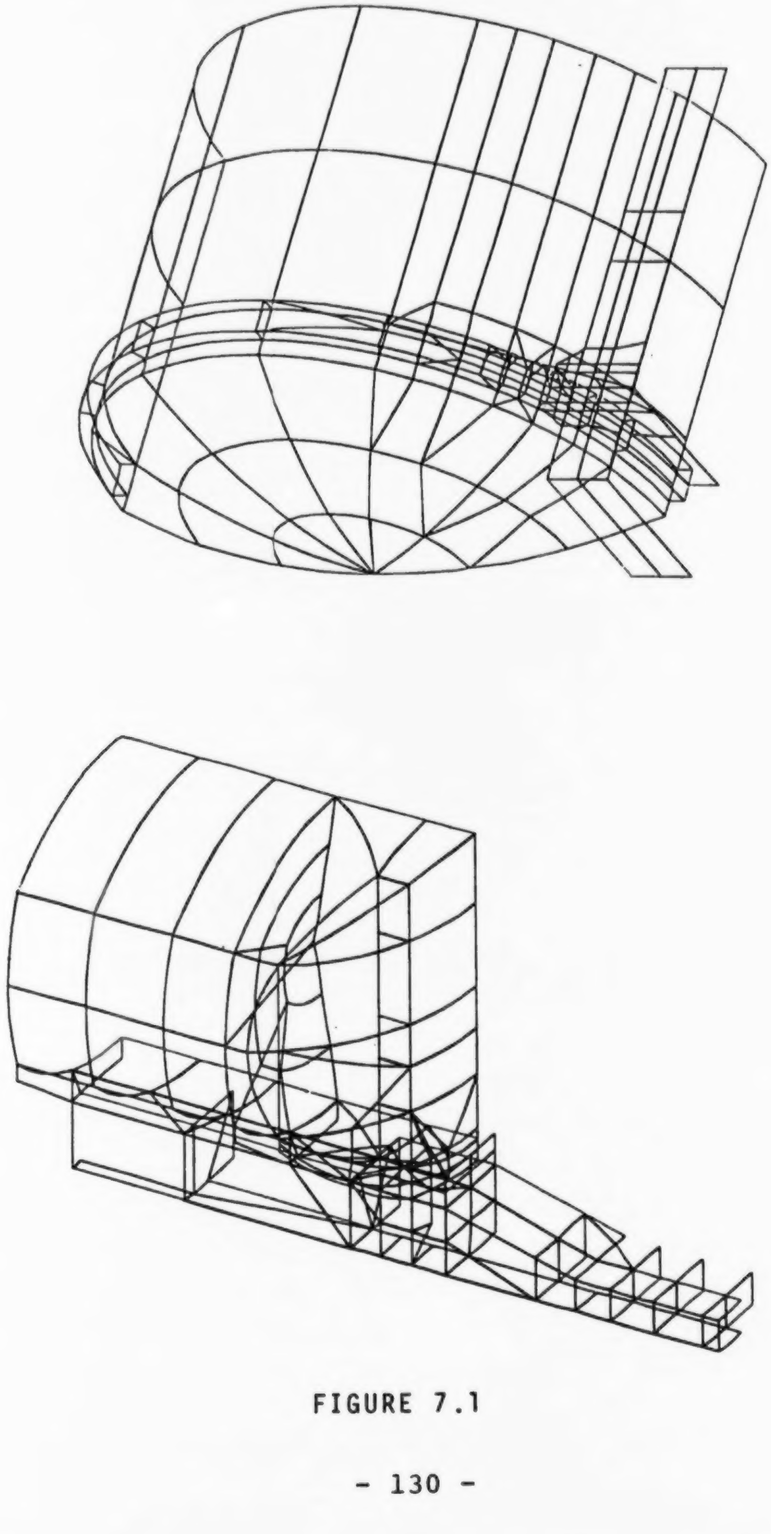

FIGURE 7.1

7.2 EXPERIMENTAL DATA

From the Suffield tests it appears the pressure in the tank rises from 80 psig to a peak of 280 psig quite rapidly but failure does not occur until sometime later. This indicates that the material temperature plays a role in the failure as would be expected. From available data on the material used in fabrication of the Suffield vessels, (ASTM-A285) it appears the strength of the steel falls off rapidly beyond 900°F. A graph of the yield strength and tensile strength is shown in Figure 7.2. A survey of the temperature data in the vapor space at the top of the tank shows the vapor temperature reached this value in all of the tests. Table 7.1 shows the temperatures and pressures achieved in the tests. There is no obvious explanation why all the vessels did not fail on the basis of these results however the failure is critically dependent on temperature and the high temperature characteristics of the material, which can vary considerably. The best that can be suggested is that the temperature should not be allowed to exceed 800°F.

	Temperatures at the top of the tank °C	Pressure MPa	Maximum principal stress due to pressure+ MPa	Approx. tensile strength MPa
BASELINE*	-	-	-	-
DRES	499 (930°F)	0.896	34.5	51.7
HOWLER	661 (1222°F)	0.659	26.5	6.89
NOVA	572 (1061°F)	0.827	31.8	13.79
DIABLO	479 (895°F)	1.31	50.3	27.58
ENIGMA	496 (926°F)	1.52	57.9	20.68

TABLE 7.1

* No results available but tank exploded.

+ Shell thickness = 5/16 in.

All tests vented successful except the BASELINE and ENIGMA

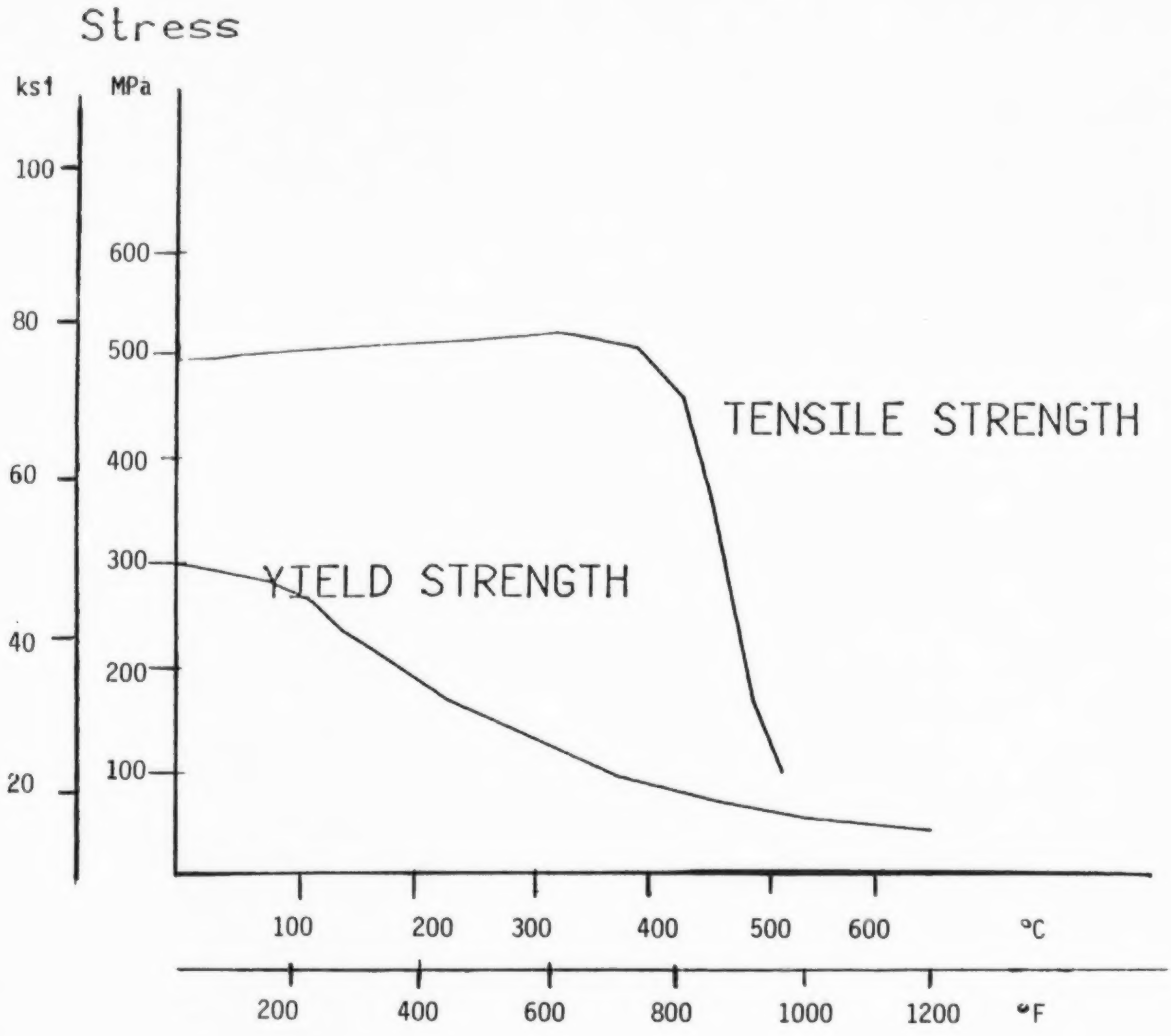

FIGURE 7.2 STRENGTH VS TEMPERATURE FOR A285 STEEL

7.3 THERMAL STRESSES DUE TO WALL TEMPERATURE VARIATIONS

Additional stresses can result from temperature differences through the thickness in the steel shell. In the worst case, if a simply supported cylindrical shell were uniformly heated externally and uniformly cooled internally the strains resulting from the variation through the thickness would be fully constrained, whilst the mean thermal strain would be unconstrained. This axisymmetric case is extreme and a circumferential variation of temperature would induce bending deflections and generate lower stress levels. Figure 7.3 illustrates a simple linear temperature variation that can be assumed to be

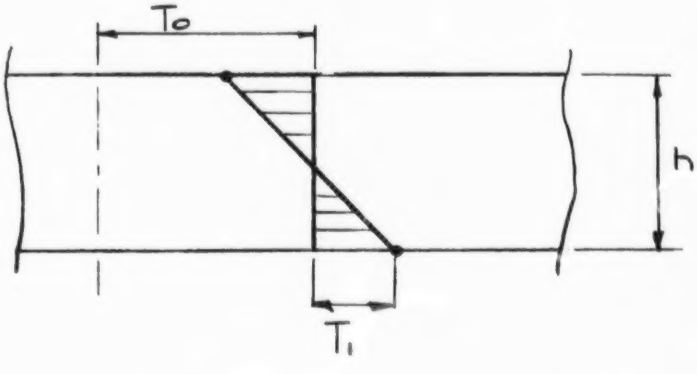

made up of two components; a constant temperature T_0 and a linear variation through the thickness T_1. The thermal stress in a cylinder caused by the linear variation is given by

$$\sigma = \frac{E\alpha T_1}{1-\nu}$$

where

σ	is the maximum stress
E	is the material Young's Modulus
ν	is the Poisson's ratio
α	is the coefficient of expansion
T_1	is the temperature variation

Under these circumstances the side of the shell which is the coolest will go into tension and potentially fail. Knowing the ultimate strength of the material and the properties it is possible to calculate the temperature differential that would cause failure and knowing this and the thickness of the shell walls the corresponding heat flux may be calculated.

Assume for ASTM 285

the ultimate strength $\sigma_f = 460$ MPa

Young's modulus E $= 210 \times 10^3$ MPa

$\nu = 0.3$

$\alpha = 15 \times 10^{-6}$

Then

$$T_1 = \frac{460 \times 10^6 \ (1 - 0.3)}{210 \times 10^9 \times 15 \times 10^{-6}}$$

$$T_1 = 102^\circ\mathrm{C}$$

Assume the wall thickness in a typical tank car is 1/4" (0.635 cm)

Also

$$Q = k\, A\, \frac{dT}{dx}$$

Where Q is the heat flux through the shell

k is the conductivity of steel (63W/mK)

A is the area 1 m^2

$\frac{dT}{dx}$ is the variation of temperature through the thickness

Hence

$$Q = 63 \times 1 \times 102 \times \frac{2}{0.00635}$$

$$Q = 2.02 \times 10^6 \text{ watts}/m^2$$

In practice a heat transfer rate of 1.0 x 10^5 watts/m^2 is considered more realistic which would in the worst case lead to an additional surface stress of 16 MPa. The pressure stresses and potential thermal stresses due to mean temperature variations around the shell are therefore considered of primary importance and not the local variation through the thickness.

In the case of the impinging flame a local hot spot will occur which will initially cause local compressive stress. However due to the degradation of the material properties with increasing temperature local yielding may take place leading ultimately to failure. A more detailed analysis of this effect will be required before a failure condition can be established. The structural failure will be dependent on the extent of the impingement area. The finite element method is a suitable tool for the study of this effect and the progressive yielding that will likely occur could be progressively followed by use of a non-linear finite element program.

7.4 THE MODEL FAILURE CRITERIA

From the arguments developed in the foregoing sections it can be concluded that the primary cause of failure is due to a combination of pressure and severely reduced material strength. It is therefore proposed that the model be terminated on this condition. The maximum steel temperature will therefore be used together with a numerical form of the material strength vs temperature curve to determine the allowable stress. This will be compared to the stress due to the current internal pressure. Failure will be considered to have occurred for the engulfing flame when the actual stress exceeds the allowable.

At this point no simple failure criteria can be postulated for the local impingement case and a separate structural model will have to be used to determine this limit.

8.0 PHYSICAL DATA

8.1 REQUIREMENTS FOR PHYSICAL DATA

To meet the project objective of developing a model, or models, which will validly describe the sequence of events which occur when LPG tanks of various designs and fitted with various protective systems are exposed to external fires of various types and intensities, it will be necessary to provide a considerable range of supporting information. Information is required in order to set the values of the parameters, to establish the functional ranges for the heat and mass flow relationships, and finally to compare the predictions of the models with the events actually observed during field trials.

Most of the physical data, including values for most of the thermal and physical properties of the materials involved in the events, is available from the standard engineering literature. Some properties, such as the temperature-stress characteristics of the particular steels used in the test vessels for the Suffield trials, as well as some of the flame and surface emissivity information are found in more obscure references or must be deduced from other data, and some required data, such as the propane boiling curve in the presence of EXPLOSAFE, are not available and must be provided. These special cases are considered in this section, including concerns with respect to the precision required of the data.

8.2 BOILING CURVES FOR PROPANE

The predictions of the models, most particulary for impinging flame events, are dependent upon the availability of propane boiling curves of adequate precision and applicability. Data are sparse for boiling propane, but boiling curves for 99% propane and for some other propane mixtures from a well-conducted investigation, carried out by Cichelli and Bonilla at Johns Hopkins University in 1945, are available [25]. No data are available on the boiling curve for any liquid in the presence of EXPLOSAFE, although in Section 3.1 we report some preliminary qualitative tests with water boiling in the presence of EXPLOSAFE sufficient to indicate that it will have a substantial effect. The Cichelli and Bonilla data were taken on horizontal flat surfaces.

There is a clear need for boiling curve data for a liquid in the presence of EXPLOSAFE. Whether the tests must be done with propane, or whether a less flammable liquid could be used and the results interpreted, is a question discussed in Section 9.2. Another question relates to the effect of the inclination of the boiling surface, since the Suffield tests show consistently high steel surface temperatures near the boiling surface, which could be a surface attitude effect. Since the surface position is located by inference from the saturation temperature readings, and such temperatures could extend a few centimeters above the true surface due to a dense population of droplets in that region, it is not entirely clear that the temperature rise is in the sub-surface region. The limited information on attitude in the literature, notably that of Thibault and Hoffman [26], leaves the question open for larger vessels. It would seem wise to select a method of test which would be sensitive to angular effects.

8.3 EXPLOSAFE EFFECTS ON HEAT TRANSFER

As has been pointed out in Section 3,on the "Role of EXPLOSAFE in Tank Car Fires", the presence of EXPLOSAFE will modify heat transfer and thermodynamic behaviour in several ways additional to its effect on the boiling curve. It acts to reduce internal liquid and vapour circulation and mixing; it functions as a radiation shield in the vapour region; it acts as a separator of liquid droplets; it modifies the volumetric thermal capacity, especially in the vapour space; it provides a parallel conduction path through liquid or vapour; it probably thickens the effective boundary layer at the wall; and it modifies bubble circulation mechanics in the liquid.

No useful engineering data of a quantitative nature from laboratory tests are available on these heat transfer effects. TP2740 reports some laboratory work on a heat transfer rig, but the results are not in a useful form and the data provided do not appear to support the conclusions reached. In any case the design of the rig is seriously flawed from a heat transfer point of view. The uncontrolled heat losses through the virtually uninsulated walls, the heat flow short circuit effects of longitudinal conduction in the walls, and strong radial heat flow components within the test section of the rig render the apparatus quite unsuitable for the production of quantitative data of useful precision. Moreover, it does not separate the radiation, conduction and convection components. It is therefore recommended that no further work be done on that apparatus.

Although it would be possible to design and conduct a series of laboratory experiments to support a close analysis of the mechanisms of influence of EXPLOSAFE, no laboratory tests, other than the boiling curve determination already mentioned, are recommended for immediate action. This is because the interaction of EXPLOSAFE in the fire events is complex, and to a very considerable extent the integrated effects of the material can be inferred from the data recorded in the field trials. It may be found necessary, after the engulfment model is first used, to make a laboratory determination of the scale effects on the mixing resistance in the liquid. The importance of such a determination will be made apparent by observations of the sensitivity of the model output to variations in this mixing factor. A description of the relevant tests, should they be needed, is given in Section 9.

8.4 THERMODYNAMIC PROPERTIES OF PROPANE

A full set of properties for the fluid modelled is essential. Data for pure propane are fortunately quite complete over the range of pressures and temperatures encountered in normal engineering use. These data cover temperatures between -75°F (-60°C) and +800°F (427°C), although they are not available in British units directly compatible with the data reported in TP2740 on the Suffield tests for the full range of values, and we prepared a working Mollier chart (pressure-enthalphy) for our analysis of the test results.

Some of the test data for the superheated propane show vapour temperatures up to nearly 650°C. Although these may be above the actual vapour temperatures due to radiation effects at the sensors, temperatures above 427°C are certainly encountered. For data in this range extrapolated values derived from thermodynamic relationships using published compressibity [24] and specific heat information can be considered adequately reliable.

Actual flame temperatures in open air combusiton of propane are usually between 1816 and 1927 °C. Very little work on the thermal radiation properties of propane gas has been reported, but for purposes of estimating the radiation from the burning flame of vented gas to the tank surface, gray gas behaviour can be assumed for the CO_2 amd H_2O products of combustion, using the techniques developed by Hottel [27]. For internal gas radiation transfer in the vapour space the product of gas pressure and mean path length is on the order of 6 atmos. m., and for the eleven atoms of propane, gray gas effective emissivities are of about 0.35 at 204 to 472 °C.

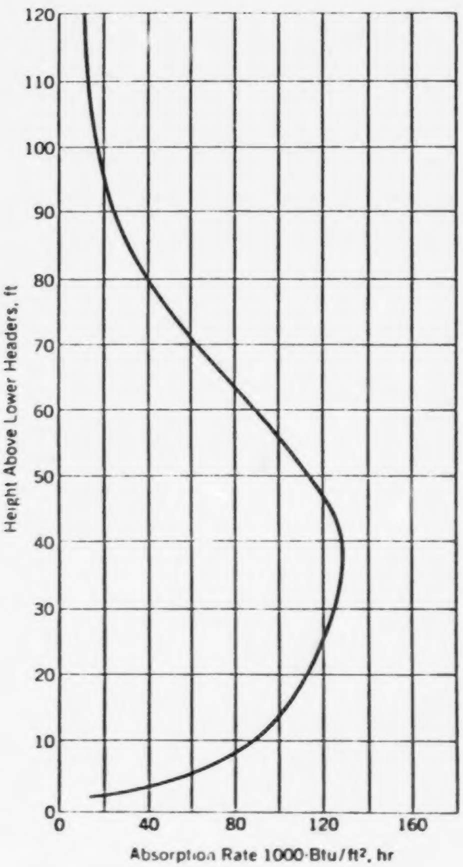

Figure 8.1 Heat absorption rates at different elevations in a furnace at maximum output. After Babcock and Wilcox.

have been estimated. This internal gas-to-surface radiation transfer is relatively unimportant when EXPLOSAFE is present because it acts as a radiation shield and moreover greatly reduces the mean path length and hence the effective emissivity.

8.5 HEAT TRANSFER COEFFICIENTS AND PROPERTIES

The flame-to-surface coefficients in both the engulfing flame and impinging jet cases are important in modelling the thermal behaviour. The coefficients for the engulfing flames are particularly difficult to estimate because of the variability of the conditions. The variables will include the wind velocity and direction, the surface emissivity characteristics of the tank, the flaming pool surface area and liquid temperature, the fuel depth, the tank geometry and the particular position considered on the tank surface. Because of the complication of such cases detailed analysis is rarely undertaken, and reliance is put on overall observations such as the absorption rate curve shown in Figure 8.1 which is used by Babcock & Wilcox for heat transfer from oil flames to boiler walls. This case is close to that for the engulfing flame, and suggests flame-to-surface coefficients on the order of 170 to 340 W/m^2K for flames assumed to be at 816 to 1650 °C. The actual coefficients can be determined for the field test cases by using the model to determine the necessary values to close the heat balance.

The effect of scale on these values is probably significant and the evaluation of this factor would be a consideration in the design of further field trials.

Data for the heat transfer rates for impinging jets are specific to the jet described. The coefficients will vary with radial displacement from the centreline of the jet,angle of impingement, jet velocity and mass flow rate, jet diameter, fuel used and air-to-fuel mixture. Such data are found in the literature of heat treatment, of gas welding and of burner design.

8.6 MECHANICAL PROPERTIES AND TANK MATERIALS

The strength of the tank steel is, of course, directly related to tank failure in a fire. The appropriate selection of tank material is related to a knowledge of the time-pressure-temperature history of the stressed parts, and the model can be used to provide this history. Conversely, in order to interpret the field trial results, a knowledge of the properties of the actual steel used is necessary.

9.0 EXPERIMENTAL WORK REQUIRED

9.1 OVERALL CONSIDERATIONS

As discussed in the previous Section, there is a hierarchy of needs for physical data, ranging from the important need for data with respect to the effect of EXPLOSAFE on the boiling curve, through to the potentially useful, but not critical determination of the radiation and heat and mass transfer coefficients at the free surface of the propane in the tank.

The only laboratory work recommended for immediate action is that concerning the EXPLOSAFE boiling curve, specifically described in Section 9.2. When the program is available for modelling, it will be possible to examine the fire events in detail and it will be apparent from the comparison of the field trial events with the model predictions whether specific further physical test data are needed, and the nature of the information required. It may not be necessary to do any further work. Of the considerable range of additional data that may ultimately be indicated to be required, the need for data on scale effects on mixing, and some further physical data on EXPLOSAFE, will no doubt be given further consideration. Some suggestions on the laboratory work which would be involved are given in Sections 9.3 and 9.4. The need for information on the characteristics of the vent valve is noted in Section 9.5.

9.2 BOILING CURVE DETERMINATIONS

The primary deficiency in physical data for use in the model is the absence of any boiling curve data on surfaces with EXPLOSAFE present, and specifically the absence of such boiling curves for propane. It is recommended that boiling curve information for propane on steel surfaces, with and without EXPLOSAFE present, be conducted.

It is proposed that pure propane be used, rather than a commercial grade which includes some other components. Although such impurities would have an effect, it is thought that this would be small, and the only clearly definable reference state is the pure state.

An examination of the reported work suggests about 50 to 100 test determinations would be necessary to provide a reasonable range of data.

It should be noted that many other techniques are available for the determination of boiling curve data and alternative proposals should recieve careful evaluation. This would be if a proposer had access to existing test apparatus which could be modified to meet the requirements.

Many related studies are reported in the literature. See bibliography references 1 to 40. A recent paper by Chawla and Chan "Heat Transfer from Vertical/Inclined Boundaries of Heat-Generating Pools" Journal of Heat Transfer, Aug. 1982, is relevant to the problem, but the flow is differently induced [28].

9.3 MIXING RESISTANCE SCALE EFFECT

The model we have developed uses a two zone liquid volume, with heat transfer from the primary zone to the secondary zone by a diffusion process that involves mainly a convective mixing mechanism. We believe that the data from the Suffield trials will provide an adequate base to set the resistance values for the tank size actually used there, that is the one-fifth scale tanks. It will not be clear until the model is operated, what the sensitivity is to this factor in the overall prediction of the fire events. If this sensitivity is high, concern about the scaling effect for use in full scale tank cars may require further testing. This factor is especially significant when EXPLOSAFE is used.

We believe that a relatively simple test can be conducted. This would involve developing an apparatus which models cross-sections of tanks. Two test sections, one having the cross-section of a full scale tank, the other a one fifth scale section, and each about 45 cms thick, could be built. The flat sides would be well insulated to provide nearly adiabatic faces. Heating from gas burners or electric sources would provide peripheral heat inputs, and the thermal mixing would be observed using a thermocouple matrix.

Conducting boiling tests with fluids as flammable as propane, especially in the region of the "Departure from Nucleate Boiling" (burnout) point, is hazardous unless proper precautions are taken. Initially tests using water might be undertaken. However the interpretation of these for the case of propane is not direct, and ultimately some tests using propane would seem to be necessary.

Because, in actual tanks, the boiling takes place on surfaces of various orientations, a form of test apparatus which would allow some separation of the surface inclination effects would be preferred. After reviewing much of the literature on experimental apparatus for the determination of the boiling curves of liquids, we have concluded that an apparatus very similar to that used by Thibault and Hoffman in the work they reported in their paper "Local Boiling Heat Flux Density around a Horizontal Cylinder under Saturated and Subcooled Conditions", presented at the 1978 International Heat Transfer Conference would be appropriate[26]. Their apparatus uses a moderately large diameter horizontal submerged tube, approximating the small curvature of the tank car surfaces better than do wires or ribbons, and moreover allows for the assessment of some of the surface attitude effects which may have a bearing on the boiling curve. The test surface was a copper cylinder 12.7 cm in diameter and 7.60 m long.

Their apparatus, by using a quenching transient technique, avoids the need for very costly high power supply rate apparatus otherwise needed to approach the burnout heat flux rate on large sufaces. By conducting a succession of tests, with and without EXPLOSAFE filling the surroundings, the effects of EXPLOSAFE over the boiling range can be examined.

Thibault and Hoffman worked with water as the fluid under test. Had propane been used,the required heat flux would have been somewhat lower, but precautions against fire or explosion would have been necessary. This would require proper venting of the vapour and other detailed precautions. One way to minimize the risk would be to conduct a full series of tests, with and without EXPLOSAFE, using water, and follow this with a number of tests using propane to establish scaling factors. However, because of the unknown effects of vapour density and latent heat on the action of the EXPLOSAFE filling matrix, there is no doubt that a higher level of confidence in the result would be achieved if propane was used throughout the test series.

Such an apparatus could, in addition to its function in establishing the mixing scale factors, be useful in other aspects of tank fire research. Notably it could be used to show the differences between the performance of different insulations or surface contours, and to confirm some of the other features of the model.

Whether the apparatus should be arranged to use propane, or a less flammable substitute, would be a matter for consideration.

Some cost savings, at the expense of the level of confidence in the results, would be obtained if the comparison vessels were built to smaller scale, such as to one tenth and one third scales. Extrapolation of the scaling factors to full scale would be straightforward, but not necessarily fully valid.

9.4 FURTHER DATA ON EXPLOSAFE

The action of EXPLOSAFE in a liquid or vapour space during heat transfer processes is, as has been pointed out, quite complex. To sort out the effects and allow for good prediction of physical behaviour in a range of conditions would require data on the thermal and fluid mechanical properties. These would include establishing the thermal diffusivity of EXPLOSAFE-liquid combinations for various temperature gradients, the radiation properties of EXPLOSAFE in vapour spaces, the effective contact resistance values at boundary surfaces, the flow resistance characteristics of the matrix, and similar factors. The need for this information is not clear at the present stage of this study.

Some of these factors can be estimated from basic physical data by computation. It is fairly direct to approximate the parallel heat flow away from a wall through the aluminum paths in an EXPLOSAFE matrix and through the surrounding liquid propane, by considering the thermal conductivities, heat flow path lengths and cross-sections, and convective flow and contact resistance effects. Our preliminary estimates show that contribution of the EXPLOSAFE to the total heat flow over the first 15 cms outward from the wall would be considerably less than 10 percent. In the vapour space the fraction of the heat conducted through the aluminum is greater, but the radiation smaller. Tests would be necessary to provide accurate data for such cases.

There is some confusion in the literature over the role of EXPLOSAFE. For instance, A.W. King in CIGT Report No. 81-16 states, "The system (EXPLOSAFE) works by conducting the heat from the overheated vapour space into the liquid via the foil network. It relies to a great extent on good wall contact for its effectiveness."[29]. It is clear that the net effect of EXPLOSAFE in the vapour space, due to combined radiation and convection effects, and including the weak matrix conduction contribution, is to reduce, not increase the vapour to liquid heat transfer rate. This was shown in Section 2.3.4. Moreover, wall contact resistance will play no part in this transfer, but may have a significant effect on local hot spot intensity. Only a careful program of laboratory investigation would provide clear data on the mechanisms controlling the effects. The overall effects can, however, be approximately modelled by matching the field test results.

9.5 VENT VALVE CHARACTERISTICS

It is, of course, necessary to have accurate data on the vent valve characteristics. Specifically the relationship, for any specific valve under consideration, of the discharge rate to the pressure and temperature of the propane vapour must be known. If such data are not available, the techniques described in the reports of the extensive work done on such valves at the University of Maryland could be used to advantage. Most valve manufacturers would be expected to be able to provide most of the performance characteristic data sought.

10.0 COMPUTER PROGRAM DEVELOPMENT

10.1 SOFTWARE CONSIDERATIONS

In view of the complicated nature of the numerical model and the amount of experimentation anticipated in the development, it is important that the program be written in a way that permits flexibility and ease of updating. By far the most significant cost in the development will be the de-bugging of the procedure and this will require a lot of iterative testing. This requirement indicates that a program development system be used that is as interactive as possible and that modularity be designed into the architecture of the program. The flow charts of the model given in this report are written with that modular structure in mind.

If the transportability of the program is to be considered important, it is recommended either FORTRAN or BASIC be the development language. In addition because of the rapid progress in powerful desk-top computers, it is also recommended that the possibility of running on such a computer be considered.

The consulting team have many years experience in the development of commercial software and recognize the importance of thorough documentation to provide backup to the developed programs. Assuming the programmed model may provide the basis for future research on this or similar projects, many different people may wish to use or add to the program. A proper set of user and programmer manuals should therefore be provided. A further aid to future model extensions would be the adherence to previously established program development standards. The team has such a set of standards which have been adopted and proven on earlier development projects. Previous software experience in the development of programs in the heat transfer field will be a major advantage.

10.2 BACKGROUND IN HEAT TRANSFER SOFTWARE

The simultaneous satisfaction of the various equations governing the heat transfer, change of state and mass flow from the rail tank car require an incremental, iterative solution. This procedure has been adopted in the THETA program in use by H.G. Engineering for heat flow problems. The techniques adopted in this program for the solution of the non-linear heat transfer process are transferable to the extensions proposed in this report. THETA provides the thermal network solution procedure which is a major part of the model described here. It is believed this program provides a very good starting point for the development of the current model.

10.3 BACKGROUND IN STRUCTURAL ANALYSIS SOFTWARE

In addition to the thermal network software H.G. Engineering have available structural analysis, finite element software. The ASAS program is a major general purpose program suitable for analysis of thermal stress problems in the tank car shell. After the temperatures have been established, it may be found desirable to investigate the state of stress existing due to the combined pressure and temperature loads. A three dimensional shell model could be built using the ASAS program.

11.0 SUMMARY

Our study of the physical evidence from the field trials and the further data available from the U.S. , has led us to believe that our understanding of the tank fire and BLEVE processes is essentially complete and correct in broad terms. Although the assignment of actual values to many of the parameters remains a problem, we are confident that the models we have developed closely represent the actual fire events in qualitative terms, and will represent them increasingly closely in quantitative terms as the model is put into use and fitted to available trial observations.

In preparing the models we have been particularly conscious of the need to make significant distinctions between different or modified designs, such as those using different insulation practices or EXPLOSAFE. We believe that the models we have presented will in fact be effective in evaluating the effects of such differences. This is particularly true since in many comparisons the effects of physical data inputs, about the values of which there may be uncertainty, will largely cancel out.

Overall we believe our model offers a substantial advance over those previously available, and that it will be a useful tool in evaluating fire related features of tank car designs.

12.0 REFERENCES

1. Canadian Transport Commission, Regulations for the Transportation of Dangerous Commodities by Rail, (Department of Supply and Services: Ottawa, 1982), 479 pages

2. Grange, S.G.M., Report of The Mississauga Railway Accident Inquiry, (Department of Supply and Services: Ottawa, 1981), 212 pages

3. Appleyard, R.D., Testing and Evaluation of the EXPLOSAFE System as a Method of Controlling the Boiling Liquid Expanding Vapour Explosion (BLEVE), prepared for Transport Canada, August 1980

4. Anderson, C., et al., The Effects of a Fire Environment on a Rail Tank Car Filled with LPG, prepared for U.S. Department of Transportation (FRA), FRA-ORD T5-31, September 1974

5. Manda, L.J., Phase 11 Report on Full-Scale Fire Tests, RPI-AAR Tank Car Safety Research and Test Project, Association of Americal Railroads, December, 1975.

6. Townsend, W., et al., Comparison of Thermally Coated and Uninsulated Rail Tank Cars Filled with LPG Subjected to a Fire Environment, Report No: FRA-ORD 75-32, prepared for the U.S. Department of Transportation, FRA, December, 1974

7. Association of Americal Railroads, Railway Progress Institute, Railroad Tank Car Safety Research and Test Project, Phase 11 Report on Analysis of 1/5 Scale Fire Test Data, Report FRA-11-2-14, April 1972, 37 pages

8. Graves, K.W., Development of a Computer Program for Modelling the Heat Effects on a Railroad Tank Car, Calspan Corporation, prepared for the U.S. D.O.T., FRA., Report FRA-ORD 75-33, January 1973

9. Sallet, D.W., et al., 1981 Safety Valve Study Review, Department of Mechanical Engineering, University of Maryland, June 4 & 5, 1981

10. Sallet, D.W. and Wu, K.F., "Thermodynamic Properties of Liquified Patroleum Gases (LPG)," FRA-ORD 76/299, February 1977, 99 pages

11. Sallet, D.W., Guhler, M. and Tsui, C.Y., "Two-Phase Flow Model Test Facility," FRA-ORD 76/298, January 1977, 23 pages

12. Sallet, D.W. and Palmer, M.E., "Extended Thermodynamic Tables of Propane, Propylene, N-Butane and Ethylene," FRA-ORD 76/300, May 1978, 157 pages

13. Sallet, D.W., Guhler, M. and Hannemann, R.J., "Unsteady Two-Phase Blowdown of a Flashing Liquid from a Finite Reservoir," Two-Phase Momentum, Heat and Mass Transfer, vol. 2, F. Durst, G.V. Tsiklauri and N.H. Afgan, editors, Hemisphere, Washington D.C., pp. 781-795, 1979

14. Palmer, M.E., Sallet, D.W. and Wu, K.F., "The Influence of Thermodynamic Properties on the Calculation of Homogeneous Mass Flow Rates," ASME paper 78-WA/HT-48, 1978

15. Sallet, D.W., Hannemann, R.J. and Guhler, M., "An Investigation into Unsteady Two-Phase Depressurization of Vessels Through Orifices and Short Pipes," ASME paper 78-WA/HT-36, 1978

16. Sallet, D.W., "On the Sizing of Pressure Relief Valves for Pressure Vessels which are Used in the Transport of Liquified Gases," ASME paper 78-WA/HT-39, 1978

17. Sallet, D.W., et al, "The Discharge of a Flashing Liquid Through Tubes," Proceedings of the 2nd Multi-Phase Flow and Heat Transfer Symposium, April 16-18, 1979

18. Sallet, D.W., "Two-Phase Flow Aspects in Sizing Pressure Relief Valves," Safety Relief Valves, R.W. Haupt and R.A. Meyer, editors, ASME, PVP-33, New York, pp. 31-41, 1979

19. Sallet, D.W., Palmer, M.E. and Rod, S.R., "The Non-Steady Flow of Fluids from Pressure Vessels," Dynamics of Fluid-Structure Systems in the Energy Industry, M.K. Au-Yang and S.J. Brown, editors, ASME, PVP-39, New York, pp. 213-228, 1979

20. Sallet, D.W., Weske, J.R. and Guhler, M., "The Flow of Liquids and Gases Through Pressure Relief Valves," Safety Relief Valves, R.W. Haupt and R.A. Meyer, editors, ASME, PVP-33, New York, pp. 13-30, 1979

21. Sallet, D.W., "Pressure Relief Valve Sizing for Vessels Containing Compressed Liquefied Gases," Pressure Relief Devices, The Institution of Mechanical Engineers, London, pp. 85-96, 1979

22. Sallet, D.W. and Palmer, M.E., "The Non-Steady Flow of Gases and Vapours from Pressure Vessels," Proc. Instn. Mech. Engrs., vol. 194, no. 26, pp. 225-230, 1980

23. Sallet, D.W. and Palmer, M.E., "The Non-Steady Outflow of Propane Vapor from a Railroad Tank Car," FRA/ORD-81/35, April 1981, 22 pages

24. Gibbs, C.W. (ed.), Compressed Air and Gas Data, (Ingersoll - Rand Co.: New York, 1969), 743 pages

25. Cichelli, M.T. and C.F. Bonilla, "Heat Transfer to Liquids Boiling Under Pressure", Chemical Engineering Progress, 41, 1945

26. Thibault, J., and T.W. Hoffman, "Local Boiling Heat Flux Density Around Horizontal Cylinder Under Saturated and Lub-cooled Conditions", 6th Interactional Heat Transfer Conference, 1978, Toronto, pp. 1-199

27. Hottel, H.C. and A.F. Sarofim, Radiative Transfer, (McGraw-Hill: New York, 1967)

28. Chawla, T.C. and S.H. Chan, "Heat Transfer from Vertical/Inclined Boundaries of Heat - Generating Boiling Pools", J. of Heat Transfer, 104, 3, Aug. 1982, pp. 465

29. King, A.W., Safety Relief Valve Literature Search and Synthesis, prepared for Transportation Development Centre, YP-3293E, August 1981, p. 34

30. Matheson Gas Products, Propane, 1974

13.0 BIBLIOGRAPHY

BOILING CURVE REFERENCES

1. Afgan, N.H., Proceedings of the IIIrd Int. Heat Transf. Conf., (1966), III, 17

2. Archambault, P. and Chevrier, J.C., Int. J. Heat Mass Transfer, 20, 1, 1977

3. Bergles, A.E. and Thompson, Jr., W.G., Int. J. Heat Mass Transfer, 13, 55, 1968

4. Bernhardt, S.H.; Sheridan, J.J.; Westwater, J.W., Amer. Inst. Chem. Engrs., Symp. 118, (1971), 21

5. Bonilla, Ch.F.; Perry, Ch.W., Trans. Amer. Inst. Chem. Engr. 37 (1941), 685

6. Bradfield, W.S., J. of Heat Transfer, 89, 269, (1967)

7. Calus, W.F.; Leonidopoulos, D.J., Int. J. Heat Mass Transf. 17 (1974), 249

8. Chen, T.S. and Mucoglu, A., Journal of Heat Transfer, Trans. ASME, Series C, Vol. 97, p. 198-203, 1975

9. Chen, T.S., Sparrow, E.M., and Mucoglu, A., Journal of Heat Transfer, Trans. ASME, Series C, Vol. 99, p. 66-71, 1977

10. Dernedde, E., Boiling Heat Transfer to Turbulent Liquid Films, M.Eng. Thesis, McMaster University, Canada, 1966

11. Gardon, R., J. Heat Transfer, C82, 396, 1960

12. Gregroyev, L.N., Teplo i Massoperenos 2, (1962), 120

13. Griswold, J., Buford, C.B., Ind. Engng. Chem. 41, (1949), 2347

14. Haase, R., Thermodyn, der Mischphasen, Springer-Verlag, Berlin, Gottingen, Heidelberg (1956)

15. Happel, O., Diss. Ruhr-Univ. Bochum (1974)

16. Hauptmann, E.G., International Journal of Heat and Mass Transfer, Vol. 8, p. 289-295, 1965

17. Hieber, C.A., International Journal of Heat and Mass Transfer, Vol. 16, p. 769-785, 1973

18. Johnson, H.A., Int. J. Heat Mass Transfer, 14, 67, 1971

19. Korner, M., Diss. Techn. Hochsch. Aachen (1967)

20. Leal, L.G., Journal of Applied Mathematics and Physics (ZAMP), Vol. 24, p. 20-42, 1973

21. Merte, Jr. H. and Clark, J.A., J. of Heat Transfer, 86, 351, 1964

22. Minkowycz, W.J. and Sparrow, E.M.,Journal of Heat Transfer, Trans. ASME, Series C, Vol. 96, p. 178-183, 1974

23. Mori, Y., Journal of Heat Transfer, Trans. ASME, Series C, Vol. 83, p. 479-482, 1961

24. Ponter, A.B. and Haigh, C.P., Int. J. Heat Mass Transfer, 12, 429, 1969

25. Ponter, H.B., Davies, E.A., Beaton, W. Ross, T.K., Int. J. Heat Mass Transf. 10, (1967), 233

26. Pressburg, B.J., Todd, J.B., Amer. Inst. Chem. Engrs. J. 3, (1957), 348

27. Redekopp, L.G. and Charwat, A.F., Journal of Hydronautics, Vol. 6, p. 34-39, 1972

28. Reinsch, C.H., Num. Math., 10, 3, 177, 1967

29. Rohsenow, W.M., Mod. Dev. Heat Transf., Acad. Press, (1963), 85

30. Shock, R.A.W., Int. J. Heat Mass Transf. 20, (1977), 70

31. Sparrow, E.M. and Minkowycz, W.J., International Journal of Heat and Mass Transfer, Vol. 5, p. 505-511, 1962

32. Stephan, K., Brennst.-Warme-Kraft 17, (1965), 571

33. Stephan, K., Korner, M., Chem. Ing. Techn. 41, (1969) 409

34. Thibault, J. and Hoffman, T.W., Submitted to Int. J. Heat Mass Transfer

35. Thibault, J., Boiling Heat Transfer Around a Horizontal Cylinder and in Tube Bundles, Ph.D. Thesis, (in preparation), McMaster University, Canada

36. Thibault, J. and Hoffman, T.W., Letter to the Editor. To be published in the Int. J. Heat Mass Transfer

37. Valent, V., Afgan, N., Warme- und Stoffubertragung 6, (1973), 23

38. Van Wijk, R.W., Vos, S.A., van Stralen, D.J., Chem. Eng. Science 5, (1956), 69

39. Verein Deutsch. Ing., Warmeatlas, Dusseldorf (1974)

40. Zuber, N., Tribus, M. and Westwater, J.W., paper 27, Second International Heat Transfer Conference, Boulder, Colorado, August 1961

OTHER USEFUL REFERENCES

41. Delichatsiss, M.A., Exposure of Steel Drums to an External Spill Fire, 15th Loss Prevention Symposium, AICHE, Detroit, Michigan, August 16-19, 1981

42. Denny, Levcon, Hall, Chelton Co., Handbook - Butane and Propane Gases, 4th ed., (Los Angeles, 1962)

43. Kemp, J.D. and C.J. Egan, Hindered Rotation of the Methyl Group in Propane. The Heat Capacity, Vapour Pressure, Heats of Fusion, and Vaporization of Propane. Entropy and Density of the Gas, J. of the American Chemical Society, 60, 7, July 6, 1938

44. Reid, R.C., Possible Mechanisms for Pressurized - Liquid Tank Explosions on BLEVE's, Science, 203, March 23, 1979, p. 1263

45. Reid, R.C. and M.E. Kim, E., The Rapid Depressurization of Hot, High Pressure Liquids or Supercritical Fluids, presented at the 1981 Annual AICHE Meeting, New Orleans

46. Segeler, Gas Engineers' Handbook, (The Industrial Press, New York, 1965)

APPENDIX

COMMON UNITS

Steel

Conductivity	63 W/m.k
Linear expansion coefficient	15×10^{-6} /K
Specific heat	420 J/kg K
Yield strength (typical)	300 MPa
Tensile strength (typical)	460 MPa
Youngs modulus (6.895 MPa = 1 ksi)	210 GPa

Propane - C_3H_8

Liquid density at 38 K	482.9 kg/m^3
Gas density at 38 K	27 kg/m^3
Boiling point	231 K
Molecular wt	44.11
Enthalpy of formation	-103.8 kJ/mol
Heat of combustion	2220 kJ/mol

1 psi = 6894.76 N/m^2 = 6.8947×10^3 MPa